UNIVERSITA' DEGLI STUDI DI VERONA

DEPARTMENT OF BIOTECHNOLOGY

GRADUATE SCHOOL OF NATURAL AND ENGINEERING SCIENCES

DOCTORAL PROGRAM IN BIOTECHNOLOGY

Cycle XXXIII

AN INTEGRATED APPROACH FOR RESOURCES RECOVERY FROM WASTEWATER

S.S.D. ING-IND/25

Coordinator: Prof. Matteo Ballottari

Signature

Tutor: Prof. David Bolzonella

Signature

PhD candidate: Alice Botturi

Signature

Table of content

List of Figure

List of Table

1 General Introduction

This first chapter includes a general introduction to this PhD thesis. Here, the potential values and applications of the current biotechnologies in the field of wastewater are assessed. This chapter shows, also, some significant correlations between this research and the 17 Sustainable Development Goals (SDGs) adopted by all United Nations (UN).

List of abbreviations

EU	European Union
BBI JU	Bio-based industries Joint Undertaking
CEAP	Circular Economy Action Plan
DM	Dry matter
GHG	Greenhouse gas
MMC	Mixed microbial culture
NZE	Net-zero energy
PHA	Polyhydroxyalkanoate
SCP	Single cell protein
SDG	Sustainable Development Goal
VFA	Volatile Fatty Acid
WWTP	Wastewater Treatment Plant

1.1 General Introduction

1.1.1 Resources recovery from municipal wastewater treatment plants (WWTPs): *cradle-to-cradle* concept

In the recent decades the wastewater resource recovery technologies have been extensively studied and elaborated by the scientific community. Traditionally the main objective of wastewater treatment plants (WWTPs) was to dispose human and industrial effluents to protect the users from health risks and to prevent nutrient pollutions in the environment (Wilsenach et al., 2003). Nowadays, there is an extra possible goal: to recover resources from wastewater such as water, energy, nutrients, fertilizers, volatile fatty acids (VFAs), extracellular polymeric substances (EPS), single-cell proteins (SCPs), polyhydroxyalkanoates (PHAs) and CO_2 (Kehrein et al., 2020). Figure 1.1 shows an overview of some key products that are potentially recoverable from WWTPs.

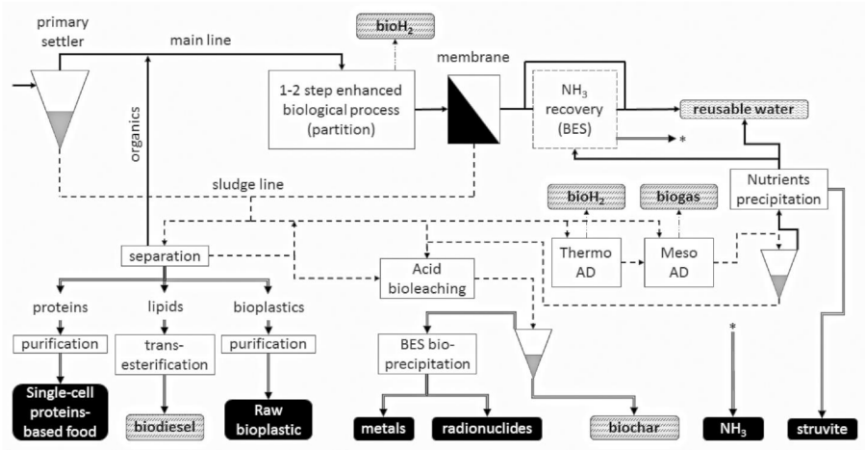

Figure 1.1 Potential resources recovery from wastewater (adopted from: Puyol et al., 2017).

Currently, our Society needs to rethink the way to produce resources, following the *cradle-to-cradle* concept. Indeed, the world's population is estimated to reach, by 2050, 9.7 billion of people and 11.2 billion by 2100 (UN, 2019); this high increase of population will lead, in turn, to an increase of products demand and, consequently, an increase of waste production and depleting of Earth's resources. The new concept from *cradle-to-cradle* aims to substitute the triple-R model (recycle, reuse and recovery), with a more efficient model. The *cradle-to-cradle* concept is mainly an economic and social way of thinking that try to create systems not only efficient but also waste free. In this context, the Sustainable Development Goals (SDGs, Figure 1.2Figure 1.2) have been set. They are seventeen goals adopted

by all the United Nations Member States in 2015. These goals are recognised by all the members as urgent calls for action by 2030 (https://sdgs.un.org/goals). Among these seventeen goals, the main goals that will be take in consideration in the present thesis are: "Zero hunger" (Goal #2); "Clean water and sanitation" (Goal #6); "Climate action" (Goal #13).

Figure 1.2 The Sustainable Development Goals (SDGs). Figure adopted from: European Commission (2020).

The water quality target has a synergic role among SDGs (Alcamo, 2019). Indeed, good water quality can satisfy most of the society's needs such as drinking water, cooking water, hygienic uses and industrial uses; furthermore, it makes a vital contribution for the ecosystem. Nowadays, water is not, anymore, the only resource that can be recovered from WWTPs; there is indeed a need to search for resource recovery applications that realize a net-zero energy (NZE) on the total environment of WWTPs (Hao et al., 2019). WWTPs represent a key platform to base the technological development focused on the *cradle-to-cradle* concept, indeed, between 50 and 100% of lost waste resources are contained in wastewater (Puyol et al., 2017). In Verstraete et al. (2009) it is reported an overall estimation of potential products that can be recovered from municipal wastewater and the relative market prices (Table 1.1).

Table 1.1 Potential products recovery from municipal wastewater (adopted from: Verstraete et al., 2009).

Potential recovery	Per m^3 sewage	Current market prices	Total per m^3 sewage (€)
Water	1 m^3	0.250 €/m^3	0.25
Nitrogen	0.05 kg	0.215 €/kg	0.01
Methane	0.14 m^3	0.338 €/m^3 CH_4	0.05
Organic fertilizer	0.10 kg	0.20 €/kg	0.02
Phosphorus	0.01 kg	0.70 €/kg	0.01
		Total	0.35

As a proof of the increase awareness on these topics, the European Union (EU) is setting new Regulations in order to try to comply what is requested by the 17 SDGs. Indeed, the importance of reach zero waste is in line with the priority of the new Circular Economy Action Plan (CEAP) which is one of the main blocks of the European Green Deal and launched in 2020. This new document presents several actions in order to try to convert all the EU products into sustainable products, focusing the attention mainly in the sectors which need most resources. Furthermore, the document set up the actions for leading global efforts on circular economy.

1.1.2 The Biomass Value Pyramid

Looking at the biomass value pyramid, showed in the following figure (Figure 1.3Figure 1.3), there are several levels of resources recovered, characterized by several economic values. In the global market, the value and the price of the resources are mainly related with their application value.

At the bottom of the pyramid there are the "lowest" value resources in terms of market price, which can be achieved, as an example, by only burning the biomass in order to obtain heat and electricity (Lange et al., 2012). The bottom of the pyramid represents, also, the resources which can be recover in higher quantity. The top of the pyramid is represented by "higher" value products, such as pharmaceutical/feed/food products. These products are characterized to have a high commercial value and are recovered in small amount.

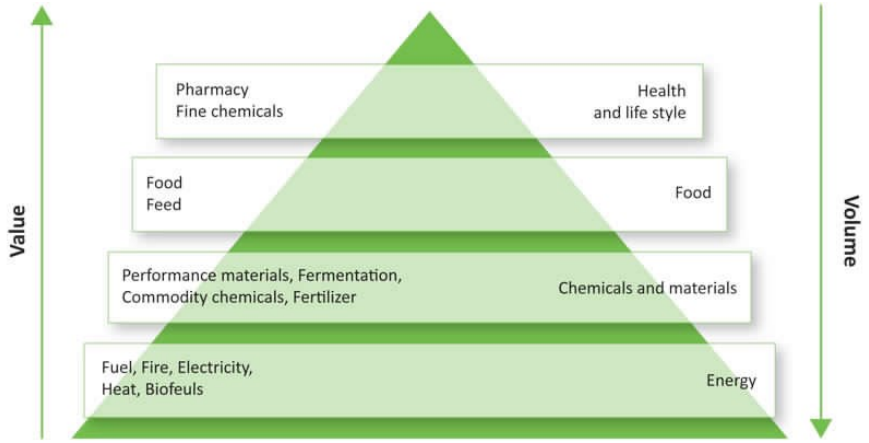

Figure 1.3 Biomass Pyramid Value (adopted from: http://www.betaprocess.eu/the-value-pyramid.php).

Biomass is a versatile energy source that can be used in several sectors, such as in the energy sector as a substitute of fossil fuel; in the chemicals and materials industries in order to replace traditional products; in the food sector as a competitor for food or feed additives; finally, in the pharmaceutical and cosmetic sector.

So, nowadays the main work for the Research and Development (R&D) groups, is to combine forces in order to optimize the way of using biomass and to find the full potentials for each biomass, also in order to meet the global targets for Circular Economy.

Indeed, the global market for bio-based products has been increasing significantly and the bio-based sector is growing and attracting investment. The seventh Bio-Based Industries Joint Undertaking (BBI JU) Call for proposal is an initiative created by the European Commission in order to encourage this market and the development of new sustainable value chains, from efficient processing of biomass feedstock to bringing bio-based products to the market (BBI JU, 2019).

Looking at the methodology for the efficient recover of resources from biomass or waste, biological methods offer the strongest promise. Examples of these methods include heterotrophic, chemotrophic, phototrophic and photosynthetic bacteria; microalgae; terrestrial plants; highly specialized metal reducing and oxidizing organisms for metal recovery; as well as accumulative bacteria from which it is possible to recover biopolymer such as PHAs, EPS, and polysaccharides.

Generally, biomass feedstocks are divided into three main categories: (1) forest products and forest residues, (2) energy crops and agricultural residues and (3) organic wastes.

There are basically two ways to upgrade the components present in the biomass; the first way is to break down the biomass into simple molecules that can be used for growing fungi or bacteria that are able to produce new building blocks for biochemicals and biomaterials. The second way is to recover directly from the biomass itself compounds like protein, cellulose or biopolymer that can be used for new products.

In the following paragraph, an overview of the main classes of products that can be recovered from WWTPs and that will be analysed in detail in the following chapters.

1.1.3 Water recovery

Our Planet is mostly water, around 70% of the Earth; however, around 97% of this resource is saline and only 3% is fresh water and can be used for drinking and irrigation (https://ec.europa.eu/environment/water/pdf/water_reuse_factsheet_en.pdf). The 68.7% of fresh water is in the form of polar icecaps and glaciers; the 30.4% is groundwater or surface water and often does not meet the needs of the population (Crook, 2007, Figure 1.4Figure 1.4). As an example, around the Mediterranean region (such as Spain, Portugal, Italy etc.) some 20% of the population lives under water stress and, specifically, during summer over 50% of the population is affected by this issue (https://www.eea.europa.eu/highlights/world-water-day-is-europe).

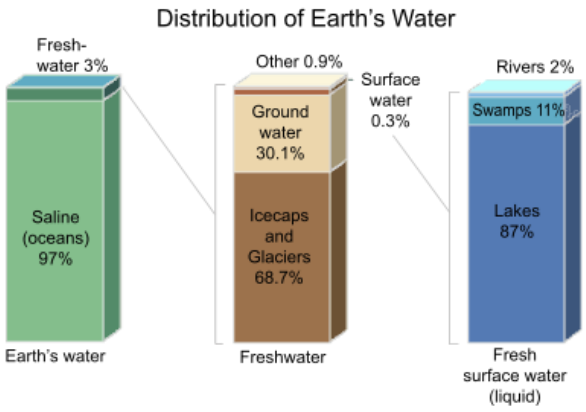

Figure 1.4 Water distribution of Earth (adopted from: https://www.e-education.psu.edu/earth103/node/701).

This problem is increasingly expanding, mainly, due to the population growth, the climate change, and the depletion of groundwater resources. It is indeed reported that by 2030 water stress and scarcity will probably affect 50% of Europe's river basins (EC, 2012). In order to avoid this, it is important to focus our strength on a more efficient manage of water resources. Water reuse from WWTPs can be an alternative and can significantly reduce the city's freshwater demand (Kehrein et al., 2020). Water is not only an essential requirement for humans, but it is also important for the economic development and for the entire ecosystem (Voulvoulis et al., 2018).

As previously described, "Clean water and sanitation" is one of the seventeen goals adopted by all the United Nations Member States (SDG #6). Recovering of reclaimed water from wastewater provides several benefits, such as reduced cost due to reduction of incoming water, reduced demand of freshwater, reduction of fertilizers used in agriculture due to the beneficial effects of recycled water, use of recycled water for industrial applications, etc.

Water is of its own a resource and it is also a transport medium for several resources. To better clarify, in Europe more than 40000 million of m^3 of wastewater are treated every year, but only 964 million of m^3 of this water is reused (https://ec.europa.eu/environment/water/pdf/water_reuse_factsheet_en.pdf).

Following this point of view, it will also take into consideration the necessity of develop processes with, among others, a low water footprint, in order to avoid the

problem of water scarcity. In the following paragraphs, some examples of processes with a low water footprint will be described in detail.

1.1.4 Biopolymers recovery

Biopolymers are polymers produced naturally by living organisms in determined conditions. Recently, due to the growing concerning in the environmental protection, the industrial interest is focused on materials that are renewable, environmentally friendly and naturally decompose (Hassan et al., 2019). The monomeric units of biopolymer are sugars, amino acids and nucleotides, and basing on the monomeric units they can be classified as polynucleotides, polypeptides and polysaccharides (Yadav et al., 2015). Depending on their origin, biopolymer can be classified as: polyesters (such as PHAs and polylactic acid, PLA), proteins (such as collagen/gelatine), polysaccharides (such as xanthan and cellulose from bacteria; pullulan from fungi; starch and carrageenan from plant/algae; chitin from animals), lipids/surfactants (such as acetoglycerides), and polyphenols (such as lignin and humic acid, Yadav et al., 2015).

1.1.4.1 Polyhydroxyalkanoates (PHAs)

Among these biopolymers, PHAs represent one of the most studied class. PHAs are polymers with similar properties than petrochemical derived plastics, such as polyethylene and polypropylene (Laycock et al., 2013). They are synthetized by several type of microorganisms as lipid inclusions storage, ranging in size from 0.2 to 0.5 µm, for energy (Poli et al., 2011).

There are more than 90 genera of Gram-positive and Gram-negative bacteria that can produce PHAs. These bacteria can be divided into two classes: the first class comprises bacteria that require limitation of nutrients (such as phosphorous, nitrogen, oxygen or magnesium) to accumulate PHAs; in the second group there are bacteria that can accumulate PHAs during the growth phase, so they do not require any nutrients limitation (Muhammadi et al., 2015).

PHA storing bacteria can be selected in a mixed microbial culture (MMC) via several approaches, such as alternating of aerobic/anaerobic environment, as well as microaerophilic/aerobic or *feast/famine* regime (Sruamsiri et al., 2020). The

latter regime consists of an alternation of cycles with changes in substrate availability, such as high content of carbon and starving periods.

MMC is usually the most economically favourable method for PHA production. Anyway, production of PHA using pure cultures and waste streams has been already studied, reporting a reduction of the overall cost of around 30-50% (Ashby et al., 2004; Coats et al., 2007).

1.1.5 Single cell protein (SCP) or microbial protein (MP): features, pros and cons

Nowadays, the food supply for more than 7.0 billion people in the World is associated with growing demand for limited resources. It is indeed reported that the world population projected to reach 9.8 billion in 2050 and 11.2 billion in 2100 (https://www.un.org/development/desa/en/news/population/world-population-prospects-2017.html). The current anthropogenic pressure on Earth's finite resource and the concomitant dynamics of climate changes, is going to generate concerns about the resilience of the contemporary feed/food chain (Matassa et al., 2016).

Especially, protein scarcity is one of the crucial and well recognized problems, mostly in the developing countries. The social changes that are occurring are expected to yield a 50% higher demand in protein (Verstraete et al., 2016). For this reason, alternative and sustainable sources of proteins should be developed and produced, as requested by the SDGs established by United Nations Member States in 2015 (Goal #2 "Zero hunger"). Global demand for protein is mainly satisfy by soybean, which is expected an annual increase of 1.6% until 2027 (Spiller et al., 2020). Europe is 70% dependent on imports of protein-rich crops, as reported in the European Commission document (2016, www.europabio.org).

Microorganisms have always been closely related to food processing, associated with several benefits. Just think, for example, to fermentation processes for dairy products production, in which lactic acid bacteria are the main actors. Microorganisms, such as bacteria, fungi, yeast and algae can also be used directly as feed or food additive (Anupama and Ravindra, 2000). These proteins produced with microorganisms are known as microbial proteins (MP) or single cell proteins (SCP).

The Imperial Chemical Industries (ICI) was the first to produce in full scale and commercialize MP called Pruteen® (Westlake, 1986). The research investigated, then, a whole range of other possibilities; however, the low price of conventional proteins for animal feed (such as soybean and fishmeal) prevented the development in the market of the alternative proteins.

In the recent years, conversely, the increase of the fishmeal price, together with the environmental concerns about the use of land for soybean, justified the return to the research and the development around MP (Matassa et al., 2016). A well-studied example of bacteria able to produce high quality protein, both for human and animal consumption, is represented by hydrogen-oxidizing bacteria (HOB, Parkin and Sargent, 2012; Pohlmann et al., 2007; Matassa et al., 2016).

The Table 1.2 shows several protein sources and their average protein content; the Table 1.3 shows the average protein content of several microorganisms.

Table 1.2 Overview of different protein sources.

Protein source	Average protein content [%DW]	Ref.
Fish	15-20	Matassa et al. (2016); Waite et al. (2014)
Pork	20	Matassa et al. (2016); Waite et al. (2014)
Chicken	31	Matassa et al. (2016); Waite et al. (2014)
Beef	25	Matassa et al. (2016); Waite et al. (2014)
Soybean	45-57	Ghasemi et al. (2011)
Wheat	12	FAO, 2015; Indexmundi (2016)

Table 1.3 Average protein content of different microorganisms.

Microorganism	Average protein content [%DW]	Ref.
Seaweed	40-60	Draaisma et al. (2013); Harun et al. (2010)
Spirulina	50-60	Templeton and Laurens (2015)
Fungi	30-70	Thrane (2007)
Bacteria	50-83	Strong et al. (2015)

New protein sources for feed or food applications are also needed for comply the Goal #13 "Climate action" as well as the Goal #6 in terms of low water footprint. Indeed, there are quite important differences in terms of footprint among traditional protein sources and innovative ones, such as SCP. The following table (Table 1.4) summarizes some of these differences, among an example of commercial SCP (FeedKind) and the two most known traditional alternatives to meat protein source (fish meal for feed application and soy protein concentrate). As it is shown in the table, the protein content ranging from 64 to 71% on dry matter (DM), with the highest value for SCP. Soy protein needs the highest land use for kg of protein produced (6.7 m^2/kg protein produced), which has a general negative impact on the environment. Water consumption is, in the same way, around 85-90% lower for SCP and fish meal, if compared with soy protein production process. Regarding greenhouse gases (GHGs) emissions, soy protein has lower emissions value if compared with SCP and fish meal (both in the range 2.2-2.6 kg CO_2/kg protein). The reason of this difference is due to the type of fermentation process for SCP production.

Table 1.4 Footprint of feed and food containing proteins (source: Carbon Trust, 2016). FeedKind is an example of commercial SCP product. DM is for dry matter.

Products	**Protein content (% DM)**	**GHGs emissions (kg CO_2e/kg protein)**	**Water consumption (m^3/kg protein)**	**Land occupation (m^2/kg protein)**
SCP (FeedKind)	71	2.2	0.01	0.0
Fish meal	64	2.6	0.02	0.01
Soy protein concentrate	66	0.8	0.14	6.66

References

Alcamo, J. (2019). Water quality and its interlinkages with the Sustainable Development Goals. *Current opinion in environmental sustainability*, *36*, 126-140.

Ashby, R. D., Solaiman, D. K., & Foglia, T. A. (2004). Bacterial poly (hydroxyalkanoate) polymer production from the biodiesel co-product stream. *Journal of Polymers and the Environment*, *12*(3), 105-112.

Coats, E. R., Loge, F. J., Wolcott, M. P., Englund, K., & McDonald, A. G. (2007). Synthesis of polyhydroxyalkanoates in municipal wastewater treatment. *Water Environment Research*, *79*(12), 2396-2403.

Crook, J. (2007). *Innovative Applications in Water Reuse and Desalination: Case Studies 2*. WateReuse Association.

EC, E. (2012). Report on the Review of the European Water Scarcity and Droughts Policy. *Communication from the Commission to the European Parliament and the Council*, *67*.

Ghasemi, Y., Rasoul-Amini, S., & Morowvat, M. H. (2011). Algae for the production of SCP. *Bioprocess Sciences and Technology: Nova Science Publishers, Inc*, 163-84.

Hao, X., Wang, X., Liu, R., Li, S., van Loosdrecht, M. C., & Jiang, H. (2019). Environmental impacts of resource recovery from wastewater treatment plants. *Water research*, *160*, 268-277.

Hassan, M. E. S., Bai, J., & Dou, D. Q. (2019). Biopolymers; Definition, Classification and Applications. *Egyptian Journal of Chemistry*, *62*(9), 1725-1737.

Kehrein, P., van Loosdrecht, M., Osseweijer, P., Garfí, M., Dewulf, J., & Posada, J. (2020). A critical review of resource recovery from municipal wastewater treatment plants–market supply potentials, technologies and bottlenecks. *Environmental Science: Water Research & Technology*, *6*(4), 877-910.

Koyande, A. K., Chew, K. W., Rambabu, K., Tao, Y., Chu, D. T., & Show, P. L. (2019). Microalgae: A potential alternative to health supplementation for humans. *Food Science and Human Wellness*, *8*(1), 16-24.

Lange, L., Bech, L., Busk, P. K., Grell, M. N., Huang, Y., Lange, M., ... & Tong, X. (2012). The importance of fungi and of mycology for a global development of the bioeconomy. *IMA fungus*, *3*(1), 87-92.

Laycock, B., Halley, P., Pratt, S., Werker, A., & Lant, P. (2013). The chemomechanical properties of microbial polyhydroxyalkanoates. *Progress in Polymer Science*, *38*(3-4), 536-583.

Matassa, S., Boon, N., Pikaar, I., & Verstraete, W. (2016). Microbial protein: future sustainable food supply route with low environmental footprint. *Microbial biotechnology*, *9*(5), 568-575.

Muhammadi, Shabina, Afzal, M., & Hameed, S. (2015). Bacterial polyhydroxyalkanoates-eco-friendly next generation plastic: production, biocompatibility, biodegradation, physical properties and applications. *Green Chemistry Letters and Reviews*, *8*(3-4), 56-77.

Parkin, A., & Sargent, F. (2012). The hows and whys of aerobic H2 metabolism. *Current opinion in chemical biology*, *16*(1-2), 26-34.

Pohlmann, A., Fricke, W. F., Reinecke, F., Kusian, B., Liesegang, H., Cramm, R., ... & Strittmatter, A. (2007). Correction: Corrigendum: Genome sequence of the bioplastic-producing "Knallgas" bacterium Ralstonia eutropha H16. *Nature Biotechnology*, *25*(4), 478-478.

Poli, A., Di Donato, P., Abbamondi, G. R., & Nicolaus, B. (2011). Synthesis, production, and biotechnological applications of exopolysaccharides and polyhydroxyalkanoates by archaea. *Archaea*, *2011*.

Puyol, D., Batstone, D. J., Hülsen, T., Astals, S., Peces, M., & Krömer, J. O. (2017). Resource recovery from wastewater by biological technologies: opportunities, challenges, and prospects. *Frontiers in microbiology*, *7*, 2106.

Spiller, M., Muys, M., Papini, G., Sakarika, M., Buyle, M., & Vlaeminck, S. E. (2020). Environmental impact of microbial protein from potato wastewater as feed ingredient: comparative consequential life cycle assessment of three production systems and soybean meal. *Water Research*, *171*, 115406.

Strong, P. J., Xie, S., & Clarke, W. P. (2015). Methane as a resource: can the methanotrophs add value?. *Environmental science & technology*, *49*(7), 4001-4018.

Verstraete, W., Van de Caveye, P., & Diamantis, V. (2009). Maximum use of resources present in domestic "used water". *Bioresource technology*, *100*(23), 5537-5545.

Verstraete, W., Clauwaert, P., & Vlaeminck, S. E. (2016). Used water and nutrients: Recovery perspectives in a 'panta rhei'context. *Bioresource technology*, *215*, 199-208.

Voulvoulis, N. (2018). Water reuse from a circular economy perspective and potential risks from an unregulated approach. *Current Opinion in Environmental Science & Health*, 2, 32-45.

Wilsenach, J. A., Maurer, M., Larsen, T. A., & Van Loosdrecht, M. C. M. (2003). From waste treatment to integrated resource management. *Water Science and Technology*, *48*(1), 1-9.

Yadav, P., Yadav, H., Shah, V. G., Shah, G., & Dhaka, G. (2015). Biomedical biopolymers, their origin and evolution in biomedical sciences: A systematic review. *Journal of clinical and diagnostic research: JCDR*, *9*(9), ZE21.

Web reference

https://sustainabledevelopment.un.org/?menu=1300

https://www.bbi-europe.eu/news/over-%E2%82%AC100-million-available-advancing-european-bio-based-sector

https://www.un.org/development/desa/en/news/population/world-population prospects-2017.html

https://www.europabio.org/sites/default/files/EU_protein_GAP_WCover.pdf

http://www.fao.org/worldfoodsituation/csdb/en/

http://www.indexmundi.com/commodities/?commodity=wheat

https://ec.europa.eu/environment/water/pdf/water_reuse_factsheet_en.pdf

https://www.eea.europa.eu/highlights/world-water-day-is-europe

https://www.un.org/development/desa/en/news/population/world-population-prospects-2019.html

https://www.carbontrust.com/resources/assessment-of-environmental-footprint-of-feedkind-protein

2 Reduction of Combined Sewer Overflows (CSOs) and possible water reuses

This chapter described the results obtained within the INTCATCH Horizon 2020 European Project; this chapter resumes the following publications:

Botturi, A., Daneshgar, S., Cordioli, A., Foglia, A., Eusebi, A. L., & Fatone, F. (2020). An innovative compact system for advanced treatment of combined sewer overflows (CSOs) discharged into large lakes: Pilot-scale validation. *Journal of Environmental Management, 256*, 109937.

Botturi, A., Ozbayram, E. G., Tondera, K., Gilbert, N. I., Rouault, P., Caradot, N., ... & Foglia, A. (2020). Combined sewer overflows: A critical review on best practice and innovative solutions to mitigate impacts on environment and human health. *Critical Reviews in Environmental Science and Technology*, 1-34.

List of abbreviations

BOD	Biochemical Oxygen Demand
COD	Chemical Oxygen Demand
CSO	Combined Sewer Overflow
CSS	Combined Sewer System
GAC	Granular Activated Carbon
RBF	Rotating Belt Filter
SSS	Separate Sewer System
TKN	Total Kjeldahl Nitrogen
TP	Total Phosphorus
TSS	Total Suspended Solids
UWWTD	Urban Wastewater Treatment Directive
WFD	Water Framework Directive
WWTP	Wastewater Treatment Plant

2.1 Introduction

2.1.1 Wastewater treatment systems

In Europe, wastewater treatment system can be classified into combined (or conventional) sewer system (CSS) and separate sewer system (SSS, Figure 2.1), basing on the way to collect and transport wastewater. In Europe most of the sewer systems (70%) are in the form of CSS, that means that municipal wastewater and storm water are collected and then carried to the wastewater treatment plant (WWTP) in a single pipeline. In the case of SSS, the sanitary sewage is carried separately from the storm water in two different sets of drainage systems. The sewage is carried to the WWTP and the storm water is discharged into water bodies without further treatment. Although the storm water may collect contaminants along its way (such as pathogens, hydrocarbons, hazardous chemicals and heavy metals) also adsorbed to grit and sediments, generally it does not require a permission from the environmental regulators for discharging into water bodies (Jotte et al., 2017).

It is also possible to have a compromise between separate and combine system; partially separate systems work in a way that combines the sanitary sewage and storm water from buildings, while transporting the storm water from the roads, streets and pavements separately, frequently through open drains.

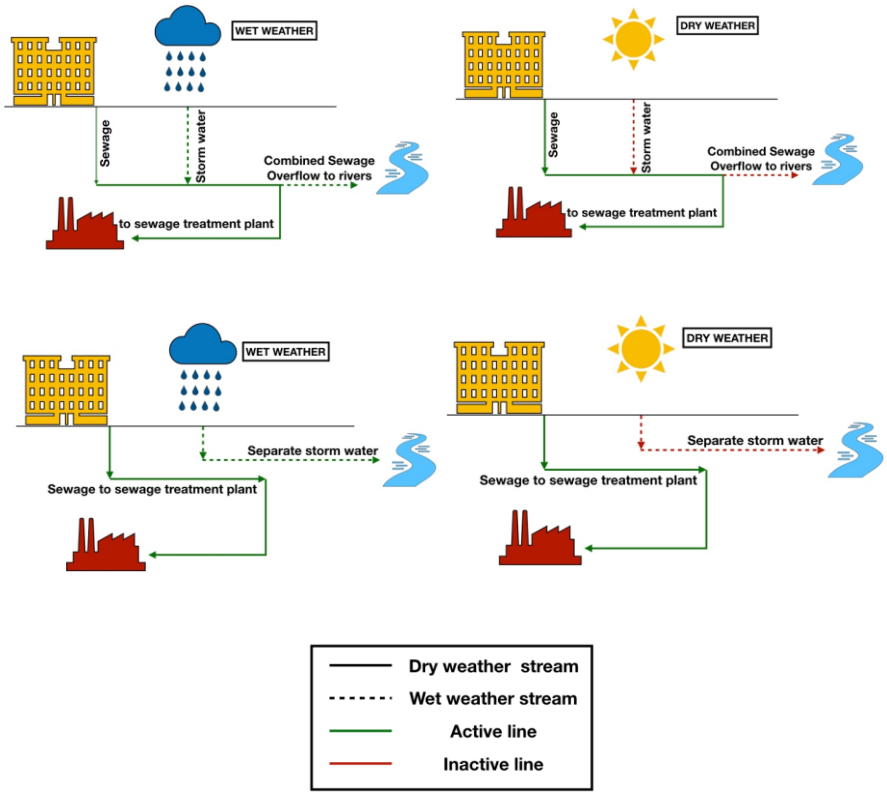

Figure 2.1 Combined (top) and separate (bottom) sewer system.

2.1.2 Combined sewer system (CSS) and combined sewer overflows (CSOs)

However, all sewer infrastructure is limited in its capacity for water intake and transport. Usually, CSS is unable to cope with the flows experienced during heavy rain events, so a relief mechanism is inserted in the wastewater network which is called combined sewer overflow (CSO) infrastructure. The excess flow is, consequently, discharged into the nearest water bodies in order to maintain the flowrates in the network and to protect properties from potential flooding (Bailey et al., 2016). However, since they contain municipal wastewater, they could potentially carry different contaminants such as heavy metals, suspended solids, nutrients, pesticides and microbial pathogens to the receiving water bodies. Although the contaminants concentrations in CSO could potentially vary depending on many factors such as the peak flow rate of municipal wastewater and its variability, size and shape of the sewage collection system etc., they could contain considerable amount of pollutants. The concentrations of pollutants in CSO could

be up to 270–550 mg/L, 260–480 mg/L, 60–220 mg/L, 4–17 mg/L and 1.2–2.8 mg/L for total suspended solids (TSS), chemical oxygen demand (COD), biological oxygen demand (BOD), total kieldahl nitrogen (TKN) and total phosphorus (TP) respectively (Metcalf and Eddy, 1991). This will lead to several problems from endangering aquatic organisms' life to limiting recreational activities for the receiving water bodies (Suarez and Puertas, 2005; Heinz et al., 2009; Phillips et al., 2012; Anne-Sophie et al., 2015; Launay et al., 2016; Al Aukidy and Verlicchi, 2017; Masi et al., 2017; Xu et al., 2018). They could also have negative impact on other chemical and physical parameters of water bodies such as pH, temperature and dissolved oxygen (Diaz-Fierros et al., 2002; Gasperi et al., 2008; Passerat et al., 2011). A range of different technologies could be applied for treating CSOs before discharging them into water bodies. Primary treatments such as constructed wetlands and settling tanks could be used for removing TSS, COD, BOD, nutrients, micropollutants, coliform bacteria and heavy metals (Krebs et al., 1999; Mell, 2010; Metcalf and Eddy, 2014). Since these treatments are not usually enough for meeting regulations on CSO quality they are often combined with secondary treatment processes such as chemical coagulation, adsorption, membrane filtration and disinfection. Up to date, limited information has been published concerning the extent and occurrence of CSO and discharge points. It is estimated that there are 2.2 million km of existing sewerage system in Europe; moreover, there are approximately 650.000 CSO stations (EurEau, 2016).

Recently, in the context of the common implementation strategy of the Water Framework Directive (WFD), the need for the control of diffuse pollution has been highlighted as the key factor to achieve a good chemical and ecological status of surface water bodies. In Europe, the Urban Wastewater Treatment Directive (UWWTD) controls the urban wastewater discharges including the CSO. The current wastewater management technique treats the CSO by a preliminary de-gritting process before its discharge into water bodies (Field et al., 1985). These overflows were not considered an important environmental concern in the past and consequently they were not controlled. Therefore, only in recent scientific projects the quality and quantity of them has been studied and the way they could be treated. Consequently, CSO are a major concern regarding the possible presence of

pollutants. For example, caffeine, a ubiquitous compound in raw domestic wastewater, have much higher concentrations in CSO than in the treated wastewater effluent (Buerge et al, 2006). Another example could be the pharmaceutical ibuprofen that has been found in CSOs in concentrations 100 times higher in comparison to treated wastewater (Philips et al, 2012). Some studies reported that the CSO and their corresponding antibiotic pollution could be responsible for the enhancement of antibiotic resistant bacteria into the environment (Scheurer et al., 2015).

2.1.3 CSO characteristics

Climatic factors such as quantity and intensity of precipitation are key factors determining the severity of CSO discharges. The characteristics of combined sewage are dependent on rainfall intensities and pollutant concentration and loads affected by wet and dry weather conditions (Sandoval et al., 2013). Moreover, during transportation in the sewer system, the physical, chemical, and biological characteristics of wastewater change (Nielsen et al., 1992). The relationship between rainfall, flood, and overflow frequencies on water quality in CSO discharges is nonlinear (Willems and Olsson, 2012). Climate change also has a major impact on CSO volumes for the regions where heavy rainfall events occur more frequently. As such, CSO discharges represent a great challenge to meeting required water quality standards in locations with CSSs. How CSOs impact the water quality of the receiving bodies should be evaluated in an integrated manner considering the flows, concentration, and season in which the impact is more destructive – in Europe this is usually during low flow regimes during summer months (Willems and Olsson, 2012). As this is also a period of increased recreational activities in surface waterbodies (Kistemann et al., 2016), severe health ramifications can be linked to CSO discharges (McBride et al., 2013). Monitoring studies indicate that the frequency of CSOs has increased in recent years (Botturi et al., 2020). An overview of pollutant ranges in combined sewage from CSO discharges is given Botturi et al., 2020. The water quality varies according to factors such as location, rainfall duration, season, etc.

2.1.4 Water quality impact of CSO discharges

The pollutants released with CSO discharges can have detrimental impacts on aquatic environments and public health. The pollutants in the untreated wastewater can increase the organic content of receiving water bodies, and oxygen depletion occurs with biodegradation, promoting eutrophication. In a comprehensive study carried out by Viviano et al. (2017), it was reported that more than 50% of the total phosphorous loads in the Lambro River resulted from CSO discharges during heavy rain events. Thermal pollution may also occur where the temperature of the CSO is different to the receiving water. Moreover, as a consequence of increased turbidity, photosynthesis is inhibited/reduced (Riechel et al., 2016). In warm seasons, low flows can limit dilution effects and, therefore, increase the problem (Montserrat et al., 2013). On the other hand, the concentrations of wastewater contaminants such as total solids, COD, TKN, and P tot can decrease due to the dilution caused by high precipitation. The study carried out by Gasperi et al. (2012a) and Gasperi et al. (2012b) showed that the parameters can be decreased almost one-third of the dry season. On the other hand, a high variation between maximum and minimum values for the parameters were determined in various studies (El Samrani et al., 2008; Li et al., 2010; Tondera, 2019; US EPA, 2004) and the highest values were reported by US EPA (2004) in which TSS, BOD_5, and TP were determined as 4420, 696, and 20.8 mg/L. The variation could be attributed to the precipitation volume, duration, location, etc. and confirmed the high stochastic nature of CSO events (Masi et al., 2017). Emerging contaminants, such as pharmaceuticals, hormones, and substances from personal care products, can be introduced into aquatic environments via CSO discharges (Del Río et al., 2013; Montserrat et al., 2013; Passerat et al., 2011). These contaminants may also be mobilized from sediments during storm events and end up in the water (Del Río et al., 2013). The runoff from urban surfaces transports additional loads of heavy metals, polycyclic aromatic hydrocarbons, and a variety of other micropollutants such as pesticides (Gasperi et al., 2014; Phillips & Chalmers, 2009). Metal contamination is another important issue in CSO discharges, which can accumulate in the sediment and affect the aquatic ecosystem, for example by inhibiting reproduction in sensitive macroinvertebrates (Schertzinger et al., 2018). A correlation between metals concentration in the sediment and the number of CSOs was determined by

Hnaťuková (2011). Recent studies revealed that, even though CSO discharges represent only a small proportion of the total annual wastewater discharge, these overflows contribute to 30–95% of the annual load for different pollutants including caffeine, ibuprofen, polycyclic aromatic hydrocarbons (PAHs), phenolic xenoestrogens, hormones, and urban pesticides (Launay et al., 2016; Phillips et al., 2012). Furthermore, Phillips et al. (2012) stated that micropollutant concentrations could be up to 10 times higher in CSO discharges than that of the treated wastewater. Despite the short duration of CSO discharges, they introduce, high loads of micropollutants into waterbodies (Musolff et al., 2009). Moreover, the concentrations of PAHs in CSO discharges were found 2000 times greater than Environmental Quality Standards (Birch et al., 2011). Gasperi et al. (2012a) and Gasperi et al. (2012b) evaluated the concentrations of priority pollutants as well as wastewater quality parameters for CSO discharges, wastewater, and storm runoff. Whereas, runoff is the major source for pesticides and dissolved metals (e.g. Zn) in CSO discharges, wastewater is the main contributor to volatile organic compounds. On the other hand, hydrophobic organic pollutants (e.g. PAHs) and particulate-bound metals (e.g. Pb and Cu) are mostly caused by in-sewer deposit erosion in the CSO discharges. Although wastewater effluents and CSO discharges are the main contributors for endocrine-disrupting compounds and personal care products in receiving water bodies, the concentrations depend on the removal rates in WWTPs, stormwater dilution factor, and the quantity of wastewater bypassed the treatment plant (Ryu et al., 2014). Studies suggest some substances suitable as markers for CSOs, especially those which are biologically degraded in WWTPs or are specific to stormwater runoff. In combined sewer networks, caffeine can be proposed as a tracer for CSO discharges (Buerge et al., 2006). Similarly, Fono and Sedlak (2005) introduced propranolol, a pharmaceutical component, as a tracer for anthropogenic discharges. CSO discharges introduce infectious pathogens originating from human faces and organic waste in the sewage, as well as from animal faces in runoff originating from wildlife (e.g. birds) or domestic animals (especially dogs) (Schares et al., 2005). They can contain antibiotic resistant bacteria (Young et al., 2013). Monitoring programs usually focus on indicator organisms, such as *Escherichia coli* and intestinal enterococci, which are, for example, relevant for the EU Bathing

Water Directive, or thermo-tolerant coliforms (WHO., 2008). They are chosen to indicate specific pollution, for example, by faecal contamination. Ideally, this should enable one to conclude that a health risk is present. Some studies have investigated and detected further bacterial pathogens such as *Campylobacter*, *Salmonella*, *Aeromonas* spp., *Pseudomonas aeruginosa*; enteric viruses such as Adenovirus and Norovirus, and human polyomavirus as well as protozoan parasites such as *Giardia lamblia* and *Cryptosporidium* (Christoffels et al., 2014; McGinnis et al., 2018; Tondera et al., 2015). Direct measurements in CSO discharges regarding *E. coli* concentrations are rare; more often, polluted river water after overflow events is sampled instead. In the few published investigations with direct measurements, the median concentrations of *E. coli* at the outlet of overflow or CSO retention tanks range from 104 to 106 MPN or CFU/100mL (Stott et al., 2018). If surface waters are used for recreational purposes, these microbial contaminations result in risks of infections with gastrointestinal illnesses, pneumonia, bronchitis, and respiratory infections (US EPA., 2004). McBride et al. (2013) revealed that the highest risks for swimmers derive from norovirus and rotavirus in such contaminated waters. Pond (2005) gives a detailed overview on infections and sequelae caused by these pathogens, some of which are chronic. The author associates the discharge of CSOs with these diseases and recommends closing recreational areas after heavy storm events and sewage treatment in general as a management strategy against possible infections. Accordingly, Tondera et al. (2016) modelled the overall impact of CSO discharges on microbial contaminations in the Ruhr River relative to other sources, for example, from WWTP effluent or diffuse pollution. The authors showed that in the river, which passes through a densely populated area in Germany, CSO discharges had the highest impact on elevated microbial concentrations up to two days after rainfall events. Moreover, Jalliffier-Verne et al. (2016) stated that high *E. coli* concentrations at raw water collection points for drinking water production correlate with the discharged concentrations from CSOs, the location of overflows, dispersion processes in the surface waterbody, and the season. In a study carried out by Riechel et al. (2019), the authors used a tracer approach using wastewater volume as a proxy for pathogen emissions to assess the relationship between different CSO outlets and bathing

water quality for Berlin, Germany. According to their results, wastewater including only 5% of the CSO volume contributes >99% of the pathogen loadings to the receiving environment. Wastewater volume was also of relevance for the determination of point sources for the hygienic impairment of the receiving environment. In another study by the same group (Seis et al., 2018), they proposed a methodology which demonstrated the shortcomings of current long-term classification as well as the potential for improvement by applying the proposed approach regarding to the microbial safety. However, USEPA's BEACH Program conducted an annual survey of the nation's swimming beaches. During the 2002 swimming season, CSOs and SSOs were responsible for only 1% and 6%, respectively, of reported advisories and closings (US EPA., 2004). Therefore, results are controversial and call for proper smart monitoring and case-by-case analyses.

2.1.5 Policy, legislation, governance, and regulation to address the challenges

The necessity of controlling CSO pollution under the urban wastewater treatment directive (UWWTD, EC, 1991) and WFD (EC, 2000) was stated by the European Union. Discharges of CSOs may affect the achievement of "good status" of waterbodies as required by the European Water Framework Directive (EWFD). The scientific community and the water sector operators are raising awareness of the environmental problems relating to CSOs and are promoting initiatives for reduce their impact and improving the quality of surface water (EurEau, 2016). Since 1998, there have been significant changes in legislation with the implementation of the water directives; the water quality and the ecological standards have been revised. New issues have arisen with an urgent need of adaptation and mitigation measures in the upgrading of urban drainage systems.

In the European legislation relating to CSOs, it is possible to distinguish between Directives aimed at protecting receiving waters and Directives to control CSO discharges (Morgan et al., 2017). The Urban Waste Water Treatment Directive 91/271/EEC (UWWTD) highlights that the collecting systems shall be constructed and managed in accordance with limiting the quantity of pollution entering receiving waters due to storm water overflows. In addition, the UWWTD requires reporting of wastewater sewerage treatment performance and a system of

preauthorization for all wastewater discharges, including CSOs. The ongoing evaluation of the UWWTD has highlighted the importance of better managing CSOs. The Bathing Water Directive 2006/7/EC (BWD) and the Habitats Directive 92/43/EEC are limited to assess the bathing waters affected by CSOs as "subject to short-term pollution". In the EU Regulation No. 166/2006 (2006) "concerning the establishment of a European Pollutant Release and Transfer Register", EU member states are obligated to report pollutant loads, specified in Annex II, to water. The threshold values are also specified in this regulation. Thus, the pollutant loads from CSO discharges should also be estimated. However, this is very challenging since CSO structures are not designed for monitoring purposes.

CSO discharges have been identified as an important problem for European countries. Germany, UK, and other countries have started to establish CSO policies and actions before Water Framework Directive (Malgrat, 2013). Sixteen EU member states have national standards that regulate storm water overflows, 11 of them have guidance documents that directly address storm water overflows (EurEau, 2016). Common approaches in standards and guidance are:

- Limit on the number of overflows (e.g. Belgium, Poland, Portugal);
- Requirements for dilution (e.g. Bulgaria, Czech Republic, Estonia);
- Other approaches: max total volume, or max number of days of overflows (e.g. Germany).

The permitted number of overflows per year proposed by CSO regulation guidelines differs according to each member country and ranges from 2 to 3 in Denmark and the Netherlands, 15 to 20 in the Galician region in Spain (Montserrat et al., 2015) and 10 in Poland (Brzezińska et al., 2016). In the UK, the requirements for solids separation depend on the number of overflows per year. The Urban Wastewater Treatment Regulation states that primary treatment must be provided within CSO structures, in which the BOD_5 of the incoming wastewater is reduced by at least 20% before discharge and the TSS reduced by at least 50% (Morris, 1999). The third periodic Asset Management Plan review (AMP3: 2000–2005) specified a timetable for water companies to reduce the number of unsatisfactory intermittent discharges caused by CSOs (McSweeney et al., 2009). In 2012, a comprehensive framework for CSO improvement has been developed through the

urban pollution management program to assess the impact of CSO discharges on receiving water quality and to develop water quality standards for the protection of aquatic life from intermittent pollution caused by CSO discharges (Morgan et al., 2017). These criteria also form the basis of CSO assessment in Ireland, as set out in the Procedures and Criteria in relation to Storm Water Overflows. On the other hand, in Italy, a list of performance indicators to describe the technical quality of the water utility management and operation were introduced in 2017 by the Italian Regulatory Authority for Energy, Networks and Environment (Regulation Number 917/2017). The section dedicated to the sewer system includes two restrictions; firstly, the adequacy of the CSO stations and secondly, the number of overflows allowed in one year in each 100 km of sewage system. Moreover, in Spain, the Royal Order RD 1290/2012 requires that all CSO discharging points for places exceeding 2000 equivalent inhabitants should be defined (Montserrat et al., 2013). In France, it is just stated that CSOs spillages must not exceed 2% of the total average annual volume for 5 years (Tabuchi, 2013) and according to the "Local Authorities General Code 2015 Order" monitoring must be ensured by the operator, municipality, and the different water policy services. However, in Germany, several guidelines describe the design and construction of CSO retention tanks at points with critical discharge (ATV-128.,128, 992; DWA., 2013b, 2013a). Capacities depend on factors like the catchment area, population density, historical rainfall patterns, and the proportion of impervious surface areas. The percentage of wastewater in a catchment that can be discharged via overflows is based on 10-year rainfall patterns and determined by the sensitivity of the receiving waterbody. In 1994, the United States Environmental Protection Agency issued the CSO control policy in the National Pollutant Discharge Elimination System program (NPDES). Within the scope of the policy, site-specific permits were developed for all CSS considering cost/performance in relation to the size of the individual systems. Additionally, a list of nine minimum measures were determined for CSOs in order to develop and adopt long-term control plans (US EPA., 2001, 2004). They include programs for control measures during installation and pollution prevention, pre-treatment applications, maximization of the storage in collection system and flow directed to the WWTP, monitoring, as well as public communication. In Canada,

although there is no federal legislation for CSOs control, some provinces, like Quebec, adopted specific rules to restrict CSOs (MDDELCC, 2014). To be in accordance with the Strategy for the Management of Municipal Wastewater Effluent, municipalities and developers have to demonstrate that new developments will not result in an increase in the frequency of CSO (Mailhot et al., 2015). According to the Canada-wide Strategy for the Management of Municipal Wastewater Effluent, CSO discharges are not entirely prohibited, but are allowed in exceptional circumstances, such as during snow-melt in spring time (Jalliffier-Verne et al., 2016). Differently, in Japan, in 2003, an amendment of "Enforcement Ordinance of Sewerage Law" related to CSO discharges abatement was issued defining the BOD5 concentration in the effluent overflow (<40 mg/L), allowing a provisional limit of 70 mg/L applicable until structure standards start to be applied. Small and midsize municipalities were obligated to implement improvements by 2013, large municipalities by 2023. Environment Protection Authority of South Australia issued a code of practice for wastewater overflow management giving a roadmap to the operators to comply with their environmental obligations. The water utility is obligated to implement an overflow abatement program, which encompasses an emergency response plan and short- and long-term measures to prevent or reduce the re-occurrence of overflows. However, in South Africa the policy related to runoff water disposal asserts that: "Urban stormwater discharged to the marine environment should not have any negative impact on the Environmental Quality Objectives of the receiving environment", it does not provide specification on treatment-at-source or land-based treatment, which are considered specific to disposal of stormwater runoff. Overall, different directives have been developed worldwide, which are mainly focused on the affirmation of the negative effects of the CSO events and allowed a number of overflows per year. Generally, the policymakers are revising and deriving the regulations to enforce authorities to take precautions and control CSO discharges. Although they pointed out the adverse impacts, in many countries no specific limits for water parameters have not been set to limit pollution from CSO discharges. This aspect is mainly related to the great variability in terms of quality and quantity of CSO characterization in the different sewer systems, previously described in Section 3.

Moreover, wide sampling campaigns and monitoring methods have to be implemented in order to quantify the hydraulic and the characterization conditions to support the legislation improvements. Finally, specific treatment technologies and control measures can be integrated into the regulations.

2.1.6 Innovative methods for CSO determination

Hydraulic conditions are the main factor to determine the proper method for monitoring CSOs. In Botturi et al. (2020) are displayed various methods used to estimate CSO volumes. Sensors and probes are also applied for monitoring purposes in most of the high-income countries, such as conductivity meters to detect occurrence and determine duration, level sensors with moderate and/or higher cost, advanced sensors (eg. UV–VIS) for also determining water quality. Where budget is limited, level sensors can be coupled with overflow equations to measure CSO volume. On the other hand, a level and a velocity sensor combined with flowmeters generate the most accurate/reliable data but require more investment cost and higher maintenance (Montserrat et al., 2013). The costs of data storage and high capacity computer systems are still an issue in CSO monitoring. Moreover, in heavy rain events, huge quantities of data must be processed and evaluated for every alarm situation in order to take immediate action (Bailey et al., 2016). The other point is the location of the CSO control system. The characteristics of the land can make the connection to the network difficult. A low-cost method was introduced by Montserrat et al. (2013) to detect the occurrence and duration of CSO events. The proposed method depends on the temperature changes between the sewer gas phase and the overflowing mixture of wastewater and storm water. Using temperature sensors for CSO detection has several advantages such as minimum capital cost, easy installation, requirement of minimum technical knowledge for integration, tolerance to extreme environmental conditions, and minimum maintenance. The authors also validated their systems and achieved detection greater than 80% of the total CSO occurrences, which showed that temperature differentiation during seasonal changes does not have a negative impact on effectiveness. However, physical features of the weir affect the detection performance. Later research, published in 2018, increased the robustness of the method proposed in Montserrat et al. (2013) by adding a second temperature sensor, improving the detection

accuracy by implementing an algorithm that accounted for the response time of the system and automatically calculated the duration of CSO events (Hofer et al., 2018). As a result, in a 7-month test phase, all 20 CSO events were recognized without false detections. Another group from France, recently developed a system called the DSM-flux (Device for Storm water and combined sewer flows Monitoring and the control of pollutant fluxes) to determine and control both the quantity and quality of CSO discharges (Maté Marín et al., 2018). The validated system can measure overflow volumes and pollutant concentration, decrease particulate pollutants from sedimentation and the erosive potential of overflows to the receiving waters. The advantages of installation of the DSM-flux system are: direct measurement at the overflow channel, installation downstream from the existing CSO structure, requirement of only one level measurement for determination of discharge values, not affected by inlet hydraulic conditions, reduced particulate pollutants and erosive potential of CSO discharges.

2.1.7 Smart CSO monitoring and control

Currently, smart network monitoring and smart data infrastructures (US EPA, 2018) are under development and application. These infrastructures are implemented in connection with a SCADA system and are mainly focused on real-time monitoring of flow rates (physically or with alternative methods) and effluent levels of CSO's with the aim of assessing potential flooding and pollution incidents. The final objective is to support decisions in real-time or quasi-real time about actions to be taken. For instance, SPRINT 226 a European project focused on the implementation of real-time sewer system control for eight European cities: Copenhagen (Denmark), Mantova (Italy), Verona (Italy), Genoa (Italy), Berlin (Germany), Vitoria-Gasteiz (Spain), Bolton (UK), and Goteborg (Sweden) (Entem et al., 1998). The project showed decent real-time control performance for overflow events of the sewer system in terms of prediction and generation of strategies to be taken into consideration (Entem et al., 1998). Another study (Seggelke et al., 2013) focused on real-time control of a CSS in a city in Germany with the aim of monitoring frequency of overflow events and investigating how to reduce them. In addition, Carbone et al. (2014) investigated a real-time control solution for an urban drainage network in Italy. It used an innovative and smart series of gates that

automatically adjusted themselves in order to optimize the storage capacity of a sewer system during rainfall events. Moreover, in the INTCATCH project, as an innovative approach to monitor water quality, autonomous and radio-controlled boats are developed and demonstrated in key catchments such as Lake Garda, Lake Yliki (Warner et al., 2018). The results revealed that monitoring the routine parameters can give an overview of the current status of the water body, as well as contribute to reducing the monitoring cost. Moreover, real-time monitoring of site-specific indicator allows determining the pollutant source which helps to derive proper catchment management strategy (Warner et al., 2018). The applications of smart data infrastructure systems can be optimized by two different methods. Whereas, the system improvements refer to increasing weirs, optimizing the efficiency curves or location of CSO control, the real-time control systems manage the operation of wastewater networks and facilities in real time (US EPA, 2018); grey (such as large concrete tanks or tunnels) and green strategies (such as bioretention facilities, green roofs, porous pavements, and stormwater planters) can be applied to control CSOs (De Sousa et al., 2012) and hybrid system of grey and green methods more advantageous than grey method-only in terms of economy, environment, and society (Gong et al., 2019). The control strategies can be optimized by hydrological model simulations supported with scenario analyses (Chen et al., 2019). In the USA, different approaches are integrated in different states to control and manage CSOs. In Philadelphia, the Water Department has a goal to reduce overflows (7.9 billion gallons of overflow water) by 2036. For this purpose, smart data technology was integrated into existing stormwater retention basins to monitor basin water level and precipitation and maximize the performance of the basin by real-time active control to selectively discharge from the basin during optimal times. On the other hand, 10 high frequency cleanout sites with remote field monitoring units were integrated in the San Antonio Water System (SAWS) in which day-to-day level trend changes can be detected by an analytical software giving data for potentially important changes in water levels. In the pilot locations, there were no sewer overflows in May/June 2016 with when nearly 16 inches of rain overwhelmed the SAWS. The real-time control system was adopted in Louisville in 1990s and actively used since 2006. The system prevents more than

1 billion gallons of CSO volume annually. In Indiana, there are 152 sensors located through the city of South Bend to maximize the capacity and performance of the city's collection system, which helped to reduce total CSO volume by roughly 70%, or about 1 billion gallons per year during the period 2008–2014. Moreover, in Greater Cincinnati, there are more than 200 CSO points, causing a discharge over 11 billion gallons of sewage into the Ohio River and its tributaries annually. One hundred and sixty-four (164) overflow points were integrated within the frame of the smart sewers network to date and sensors were installed through the watershed (US EPA, 2018). The monitoring technology should be pursued in the catchment base, and economical analysis should be carefully proceeded to decide to integrate the best smart strategy.

2.1.8 Innovative treatment alternatives

Different strategies are developed to reduce the impacts of CSOs, such as increasing storage capacity, detention/retention facilities, as well as sewer separation to fulfil the requirements of the related regulations (Figure 2.2).

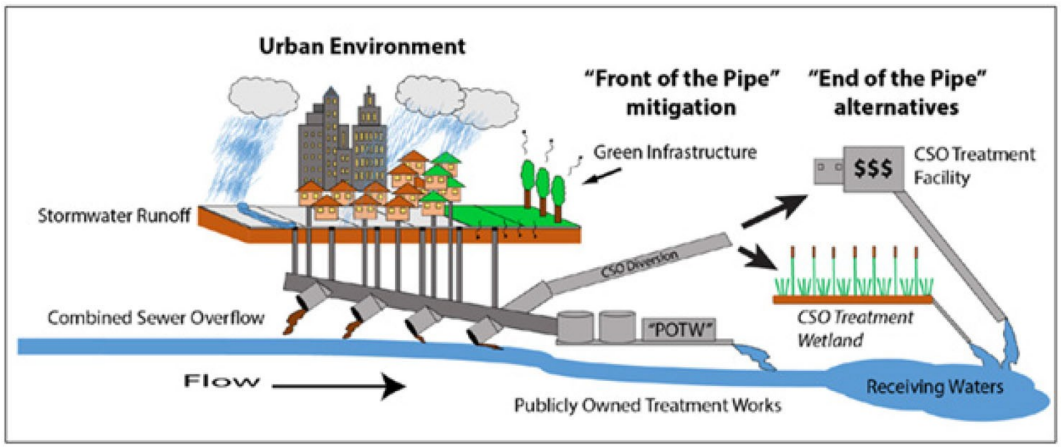

Figure 2.2 Management strategies for CSO (source: Levy et al. (2014)).

However, converting CSS into a separated system can be prohibitive due to cost and it does not always guarantee pollution reduction (Li et al., 2010). The latest information on treatment technologies, grouped as natural and technological treatment, and their performances in treating CSOs will be summarized in the following paragraphs.

2.1.8.1 Natural extensive treatments

Green infrastructure and nature-based solutions (NBS) use natural processes to contribute to the improved, sustainable management of water as well as enhancing

natural capital and biodiversity. Green infrastructure is recognized to deliver multiple benefits by combining continuous treatment of CSOs with additional services in terms of flood protection, increased biodiversity, climate change resilience, and recreational activities. There is growing recognition that green infrastructure are flexible, multipurpose alternatives to traditional, often costlier treatment solutions that can be applied in diverse wastewaters (Vymazal, 2011) including treatment of residential, municipal, and agricultural storm water and wastewater and urban run-off. They are incorporated into and promoted in Europe by the European Commission Strategy on Green Infrastructure (EC., 2013) and in the UK; an example is the London Environment Strategy (GLA, 2018). Green infrastructure is therefore an increasingly important possible solution for pollution mitigation. As well as being an environmentally friendly alternative, green infrastructures are flexible in terms of size, cost-effective and have a discrete layout (Fu et al., 2019). Of the green infrastructure techniques, constructed wetlands (CW) have a long history of wastewater treatment and have many applications for CSO treatment (Levy et al., 2014; Masi et al., 2017; Pálfy et al., 2018, 2016; Rouff et al., 2013; Tondera, 2019).

2.1.8.2 Technological compact treatments

Minimizing the negative impact of CSOs in the receiving waters can be achieved by in-line treatment methods such as settling without additives, which is the most commonly applied method, and chemical coagulation before discharge. Coagulation and flocculation are an effective method to remove organic materials with organic/inorganic polymers as coagulants and flocculants to get better sedimentation. In a study carried out by El Samrani et al. (2008), effects of different commercial coagulants – namely, ferric chloride solution (CLARFER) and aluminum salts (WAC HB) – were evaluated on turbidity and heavy metal removal from samples collected during rainy weather at the inlet of Boudonville retention basin. The results showed that both coagulants provided excellent removal of heavy metals; indeed, the concentrations of Cu, Zn, and Pb in the treated water complied with the water legislation. Regarding flocculation treating CSOs, Gasperi, Laborie, et al. (2012), Gasperi, Zgheib, et al. (2012) examined the performance of a full-scale ballasted flocculation unit (BFU) implemented at the bypass of the WWTP

located downstream of Paris on the Seine River. Ferric chloride (FeCl3) and anomic polymer were, respectively, used as coagulant and flocculant according to the turbidity levels entering BFU, and high surface area was achieved by microsand to enhance flocculation, assist flock formation, and act as ballast, which aids rapid settlement. The performance of the system was evaluated during the wet period, in which the bypassed combined sewage was treated only with BFU and bio-filtration in order to remove nitrogen, before discharge. Significant removal rates (>80%) were achieved for the compounds with a strong hydrophobic character (log Kow > 5.5) and removal rates of 50–80% were achieved for intermediate hydrophobic compounds (4 < log Kow < 5.5). On the other hand, low hydrophobic compounds (log Kow < 4) were poorly (<20%) to weakly removed (<50%). The authors concluded that it is a promising process to treat CSO waters in order to remove various compounds. Another possibility to remove very small particles or dissolved substances especially is by adsorption. Although Jung et al. (2015) investigated positive removal of micropollutants such as acetaminophen and naproxen (94.1% and 97.7%, respectively) from artificial combined sewage with biochar in a lab scale study, there is no application on a large scale yet, since removing the adsorbent from the wastewater matrix is difficult. Easier is the combination of a sand filter or vertical-flow CW containing an activated layer, such as investigated by Bester and Schäfer (2009). They evaluated the performance of an activated soil filter (bio filter) in order to eliminate diverse xenobiotics from combined sewage, storm water, and wastewater. The results indicated that the removal efficiency of organic micropollutants depends on the application of an organic layer in the filter, enabling higher removal efficiency. In a comprehensive study of sanitary sewer overflow treatment with fixed media biofilters, results showed that, all bioreactors can remove TSS, ammonia, and phosphorous effectively (Tao et al., 2010). Moreover, BOD5 reduction efficiency of 84 ± 9% can be reached with sand bioreactors. In another study, Kumordzi et al. (2016) focused on to remove the most abundant heavy metal, namely Zn2þ, in simulated CSOs by a composite catalyst of TiO_2 and Graphene under various process conditions such as pH, light intensity, catalyst loading, and light source in a lab-scale system. The adsorption and photo-reduction of Zn^{2+} enhanced with TiO_2-G under the solar spectrum. On the other hand,

adsorption is not the best solution in case of high clogging risk and water volume. Rotating belt filter is another option for CSO treatment in terms of their minimal footprint and also easier implementation (Gutierrez, 2015). Within the scope of INTCATCH Horizon2020 Innovation funded European project, a demo plant, with the aim of treating CSOs before their discharge into Garda Lake, was installed at Villa Bagatta. Additional aims considered the concept of technological innovation and public participation in integrated and smart management of water infrastructure and basins (Figure 3). The pilot plant has a compact modular design, composed of three mains sections: rotating belt filtration (RBF), filtration on granular activated carbon (GAC), and disinfection by UV treatment (Figure 4). Despite the fact that the processes used in this project used for decades for wastewater treatment, they have not been applied specifically for the treatment of CSO discharges. The plant can treat 54 m^3/h. The Rotating Dynamic Filter (Salsnes Filter, SF1000) accomplished the sieving of the CSOs through a mesh size of 350 mm and the retained solids are thickened using an embedded screw press unit, achieving a total solid concentration of 20–35%. The outlet CSOs is stored in an existing concrete open tank where it may be pumped up to 3.6 m^3/h to the GAC filtration system. Following the GAC system, is an ultraviolet disinfection unit with four modules (Trojan Technologies, UV3400K) installed in the open channel. Electrical conductivity, pH, and multiple parameters simultaneously derived by UV/Vis optical spectrometry (Intelligent Spectral Analyzer, ISA) are installed to monitor the system.

Data are gathered and transmitted to cloud computing which is also integrating sustainability evaluation and assessment tools in order to provide eco-efficiency indicators of the treatment and management system. The plant reached satisfactory removal efficiencies for TSS (90%), COD (69%), and *E. coli* (99%). However, further treatment is required for efficient nutrient removal in which TN and TP removal of around 41% and 19%, respectively (Botturi et al., 2020). The innovations of this project are its modular structure, compactness, rapid treatment, and resilience of the system which enables to re-shape of the configuration according to the treatment requirements. To sustain the safety of the water quality of receiving water bodies used for recreational purposes, microbial loads from

CSOs should be reduced. Since quality and quantity of CSOs are very variable, it is a challenge to find suitable disinfection technologies which can be operated spontaneously for a short period at full capacity. The most applied disinfection methods for the treatment of WWTP effluent are chlorine compounds, ozone, and ultra-violet (UV). However, these are not ideal for CSO treatment due to the high concentrations of solids and dissolved organic compounds: using chlorine compounds can lead to the formation of toxic, mutagenic, and carcinogenic chlorinate by-products (Bayo et al., 2009; Nurizzo et al., 2005). Undesirable by-products can also be the result when using ozone. Tondera et al. (2015) evaluated the effects of ozonation on diluted wastewater in a pilot-scale application. Although the reduction of pathogenic bacteria, viruses, and protozoan parasites was promising and more effective than UV irradiation for the tested conditions, the operation of an ozone generator under these conditions is difficult to manage and both installation and operation is costly. Suspended solids and turbidity in CSOs are also limiting parameters on the disinfecting effects of UV radiation (Tondera et al., 2015). In another study, Gibson et al. (2016) evaluated the effects of chemical pre-treatment of CSOs for subsequent UV disinfection. When applying 20 mg/L alum, the UV light transmission of the raw CSO increased from 30% to 60% after settling. The high charge density cationic polymer improved the removal of turbidity but did not affect UV transmittance (UVT) and TSS. The use of alum (metal coagulants) can achieve a UVT of 78%, while the use of cationic polymers reached a value of 60%. Pre-treatment to remove particles via CSO–CWs, as described above, not only increases the removal of microbial loads, but also allows reduction of dissolved parameters. In addition, no chemical addition is required, but space availability and installation costs are critical.

Alternative treatment with peroxy acids was investigated in several recent studies. Peracetic acid (PAA) requires a reaction time of several hours (Chhetri et al., 2014). The influence of particles on the removal efficiency gave controversial results: While Chhetri et al. (2016) found that bacterial reduction was more mostly efficient with a pre-treatment by particle separator and an additional coagulation with poly-aluminium-chloride, McFadden et al. (2017) could not find an effect of particle removal on the efficiency of CSO treatment with PAA. As an alternative to PAA,

performic acid (PFA) requires only a short contact time. Under real scale conditions, Chhetri et al. (2015) showed a reduction of 2.0 $\log_{10}$ of *E. coli* and 1.3 $\log_{10}$ of intestinal enterococci (contact time of 20 min, 8 mg/L min reduced approximately), and Tondera et al. (2016) proved additional reduction of coliform bacteria, Aeromonas spp. and *P. aeruginosa* with a $\log_{10}$ reduction between 1.8 and 2.9 (contact time of max. 30 min, 12–24 mg/L min). Additionally, a reduction of somatic coliphages with 2.7 ± 1.7 $\log_{10}$ could be shown. Another advantage of using PFA is that the commercially available reaction chamber providing PFA seems to be tolerant to long standstills, which can occur during dry seasons without CSOs.

2.2 Focus of this work

The principal goal of this work, within the European Project, was to demonstrate and verify the efficiency of a pilot plant for CSO treatment. Furthermore, the idea was to involve citizen science and make this environmental issue derived from the water pollution more evident.

2.3 Materials and methods

2.3.1 Villa Bagatta pumping station

The Villa Bagatta pumping station operated as shown in the Figure 2.3 The municipal wastewater coming from the pipeline, flowed into the “black water tank” where were placed four pumps (P1, P2, P3, P4, each with a nominal power of 18.5 kW), that pumped the wastewater for its further transport by gravity to the WWTP. Then, an underground “overflow tank” was implemented for the collection of the excess wastewater derived from the first tank. Inside the “overflow tank” there were two pumps (P5 and P6, each with a nominal power of 22 kW), which pumped the excess wastewater to an “overflow screening” for a preliminary degritting; then the treated wastewater was stored in another underground tank equipped with a pump (P9, with nominal power of 33 kW) for discharging the wastewater into the Lake through a pipeline with 1.3 km distance from the coast.

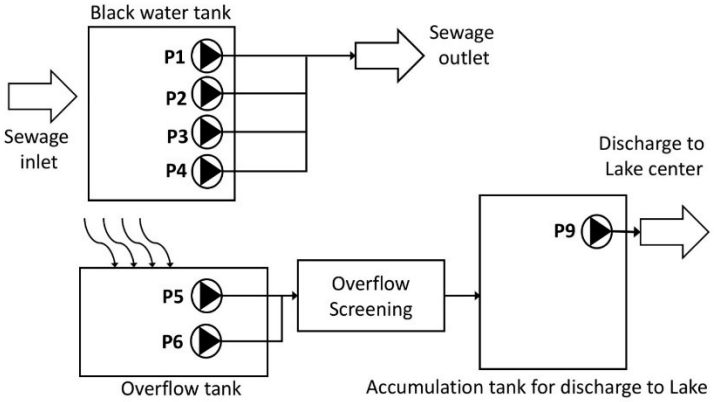

Figure 2.3 Villa Bagatta pumping station scheme.

2.3.2 Demo plant for CSOs treatment

In order to study and optimize the optimal CSO treatment, a demonstrative pilot plant was installed in a sensitive area near Lake Garda (Lazise, Verona, North of Italy, Figure 2.4). The sewage system of the municipalities around Lake Garda consists of a set of pipelines located in the ground and through the Lake, which collects mainly municipal wastewater, and carry them to the WWTP of Peschiera del Garda (Verona, North of Italy, project potential of 300.000 population equivalent, PE). In detail, in Lazise (Verona, North of Italy) where the demo plant was located, there is the pumping station of Villa Bagatta. The pumping stations are designed to handle wastewater that is fed from underground gravity pipelines and stored in an underground well, where electrical instrumentation is present to detect the level of wastewater.

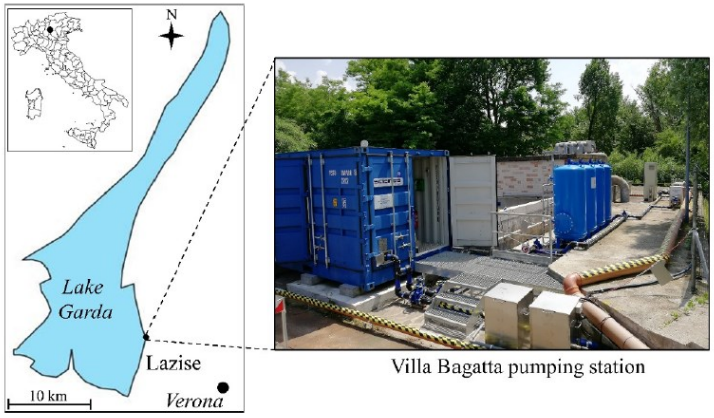

Figure 2.4 Demo plant location.

After several literature studies, the best treatment combination was projected and implemented at Villa Bagatta (Lazise, Verona, North of Italy); it consisted of (Figure 2.5):

- Dynamic rotating belt filter (RBF) for the removal of solids by a machine placed in a container provided by Salsnes (Norway);
- Adsorption treatment on granular activated carbon (GAC) consisting of four filters mounted on a skid;
- Disinfection with UV lamps provided by Trojan UV (Canada).

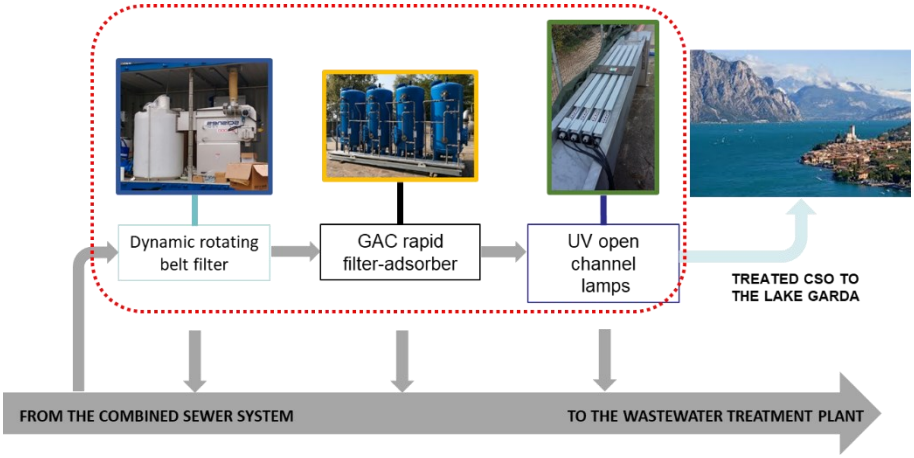

Figure 2.5 Schematic representation of the Villa Bagatta demo plant.

2.3.2.1 Dynamic rotating belt filter (RBF)

Figure 2.6 Dynamic rotating belt filter (RBF).

Dynamic RBF system (provided by Salsnes, Figure 2.6) is designed primarily for the TSS removal. It consists of continuous rotating filtration separating solids from liquids, sludge removal using an air knife, and a control power panel which supplies power and control to the system. It can accommodate filters with different mesh sizes. A wide range of mesh sizes have been tested for different samples taken on days with different weather conditions. The performance of the mesh filters has been compared based on the TSS removal percentage. In results, a mesh size of 90 µm was chosen for the filtration and the removal of TSS and COD have been analysed for different dilution factors.

2.3.2.2 Granular Activated Carbon (GAC) rapid adsorption

The adsorption system contains four filters each with 3.6 m^3/h capacity and an average contact time of 5 minutes (Figure 2.7). The first filter is a sand filter, the second one contains ST100 activated carbon and the last two ones consist of ST300 activated carbon. The system is able of working in different modes, either individually for each filter or with a combination of filters in parallel and series. Batch experiments have been carried out on the two types of granular activated carbons (ST100 and ST300) in order to investigate the performance of the filters. Soluble COD removal has been tested with carbon dosage of 2, 5, 10, and 20 g/l over time span of 3 h. Both equilibrium and kinetics modelling of the adsorption process have been studied to see the performance of GAC system.

Figure 2.7 Granular Activated Carbon (GAC).

Equilibrium of adsorption process could be modelled according to linear (Eq. 2.1), Freundlich (Eq. 2.2) or Langmuir (Eq. 2.3) isotherms with the following equations:

$$q_e = \frac{x}{m} = kC_e \qquad Eq.2.1$$

$$\frac{C_e}{q_e} = \frac{C_e}{q_0} + \frac{1}{q_0 k_l} \qquad Eq.2.2$$

$$\log\left(\frac{x}{m}\right) = \log\ (k_f) + \left(\frac{1}{n}\right)\log C_e \qquad Eq.2.3$$

Where k is the linear constant, k_l and q_0 are the Langmuir constants, k_f is the Freundlich constant, 1/n is a measure of adsorption capacity and intensity (Nayl et al., 2017), C_e is the equilibrium concentration of COD (mg/L) and x/m is the adsorption capacity (mg/L).

On the other hand, kinetics of the adsorption process has been modelled using the second-order kinetic model (Eq. 2.4):

$$\frac{dq_t}{dt} = k_2(q_0 - q_t)^2 \qquad Eq.2.4$$

Integrating this equation over time using t=0, q_t=0 and t=t, q_t=q_t as boundary conditions the following equation (Equation 2.5) is obtained for modelling the kinetics of the adsorption process:

$$\frac{1}{q_t} = \frac{1}{k_2 q_e^2} + \frac{1}{q_e}t \qquad Eq.2.5$$

The first filter (sand filter) was investigated individually and removal efficiency of different conventional parameters (TSS, COD, TKN, TP) was analysed. Then the whole system, including sand filter and the other 3 granular activated carbon filters, was set up in parallel and series and the performance of each mode has been observed.

2.3.2.3 UV disinfection

Figure 2.8 UV disinfection system.

UV disinfection system provided by Trojan Technologies (Figure 2.8), is the final step of the treatment that contains four modules each with four UV lamps. There is a control system connected to the UV sensor for controlling the intensity of the lamps. Several tests using various dilution factors have been carried out and the performance of the system was analysed for removal of *E. coli*.

2.3.3 Wastewater characterization during dry conditions

During the drafting phase of the experimental activities, the average composition of the wastewater collected in the pipeline in the east side of the Lake Garda during dry weather is defined. In August 2017, a sampling campaign was carried out two times a week for three weeks in order to have enough variability of wastewater characteristics. The analysis was performed for TSS, COD, TKN, TP, alkalinity and *E. coli*. In detail, the 18 raw wastewater samples were taken from 3 sampling points along the pipeline (as shown in Figure 2.9).

Figure 2.9 Points of the sampling campaign along the Garda Lake.

In the absence of real overflow events, the raw wastewater collected from the public sewers near the Lake Garda was diluted (1:3, 1:5, 1:10) with the Lake water in order to simulate different overflow conditions for the purpose of this study. The following table (Table 2.1) shows the characteristics of the collected raw wastewater and the Lake Garda water used for dilution.

Table 2.1 Characterization of raw wastewater, Lake water and the consequent simulated CSOs after dilution.

Parameter	Unit	Raw WW	Lake water	Simulated CSO		
				1:3	1:5	1:10
pH		7.55 ± 0.3	8.28 ± 0.93			
TSS	**mg/L**	270 ± 105	NA	90 ± 35	54 ± 21	27 ± 10
COD	**mg/L**	464 ± 171	5.3	158 ± 58	97 ± 36	51 ± 19
P-PO_4	**mg/L**	4.4 ± 1.7	0.011 ± 0.004	1.5 ± 0.6	0.9 ± 0.3	0.5 ± 0.2
TP	**mg/L**	7.2 ±1.8	0.008 ± 0.005	2.4 ± 0.6	1.5 ± 0.4	0.7 ± 0.2
N-NH_4	**mg/L**	65 ± 18	0.016 ± 0.012	21.6 ± 6.2	12.9 ± 3.7	6.5 ± 1.9
TKN	**mg/L**	78 ± 24	NA	26.3 ± 8.2	16.1 ± 5.0	8.3 ± 2.6
Alkalinity	**mg/L**	391 ± 55	137.2 ± 36.9	196 ± 27	157 ± 22	128 ± 18
E. coli	**CFU/100 ml**	1.83E+07 ± 7.26E+06	NA	6.1E+06 ± 2.4E+06	3.66E+06 ± 1.5E+06	1.83E+06 ± 7.3E+05

2.3.4 Experimental procedure

The performance of each process unit has been evaluated individually. Dynamic RBF was analysed in order to choose the best mesh size of the filter. This has been evaluated based on the TSS removal of the filter for each mesh size. The evaluation of sand filter and GAC was carried out using the whole system in parallel and in series. The sand filter itself has been considered individually as well. Finally, UV disinfection process was studied for the pathogen removal.

After this phase of the study, different scenarios with different combination of these process units have been simulated based on the obtained removal efficiencies of each unit and the performance of the scenarios have been investigated in terms of TSS, COD, soluble COD, TN, TP, P-PO_4 and E. *coli* removal efficiencies. All scenarios have been compared at the end to find the best scenario to treat CSO. Table 2.2 shows the configuration of different scenarios used in this study. Finally, the best-case scenario was applied to the real overflow event to evaluate the results in comparison with the simulated scenario. The real CSO samples were taken from

the Villa Bagatta station in the event of intense rain and the dilution factor was calculated based on the dry weather real concentrations and found to be 1:11, close to the highest dilution factor used in the simulation of heavy rain events (1:10).

Table 2.2 Different configurations for the CSO treatment process.

Scenario	RBF	Sand filter	GAC	UV
Scenario 0	-	-	-	-
Scenario 1	+	-	-	-
Scenario 2*	+	+	-	-
Scenario 2	+	+	+	-
Scenario 3*	+	+	-	+
Scenario 3	+	+	+	+
Scenario 4	+	-	-	+

2.4 Results and discussion

2.4.1 Single unit performance

2.4.1.1 Dynamic rotating belt filter (RBF)

Figure 2.10 shows the results of TSS removal for different mesh sizes of the filter. Although the average TSS removal of 75 µm filter was lower than the 90 µm, in some cases higher removal was also observed. It can be concluded that moving from 90 to lower size does not improve the filtration efficiency on average. Therefore, a 90 µm mesh size should be enough to obtain the desired level of TSS removal from the RBF system.

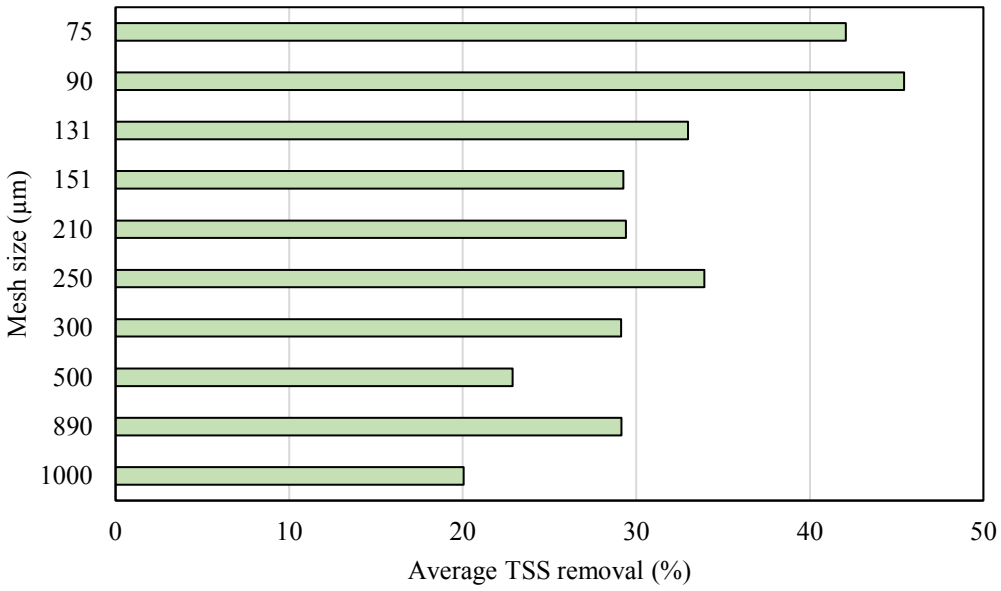

Figure 2.10 Average TSS removal efficiency for different filter mesh size in the dynamic RBF system.

Table 2.3 shows the TSS and COD effluent concentrations for the experiments with different dilution factors, having used the 90 µm mesh size for the filter and duration of 2–3 h. Obviously, the concentrations are still beyond the acceptable limits of the common water quality regulations, suggesting the need for further treatment of the CSO. It can be seen that at least 31% and 30% of TSS and COD removal respectively (for 1:10 that is the simulation of heavy rain events) can be achieved with RBF and this value would be increased to 45% and 39% in case of 1:3 dilution factor. Based on the influent concentration of TSS that was around 90 mg/L, the results of TSS and COD removal are in-line with the other studies using rotating belt filters (Razafimanantsoa et al., 2014).

Table 2.3 TSS and COD concentration at the inlet and outlet of dynamic RBF process.

Dilution		Treated water			Recovered sludge	
	Parameter	Influent (mg/L)	Effluent (mg/L)	Removal efficiency (%)	TS (%)	g/m^3 treated
1:3	TSS	84±6	47±14	45±13	27.2±0.5	23.4±2.2
	COD	119±3	72±15	39±14		
1:5	TSS	91±21	52±16	42±11	25.0±3.4	28.4±14.0
	COD	141±19	91±23	36±12		
1:10	TSS	90±49	62±35	31±4	26.1±0.2	32±13.4
	COD	143±72	101±23	30±12		

Franchi and Santoro (2015) suggested that the addition of polymer in upstream of the filter improves the flocculation and increase the TSS removal of the system considerably. This could be an additional step towards improvement of the result of dynamic RBF for CSO treatment. However, for remote areas such as Villa Bagatta it was not considered technically, practically and economically sustainable for operational issues. The water utility considered the use of chemicals as unfeasible and possibly of interest only for CSOs just before the WWTP, where operators can routinely intervene for maintenance and performance optimization.

2.4.1.2 Rapid filtration on GAC system

The Figure 2.11 shows the result of batch tests in terms of soluble COD removal and adsorption capacity (x/m) with different carbon dosage. CODs removal is increased with the increase of carbon dose. This might be related to an increase in total surface area of the activated carbon and consequently more active site available on the activated carbon for the adsorption of COD (Nayl et al., 2017).

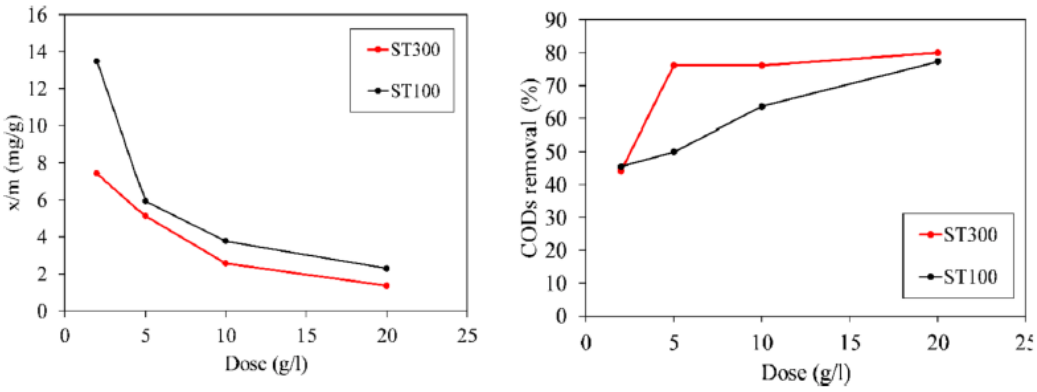

Figure 2.11 CODs removal and adsorption capacity of GAC filters with different carbon dosage.

The plot of t/qt vs time (Figure 2.12) shows that the second-order kinetic model fits well the experimental data.

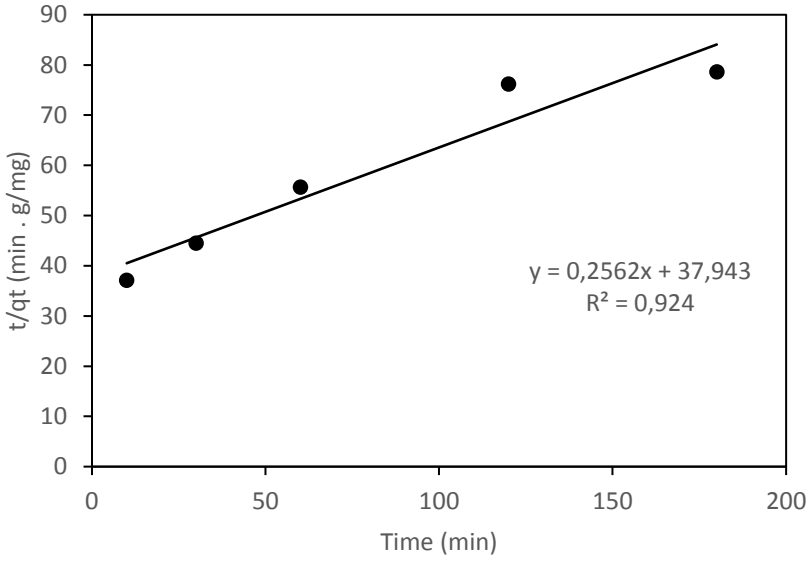

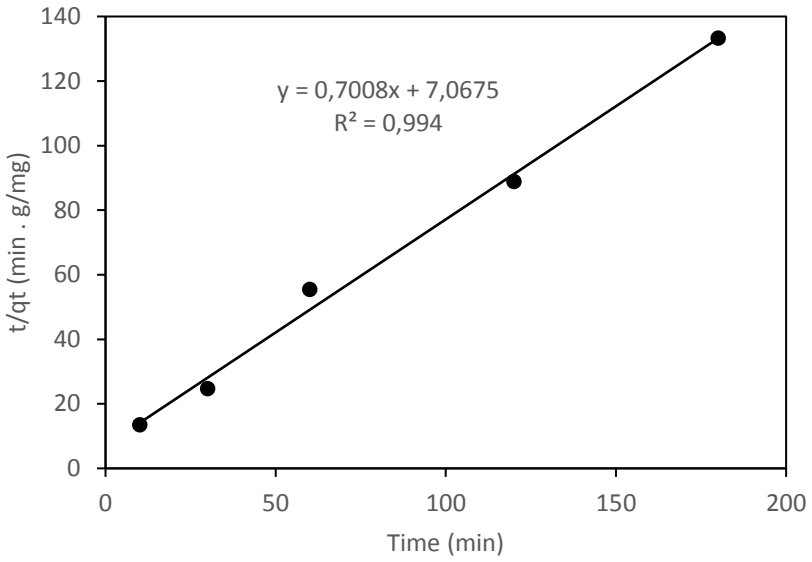

Figure 2.12 Second-order kinetic model of the adsorption process at 20 g/l carbon dose, up: ST100, down: ST300.

The calculated adsorption capacity (q_e) for the GAC ST100 and the GAC ST300 were 3.9 and 1.42 mg/g, respectively. While the second-order kinetic rate constant (k_2) for both carbon filter at dose of 20 g/L were: 1.73E-03 and 6.95E-02 for ST100 and ST300, respectively. The kinetic model could be used to predict the adsorption capacity of the GAC filters for COD removal. The results of equilibrium modelling show that Langmuir isotherm model fits well the experiments for ST100 filter, while none of the models fits considerably good the ST300 data (best results obtained with linear isotherm model, R2 ¼ 0.73). The results suggest that for ST100 filter, Langmuir isotherms can perfectly explain the adsorption process for CSO treatment. However, more experiments would be required for ST300 to obtain a better fit of the model. The results of TSS, COD, CODs, TKN and TP removal for the sand filter individually as well as their concentration in influent and effluent are presented in Table 2.4.

Table 2.4 Concentrations of conventional parameters at inlet and outlet of the sand filter.

Dilution	Parameter	Influent (mg/L)	Effluent (mg/L)	Removal efficiency (%)
1:3	**TSS**	81	31	62
	COD	182	102	44
	CODs	58	51	12
	TKN	28	24	13
	TP	5.2	3.9	25
1:5	**TSS**	38	11	92
	COD	79	42	47
	CODs	14	14	0
	TKN	15	10	32
	TP	6.5	6.5	0
1:10	**TSS**	33	2	99
	COD	72	41	43
	CODs	24	14	40
	TKN	8	2	79
	TP	5	3.9	23

The results demonstrate the sand filter is considerably effective for TSS and COD removal with 62–99% and 44–47% removal, respectively. However, it does not effectively remove the nutrients. The Table 2.5 shows the results of the whole GAC system in both parallel and series modality. In this case, the significant effect of the system on TSS and total COD removal still exists. The results suggest that the GAC system can remove TSS and total COD up to 94–97% and 50–55%, respectively, regardless of the system configuration that is in-line with other literatures (Aziz et al., 2011; Osman et al., 2013; Sanou et al., 2016; Sun et al., 2016). However, soluble COD removal is not very efficient, suggesting that most of the total COD removal is associated with the particulate form. COD fractionation of the municipal wastewater suggests that particulate slowly biodegradable COD and particulate inert COD account for 40–65% and 7–15% of total COD respectively (Ekama et al., 1986; Henze, 1992; Orhon and Cokgor, 1997; Pasztor et al., 2009). In case of wet weather, combined wastewater with stormwater could have substantially higher

particulate inert COD content up to 69% of total COD (Zawilsky and Brzezinska, 2009).

Table 2.5 Concentrations of conventional parameters at inlet and outlet of the GAC rapid adsorption in both parallel and series configurations.

Dilution	Parameter	Parallel			Series		
		Influent (mg/L)	Effluent (mg/L)	Removal efficiency (%)	Influent (mg/L)	Effluent (mg/L)	Removal efficiency (%)
1:3	TSS	51 ± 27	23 ± 10	68 ± 6	42	10	76
	COD	118 ± 56	74 ± 19	53 ± 10	89	65	26
	CODs	53 ± 7	44 ± 5	21 ± 10	56	56	0
	TKN	28	20 ± 3	28 ± 11	NA[a]	NA	NA
	TP	5.2	3.7 ± 0.6	29 ± 11	NA	NA	NA
1:5	TSS	25 ± 11	9 ± 3	91 ± 6	18	1	94
	COD	61 ± 16	49 ± 12	53 ± 12	56	38	32
	CODs	27 ± 11	15 ± 10	27 ± 36	37	37	0
	TKN	15	6 ± 3	57 ± 21	NA	NA	NA
	TP	6.5	5.9 ± 1.2	9 ± 19	NA	NA	NA
1:10	TSS	24 ± 9	5 ± 4	97 ± 3	14	1	93
	COD	60 ± 10	41 ± 11	55 ± 10	56	28	50
	CODs	27 ± 9	11 ± 6	52 ± 33	37	28	25
	TKN	8	5 ± 2	43 ± 25	NA	NA	NA
	TP	5.0	4.4 ± 1.2	12 ± 24	NA	NA	NA

[a] Not available.

Therefore, having the GAC adsorption in the CSO treatment line could substantially reduce particulate non-biodegradable and slowly biodegradable fractions of COD. The COD removal could be also affected by the pH of the solution and it will be higher in more acidic environments (pH around 5) comparing to the level of this experiment which is around 7–8 (El-Naas et al., 2010; Njoku and Hameed, 2011). This adsorption system, as expected is not very effective for nutrient removal and low removal rates confirm this. Although the data for nutrients are not available for the configuration in series, it is expected to obtain similar results to the parallel mode. This is mainly due to the short contact time of the adsorption that does not let the nutrients adsorption to increase very as much as it is required (Pan et al., 2011). Specific nutrients removal processes, such as chemical precipitation, are required to achieve higher removal rates. In general, average contact time of 5 min would be enough for each filter to achieve the TSS and COD removal percentages in the experiments which shows a great potential in terms of rapidness of the process since the conventional GAC treatments reported much longer contact times in order to achieve such high removal efficiencies (Sanou et al., 2016; Nayl et al., 2017).

2.4.1.3 UV disinfection

The final unit step of the treatment line, UV disinfection, showed high removal efficiencies of *E. coli* and total coliform in almost all the dilution cases with 20–30 s of contact time and 0.6–3.1 mW/cm^2 of intensity (Table 7). This is confirmed by

other studies that high intensity UV disinfection is very effective in removing coliform bacteria contaminants for meeting regulations of different effluents (Darby et al., 1993; Das, 2001; Neis and Blume, 2002; Do Couto et al., 2015). The surprisingly lower total coliform removal for 1:10 dilution factor could be related to measurement error of the effluent concentration and it is expected that in this case very high removal rate could be achieved as well. Therefore, this process is essential for removing coliform bacteria contaminants and needs to be considered in the treatment line. The Bathing Water Directive (EEC, 2006) has indicated a limit of 500 and 1000 CFU/100 ml for *E. coli* in inland waters corresponding to excellent and good quality status respectively. The experiments show that the effluents for the 1:5 and 1:10 dilution factors (100 CFU/100 ml) do not exceed this limit. Some studies reported that higher TSS concentration in the solution would affect the UV disinfection negatively by decreasing the disinfection rate and promoting the tailing effect (Liang et al., 2013; Qian et al., 2016; McFadden et al., 2017; Carré et al., 2018). Suspended particles, particularly those larger than 20 μm, provide protection to the bacteria during the disinfection process and will lead to a decrease in disinfection efficiency (Madge and Jensen, 2006). In this study, all the disinfection experiments have been carried out after dynamic RBF and either before or after GAC adsorption process. Consequently, some level of TSS removal (30–40%) was already achieved before disinfection process. However, a decrease in pathogen removals can be seen in the experiments without GAC adsorption prior to UV disinfection. The E. coli concentration in the final effluent after UV disinfection for the experiment with 1:3 dilution factor was obtained 4000 CFU/100 ml and 40000 CFU/100 ml with and without GAC pre-treatment respectively. This difference could be quite substantial in terms of meeting the regulations for discharging CSO in water bodies, although it is not very visible looking at removal % values (99.96% and 99.60% respectively).

2.4.2 Simulated treatment scenarios

The results of the scenario 0 in which no specific treatment step was applied, and the plant consists of the only existing coarse screening process showed no removal for any of the parameters as expected. In scenario 1 however, where only dynamic RBF was considered TSS and COD removal were observed with the average

removal percentage (among three dilution factors) of 38.9% and 34.9% respectively. Therefore, rotating dynamic filtration is not very effective if considered as the only unit for treatment. Moving to scenario 2* and 2, the effect of adding an adsorption unit is considerably visible. In both cases, TSS and COD removal were increased significantly and reached up to 91.1% and 64.2% respectively for scenario 2* and to 87.2% and 69.9% respectively for scenario 2. It can be concluded that the combination of RBF and GAC adsorption could lead to very effective TSS and COD removal for CSO streams. In addition, the removal of other parameters was observed in these two scenarios. CODs, TN, TP and PO_4–P average removals of 17.5%, 40.7%, 13.1% and 3.7% were achieved with scenario 2*, while these values for scenario 2 were 32%, 31.8%, 25.6% and 14.8% respectively. These results suggest that the RBF/GAC treatment system is not very effective on nutrients removal and further specific N and P removal processes would be required for meeting strict regulations on nutrient discharges in sensitive water bodies when it is necessary. The Table 2.6 summarizes the results of all the scenarios in terms of average removal for different dilution factors. The best results were corresponded to the scenario 3* and 3, in which a UV disinfection unit was added to scenario 2* and 2 configurations respectively. Comparing the results, as it is expected, no further significant improvement was observed on the TSS, COD, CODs, TN, TP, PO_4–P removal and the effect of UV disinfection process is mainly on the *E. coli* removal. The process was able to remove *E. coli* completely in all the cases. The result of the scenario 4 was very similar to scenario 1 (both with dynamic RBF and without sand filter/GAC) in terms of TSS and COD removal. On average, 39.4% and 34.9% were achieved respectively. The only difference is in *E. coli* removal which was achieved in scenario 4 with the addition of the UV disinfection unit. The *E. coli* removal in scenario 4 would not be probably achievable in real cases because of low TSS removal of the system. It is good to mention that even a slight decrease in removal % of *E. coli* could mean 10 times greater number of cells in the final effluent which is quite considerable for coliform bacteria. As it is expected, high TSS concentration would decrease the efficiency of disinfection process (Liang et al., 2013; McFadden et al., 2017). Therefore, in order to achieve

high *E. coli* removal both dynamic RBF and GAC adsorption would be required to remove TSS prior to disinfection process.

Table 2.6 Average removal efficiencies for different configurations of CSO treatment system.

	Scenario 1	Scenario 2*	Scenario 2	Scenario 3*	Scenario 3	Scenario 4
TSS	38.9±8.1	91.1±10.9	87.2±9.1	91.2±10.7	91.7±8.1	39.4±7.3
COD	34.7±4.8	64.2±3.0	69.9±1.4	64±3.4	69.9±1.4	34.9±4.7
CODs	0	17.5±21.1	32±18.0	18.4±20.5	32±19	1.2±1.0
TN	0	40.7±34.5	31.8±8.2	40.7±34.5	41.6±15.2	0
TP	0	13.1±12.5	25.6±10.0	13.1±12.5	18.9±8.9	0
PO_4-P	0	3.7±6.4	14.8±4.6	3.7±6.4	14.8±4.6	0
E. coli	0	0	0	100±0	100±0	99.9±0.2

2.4.3 Comparison of the scenarios

The Figure 2.13 shows the comparison of TSS, COD, CODs, TN, TP, PO4–P and *E. coli* removal at dilution factor 1:3 for all the scenarios. Looking at the results, significant TSS and COD removal can be achieved in the scenarios 2*, 2, 3* and 3. These are the ones with either sand filter or the whole GAC adsorption system. This suggests that only dynamic RBF is not enough for effective TSS and COD removal. Between these four scenarios, only 3* and 3 have the UV disinfection and consequently can remove *E. coli*. It can be concluded that the scenario 3 has the best results amongst all and it can perform efficiently for all dilution factors. Thanks to the UV disinfection process it can remove completely the *E. coli* out of the system and through the combination of RBF, sand filter and GAC it has the highest TSS and COD removal between all the cases. Although it shows highest nutrients removal of around 30%, still it is not very effective in that objective probably due to the short contact time in the adsorption process and as mentioned before, specific nutrient removal and recovery processes are required in combination of this treatment line for that purpose.

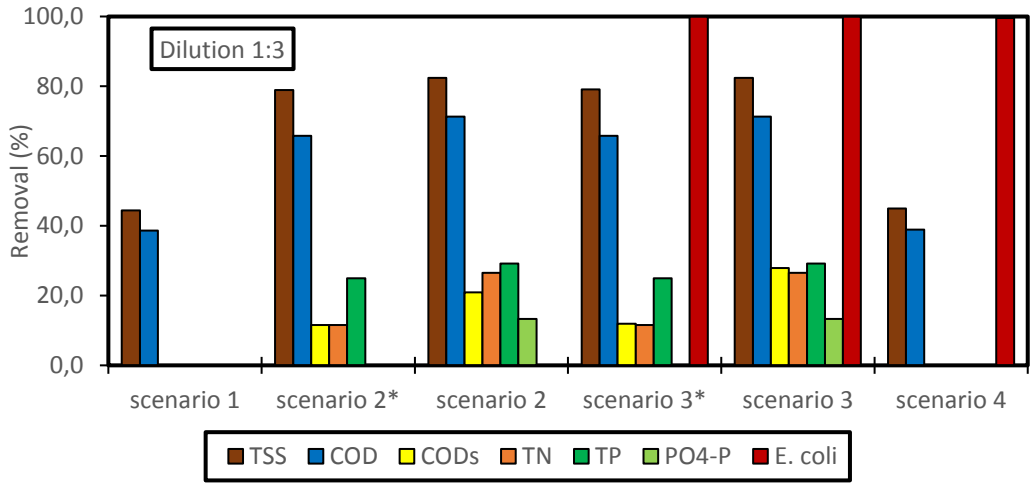

Figure 2.13 Removal efficiencies comparison between different treatment scenarios at 1:3 dilution factor.

2.4.4 Effect on dilution on TSS and COD removal

Changing the dilution factor of the samples will result in various initial concentration of the parameters. The result of dynamic RBF single unit treatment showed that TSS and COD removal decreases with the increase of dilution factor that means a decrease in initial concentration of TSS and COD in the influent. Higher initial concentration means higher solids and organic matter available to be retained by the mesh and form the filtration cake. On the other hand, the treatment with only sand filter demonstrated that the TSS removal increased with the increase of dilution factor (decrease of the initial concentration). This could be dependent on the fact that the ratio of the initial adsorbate molecules to the available adsorption sites increases with the higher initial concentration and consequently there will be lower removal efficiency (Devi et al., 2008). In the case of COD removal, an increase was observed moving from high to medium dilution followed by a slight decrease from medium to low dilution. This behaviour could be associated to the saturation of the filter that decreases the above-mentioned ratio at certain point. The whole GAC adsorption system showed that COD removal generally increased with the decrease of dilution factor that could be due to the increase of driving forces (Devi et al., 2008) and to the fact that at lower concentrations free sites are less accessible on adsorbent surface (Tazerouti and Amrani, 2009). TSS removal results were similar to the results of sand filter treatment and increased with the increase of initial concentration. Considering the treatment scenarios, scenarios 1 and 4 which include only the RBF process have similar results to the RBF single unit that

is TSS and COD removal increase with the decrease of the dilution factor. Scenario 2* and 3* that have RBF in combination with sand filter have significantly higher TSS removal at higher dilution factors according to the result of single unit process of sand filter. Although, in these scenarios the removal at lower dilution factor is also considerably higher than single unit process. In addition, for the COD removal they behave the same as the single unit process with an increase from high to medium dilution and then a decrease from medium to low. However, these changes are less visible in these scenarios that are affected also with the result of dynamic RBF. For scenarios 2 and 3 with RBF, sand filter and GAC adsorption, TSS removal still behaves the same and increases with dilution factor accordingly. However, COD removal is constantly increasing from high to low dilution factor that could be due to the effects of all three treatment steps together.

2.4.5 Validation through real CSO treatment

Scenario 3, which had the best overall results, was applied for treating the real CSO samples taken from Villa Bagatta station in the intense rain event. The real event has been recorded only once during 2 years at the Villa Bagatta pumping station. During the event the pumping station was activated 3 times for 1.5–4.5 h. The treatment plant achieved TSS, total COD, soluble COD and TP removal of around 95%, 88%, 78% and 25% respectively that was comparable to the simulated event of heavy rainfall (97.8%, 55.3%, 52.7% and 14.3% respectively for 1:10). *E. coli* was also removed with 99.96% removal percentage that is quite the expected result based on the simulated events with the UV disinfection process.

2.5 Conclusion

The innovative compact pilot plant implemented in this study for advanced treatment of CSOs achieved high removal efficiencies for various contaminations particularly for TSS, COD and *E. coli*. Although, each unit process has been previously applied for wastewater treatment, they have not been used for treating CSOs particularly in presented small size and innovative configuration. Franchi and Santoro (2015) investigated the use of dynamic RBFs for primary treatment and showed that between 30 and 70% TSS removal could be achieved depending on the mesh size and influent TSS concentration. In addition, 20–40% BOD removal could also be obtained. This could be very beneficial for the subsequent biological

treatment in terms of reducing power consumption in aerobic stage. Razafimanantsoa et al. (2014) obtained similar results for municipal wastewater. However, the use of these filters specifically for CSOs has not been investigated. Given the highly diluted nature of CSOs, 38.9% and 34.7% average TSS and COD removal have been achieved in this study. The addition of sand filter/GAC adsorption has increased the average TSS and COD removal to 91.7% and 69.9% respectively. These results are quite significant given the short contact time of filtration/adsorption which is about 5 min on average. Similar removal efficiencies have been observed in studies using sand filter (Mulligan et al., 2009; Paredes et al., 2016) and GAC adsorption (Huggins et al., 2016; Paredes et al., 2016; Tee et al., 2016) for COD and TSS, however, the contact time is substantially higher in conventional filtration/adsorption studies. UV disinfection is an attractive alternative to chemical disinfection processes (Yang et al., 2014; Song et al., 2016) due its lower operational costs and lack of toxic by-products (Paredes et al., 2018). Nearly complete removal of *E. coli* has been achieved in this study using UV disinfection with 20–30 s contact time. In terms of nutrients removal (N and P), the results show relatively moderate to low removal efficiencies. 41.6% and 18.9% average removal efficiencies have been achieved for total N and total P respectively. This is not surprising since most effective methods for nutrients removal and recovery are either biological or chemical (Batstone et al., 2015; Daneshgar et al., 2018; Monfet et al., 2018) in which up to more than 90% removal could be achieved. Depending on the N and P load in the raw wastewater and the characteristics of the overflow event, this could be problematic since high discharge of nutrients in the water bodies will have negative effects in the form of eutrophication phenomenon (Pan et al., 2018). Therefore, a further possible improvement could be the addition of a chemical precipitation process for increasing nutrients removal and at the same time recovering them in the form of valuable products such as struvite, calcium phosphate, iron phosphate, etc. However, this would add to the operational cost of the treatment process. The final *E. coli* concentration is 375 CFU/100 ml that is under the limit of the “excellent” and “good” status of Bathing Water Directive (EEC, 2006) for inland and coastal waters respectively (500 CFU/ 100 ml). TSS and total COD concentrations in the

final treated water were 8 and 24 mg/L, respectively. Although, in the BWD there is no specific limit defined for the TSS and COD concentrations, the obtained values meet the Urban Waste Water Directive (EEC, 1991) that defines the TSS and COD limits of 35 mg/L and 125 mg/L O_2 respectively in the discharge of wastewater treatment plants. These results validate the performance of the treatment system obtained through the simulated CSO events for a real case scenario and suggest the potential of its application as a specific CSO treatment solution for the sensitive areas that require the reduction of contaminants for water bodies discharges. Different CSO control strategies are available including treatment, conveyance, off-line storage, sewer separation and inflow reduction. Not much data is available for the cost of each control strategy. However, some reports have given some approximations. Hernandez-Sancho et al. (2015) reports average investment costs of separate sewerage system in Walloon region of Belgium to be 865 €/m compared to combined system which is 395 €/m. EPA (2007) reported that the cost of sewer separation, as the most expensive approach in many cases, could be approximately between 10000 and 50000 \$/1000 m^2 of area that is being subjected to the separation procedure. Conventional physical/chemical treatment could cost between 530 and 790 \$/m^3 of water being treated (EPA, 2007). Iglesias et al. (2010) reported 28–48 €/m^3 day of establishment costs for physical/chemical treatment with filtration and disinfection in Spain while this cost is about 9–22 €/m^3 day for only filtration and disinfection treatment. Another study reports a 4.63\$/m^3 cost of sewer separation and physical/chemical treatment for a case study in Washington, USA (Harrison and Kasthuri, 2012). The preliminary results of the cost assessment for the proposed compact treatment plant in this study suggests that using dynamic RBF and GAC adsorption would lead to a cost of at least 1.2 €/m^3, which is substantially lower than sewer separation or physical/chemical treatments even with further addition of UV disinfection cost. The energy consumption of dynamic RBF is about 0.11 kWh/m3 that is much lower than 0.4–0.7 kWh/m^3 for conventional treatments in Italy (Guerrini et al., 2017) although considering the GAC and UV disinfection process this consumption will be higher. Obviously, this assessment is highly site-specific and is carried out for the case of Villa Bagatta pumping station that experiences very low number of overflow events during the year. Nonetheless, it

could give an idea that the compact CSO treatment plant could be potentially an attractive approach for water utilities in small catchments as an economic CSO control strategy. An advanced compact treatment approach has been proposed in this study to treat the CSO discharging into the Lake Garda in Italy. The performance of the system has been evaluated for removal of conventional wastewater parameters and coliform bacteria contamination. The system showed high average removal of 91.7%, 69.9% and 100% for TSS, COD and *E. coli* respectively while moderate efficiencies for nutrients removal (41.6% for N and 18.9% for P) have been achieved. Further chemical processes, such as precipitation, could be applied to improve nutrients removal for meeting regulations. The compactness, rapidness and modularity of this treatment system, makes it an attractive solution for water authorities and utilities dealing with the CSO contaminations. This study showed the great potential of proposed treatment system specifically used for CSO in order to meet the regulations on water qualities discharging into natural water bodies.

Reference

Al Aukidy, M., & Verlicchi, P. (2017). Contributions of combined sewer overflows and treated effluents to the bacterial load released into a coastal area. *Science of the total environment*, *607*, 483-496.

Anne-Sophie, M. H., Dorner, S. M., Sauvé, S., Aboulfadl, K., Galarneau, M., Servais, P., & Prévost, M. (2015). Temporal analysis of *E. coli*, TSS and wastewater micropollutant loads from combined sewer overflows: implications for management. *Environmental Science: Processes & Impacts*, *17*(5), 965-974.

Bailey, J., Harris, E., Keedwell, E., Djordjevic, S., & Kapelan, Z. (2016). The use of telemetry data for the identification of issues at combined sewer overflows. *Procedia engineering*, *154*, 1201-1208.

Bayo, J., Angosto, J. M., & Gómez-López, M. D. (2009). Ecotoxicological screening of reclaimed disinfected wastewater by Vibrio fischeri bioassay after a chlorination–dechlorination process. *Journal of Hazardous Materials*, *172*(1), 166-171.

Bester, K., & Schäfer, D. (2009). Activated soil filters (bio filters) for the elimination of xenobiotics (micro-pollutants) from storm-and waste waters. *Water research*, *43*(10), 2639-2646.

Botturi, A., Ozbayram, E. G., Tondera, K., Gilbert, N. I., Rouault, P., Caradot, N., ... & Foglia, A. (2020). Combined sewer overflows: A critical review on best practice and innovative solutions to mitigate impacts on environment and human health. *Critical Reviews in Environmental Science and Technology*, 1-34.

Brzezińska, A., Zawilski, M., & Sakson, G. (2016). Assessment of pollutant load emission from combined sewer overflows based on the online monitoring. *Environmental Monitoring and Assessment*, *188*(9), 502.

Buerge, I. J., Poiger, T., Müller, M. D., & Buser, H. R. (2006). Combined sewer overflows to surface waters detected by the anthropogenic marker caffeine. *Environmental science & technology*, *40*(13), 4096-4102.

Diaz-Fierros T. F., Puerta, J., Suarez, J., Diaz-Fierros V. F. (2002). Contaminant loads of CSOs at the wastewater treatment plant of a city in NW Spain. *Urban Water*, *4*(3), 291-299.

EurEau, (2016). Combined Sewer Overflows A Challenge for Policy Makers and the Water Sector, Storm Water Overflows Commission Study. European Commission, Directorate General for Environment Unit C.2 - Marine Environment & Water Industry.

Field, R. (1985). URBAN RUNOFF: POLLUTION SOURCES, CONTROL, AND TREATMENT 1. *JAWRA Journal of the American Water Resources Association*, *21*(2), 197-206.

Gasperi, J., Garnaud, S., Rocher, V., & Moilleron, R. (2008). Priority pollutants in wastewater and combined sewer overflow. *Science of the total environment*, *407*(1), 263-272.

Gasperi, J., Laborie, B., & Rocher, V. (2012a). Treatment of combined sewer overflows by ballasted flocculation: Removal study of a large broad spectrum of pollutants. *Chemical Engineering Journal*, *211*, 293-301.

Gasperi, J., Sebastian, C., Ruban, V., Delamain, M., Percot, S., Wiest, L., ... & Gromaire, M. C. (2014). Micropollutants in urban stormwater: occurrence, concentrations, and atmospheric contributions for a wide range of contaminants in three French catchments. *Environmental Science and Pollution Research*, *21*(8), 5267-5281.

Gasperi, J., Zgheib, S., Cladière, M., Rocher, V., Moilleron, R., & Chebbo, G. (2012b). Priority pollutants in urban stormwater: Part 2–Case of combined sewers. *Water Research*, *46*(20), 6693-6703.

Hnaťuková, P. (2011). Geochemical distribution and mobility of heavy metals in sediments of urban streams affected by combined sewer overflows. *Journal of Hydrology and Hydromechanics*, *59*(2), 85-94.

Heinz, B., Birk, S., Liedl, R., Geyer, T., Straub, K. L., Andresen, J., ... & Kappler, A. (2009). Water quality deterioration at a karst spring (Gallusquelle, Germany) due to combined sewer overflow: evidence of bacterial and micro-pollutant contamination. *Environmental Geology*, *57*(4), 797-808.

Jotte, L., Raspati, G., & Azrague, K. (2017). Review of stormwater management practices. *Klima 2050 Report No*, *7*.

Kistemann, T., Schmidt, A., & Flemming, H. C. (2016). Post-industrial river water quality—Fit for bathing again?. *International Journal of Hygiene and Environmental Health*, *219*(7), 629-642.

Krebs, P., Holzer, P., Huisman, J. L., & Rauch, W. (1999). First flush of dissolved compounds. *Water Science and Technology*, *39*(9), 55-62.

Launay, M. A., Dittmer, U., & Steinmetz, H. (2016). Organic micropollutants discharged by combined sewer overflows–characterisation of pollutant sources and stormwater-related processes. *Water research*, *104*, 82-92.

Levy, Z. F., Smardon, R. C., Bays, J. S., & Meyer, D. (2014). A point source of a different color: Identifying a gap in United States regulatory policy for "green" CSO treatment using constructed wetlands. *Sustainability*, *6*(5), 2392-2412.

Masi, F., Rizzo, A., Bresciani, R., & Conte, G. (2017). Constructed wetlands for combined sewer overflow treatment: ecosystem services at Gorla Maggiore, Italy. *Ecological Engineering*, *98*, 427-438.

McBride, G. B., Stott, R., Miller, W., Bambic, D., & Wuertz, S. (2013). Discharge-based QMRA for estimation of public health risks from exposure to stormwater-borne pathogens in recreational waters in the United States. *Water Research*, *47*(14), 5282-5297.

McFadden, M., Loconsole, J., Schockling, A. J., Nerenberg, R., & Pavissich, J. P. (2017). Comparing peracetic acid and hypochlorite for disinfection of combined sewer overflows: Effects of suspended-solids and pH. *Science of the Total Environment*, *599*, 533-539.

Mell, I. C. (2010). *Green infrastructure: concepts, perceptions and its use in spatial planning* (Doctoral dissertation, Newcastle University).

Metcalf, L., Eddy, H. P., & Tchobanoglous, G. (1979). *Wastewater engineering: treatment, disposal, and reuse* (Vol. 4). New York: McGraw-Hill.

Metcalf, L., Eddy, H. P. (2014). *Wastewater engineering: treatment and resource recovery,* fifth ed. McGraw-Hill Education, New York, NY, USA.

Montserrat, A., Gutierrez, O., Poch, M., & Corominas, L. (2013). Field validation of a new low-cost method for determining occurrence and duration of combined sewer overflows. *Science of the total environment*, *463*, 904-912.

Nielsen, P. H., Raunkjær, K., Norsker, N. H., Jensen, N. A., & Hvitved-Jacobsen, T. (1992). Transformation of wastewater in sewer systems–a review. *Water Science and Technology*, *25*(6), 17-31.

Nurizzo, C., Antonelli, M., Profaizer, M., & Romele, L. (2005). By-products in surface and reclaimed water disinfected with various agents. *Desalination*, *176*(1-3), 241-253.

Pálfy, T. G., Meyer, D., Troesch, S., Gourdon, R., Olivier, L., & Molle, P. (2018). A single-output model for the dynamic design of constructed wetlands treating combined sewer overflow. *Environmental Modelling & Software*, *102*, 49-72.

Passerat, J., Ouattara, N. K., Mouchel, J. M., Rocher, V., & Servais, P. (2011). Impact of an intense combined sewer overflow event on the microbiological water quality of the Seine River. *Water research*, *45*(2), 893-903.

Phillips, P., & Chalmers, A. (2009). Wastewater Effluent, Combined Sewer Overflows, and Other Sources of Organic Compounds to Lake Champlain 1. *JAWRA Journal of the American Water Resources Association*, *45*(1), 45-57.

Phillips, P. J., Chalmers, A. T., Gray, J. L., Kolpin, D. W., Foreman, W. T., & Wall, G. R. (2012). Combined sewer overflows: an environmental source of hormones and wastewater micropollutants. *Environmental Science & Technology*, *46*(10), 5336-5343.

Riechel, M., Matzinger, A., Pawlowsky-Reusing, E., Sonnenberg, H., Uldack, M., Heinzmann, B., ... & Rouault, P. (2016). Impacts of combined sewer overflows on a large urban river–Understanding the effect of different management strategies. *Water research*, *105*, 264-273.

Scheurer, M., Heß, S., Lüddeke, F., Sacher, F., Güde, H., Löffler, H., & Gallert, C. (2015). Removal of micropollutants, facultative pathogenic and antibiotic resistant bacteria in a full-scale retention soil filter receiving combined sewer overflow. *Environmental Science: Processes & Impacts*, *17*(1), 186-196.

Sandoval, S., Torres, A., Pawlowsky-Reusing, E., Riechel, M., & Caradot, N. (2013). The evaluation of rainfall influence on combined sewer overflows characteristics: the Berlin case study. *Water science and technology*, *68*(12), 2683-2690.

Suarez, J., & Puertas, J. (2005). Determination of COD, BOD, and suspended solids loads during combined sewer overflow (CSO) events in some combined catchments in Spain. *Ecological Engineering*, *24*(3), 199-217.

Viviano, G., Valsecchi, S., Polesello, S., Capodaglio, A., Tartari, G., & Salerno, F. (2017). Combined use of caffeine and turbidity to evaluate the impact of CSOs on river water quality. *Water, Air, & Soil Pollution*, *228*(9), 330.

Willems, P., & Olsson, J. (2012). *Impacts of climate change on rainfall extremes and urban drainage systems*. IWA publishing.

Xu, Z., Wu, J., Li, H., Chen, Y., Xu, J., Xiong, L., & Zhang, J. (2018). Characterizing heavy metals in combined sewer overflows and its influence on microbial diversity. *Science of the Total Environment*, *625*, 1272-1282.

3 Recovery of high-added value microbial cells rich in polyhydroxyalkanoates (PHAs) to be used for industrial applications

This chapter describes a project related to the recovery of high added value biomass using fermented waste, for possible industrial applications. Part of this chapter derived from the following publication:

Botturi, A., Battista, F., Andreolli, M., Faccenda, F., Fusco, S., Bolzonella, D., ... & Frison, N. (2021). Polyhydroxyalkanoated-Rich Microbial Cells from Bio-Based Volatile Fatty Acids as Potential Ingredient for Aquaculture Feed. *Energies*, 14(1), 38.

List of abbreviations

CDM	Cell Dry Mass
COD	Chemical Oxygen Demand
sCOD	Soluble Chemical Oxygen Demand
CSTR	Continuous Stirred Tank Reactor
D	Dilution rate
HAc	Acetic Acid
HPr	Propionic Acid
HRT	Hydraulic Retention Time
MCL	Medium Chain Length
MLSS	Mixed Liquor Suspended Solids
MLVSS	Mixed Liquor Volatile Suspended Solids
MMC	Mixed Microbial Culture
OD	Optical Density
OLR	Organic Loading Rate
P	Productivity
PHA	Polyhydroxyalknoate
PHB	Polyhydroxybutyrate
PHB–HV	Polyhydroxybutyrate-hydroxyvalerate
SCFA	Short chain fatty acid
TKN	Total Kjeldahl Nitrogen
VFA	Volatile Fatty Acid
WWTP	Wastewater Treatment Plant
X	Active biomass
Y_{PHA}	PHA Yield
Y_X	Biomass Yield

3.1 Introduction

As described in the General Introduction, polyhydroxyalkanoates (PHAs) are polyesters that are accumulated as energy and carbon storage by several type of bacteria. This class of bacteria includes both bacteria able to produce PHAs during the growth phase (so with a nutritionally balance growth medium) and under limitation of nutrients (so called accumulation phase). From the industrially point of view, PHAs can be produced both with pure bacterial cultures and mixed microbial cultures (MMCs). Below, some information about pure and mixed cultures.

3.1.1 PHA production by pure culture bacteria

Using pure culture for biotechnological application is a well-recognized and wide studied method for industrial production of several compounds. Also, for the PHA production at industrial scale, the use of pure culture (both wild-type and recombinant) is the most applied method. As an example, *Ralstonia eutropha* (or *Cupriavidus necator*) is the main strain used for industrial production of PHA. Companies like Tianan Biologic Materials (China), PHB industrial (Brazil), and Mitsubishi gas chemicals (Japan) are some of those are producing commercial polymers from *Ralstonia eutropha* (Poltronieri and Kumar, 2017). Anyway, the use of pure culture for PHA production is affected by high production cost. One of the principal contributors to the high cost is related to the use of high purity substrates with high market price (such as glucose, maltose, sucrose or other sugar based compounds such as corn), which is reported to account for around 45% of the total production cost (Kourmentza et al., 2017). Consequently, the research activities are mainly focused on the use and the valorisation of waste, developing bioprocesses for bioproducts recovery (Kourmentza et al., 2017). Some examples are reported in Alsafadi and Al-Mashaqbeh (2017), where several haloarchaea are tested for PHA production capacity using olive mill wastewater; spent coffee grounds and cheese whey (Kucera et al., 2018); or wheat bran and digested potato waste (Van-Thuoc et al., 2008). Generally, food waste is the primary candidate as carbon source for PHA production, since is widely available and inexpensive. In the field of PHA production, it is possible to choose a specific class of bacteria basing on the type of waste available; in case of waste rich in carbon and nutrients, it is better to select

growth associated PHA producers (such as *Alcaligenes latus* and *Paracoccus denitrificans*); on the contrary, in case of substrate that lack an essential nutrient (such as nitrogen or phosphorous) PHA accumulation using non-growth associated bacteria may be preferable, as an example *Cupriavidus necator*. However, it is important to set up a nutrient feeding strategy in order to obtain a balance between cellular growth and polymer formation (Valentino et al., 2013). This evaluation derived mainly from which product is to be achieved and in which industrial market it is commercialized.

3.1.2 PHA production by mixed microbial culture (MMC)

PHA production using MMCs is a well-studied process. The production process is usually divided into the following phases:

- Substrate pre-treatment, in order to make the substrate more available;
- Separation unit in solid and liquid fraction. The solid fraction can be used for biogas production while the liquid fraction is usually used for acidogenic fermentation to increase the concentration of the volatile fatty acids (VFAs) which are the main PHAs precursors;
- Selection process, usually with *feast/famine* regime, in order to remove those bacteria which are not able to store PHAs;
- Accumulation stage, in order to obtain the maximum PHA storage and recovery.

The use of MMC and waste as feed represent a good alternative from the economical point of view. Nowadays, the production of PHA via MMCs is increasingly considered as an integrated part of the wastewater treatment plants (WWTPs, Tamis et al., 2014; Sagastume et al., 2016).

Besides the production of biogas through anaerobic digestion in the WWTPs, other technologies with the aim of producing higher-value end-products can be taken into consideration, with an interesting economical value (Crutchik et al., 2020).

The transition to circular bioeconomy is an important method for try to convert waste stream to bio-based products that can be reused for several applications in several industrial sectors (Mohan et al., 2019).

3.1.3 Polyhydroxyalkanoates possible industrial applications

PHAs and biomass enriched in PHAs can have different applications, besides the substitution of petroleum-based materials in the bioplastic sector. It is well recognized that PHAs represent a great opportunity for polymer industry because they are biodegradable and with properties very similar to the traditional plastic. PHAs can be used also in other fields such as agricultural, medical, feed/food industry. As far as the medical field is concerned, PHAs were used for implants, drug carriers, tissue engineering, biocontrol agent, inhibitors of cancerous growth and memory enhancing molecules (Kalia, 2019). PHAs have also the potential to meet the requirements for packaging material, due to their properties and permeability (Chen 2010; Wang and Chen, 2017). Specifically, in Albuquerque and Malafaia (2018) it is reported that copolymers of PHA having high hydroxyvalerate and medium chain length (MCL) PHA content can have more interesting properties due to the high flexibility. Furthermore, and this is an interesting and less know application, it is described in Defoirdt et al. (2009) that PHAs may have beneficial effects in the metabolism of some animals. As an example, it is well known that short-chain fatty acids (SCFAs, like formic, acetic, propionic, butyric, valeric and lactic acid) exhibit antimicrobial activity (Huang et al., 2012; Bergeim, 1940; Van Immerseel et al., 2003; Defoirdt et al., 2006) as well as positive effect on the gastrointestinal health of animals (Defoirdt et al., 2009). However, currently SCFAs smell bad, characteristic that make them not easily usable in the food/feed sector. So, Defoirdt et al. (2009) reported some evidence about the possible application of PHAs (which are polymers of β-hydroxy SCFAs, and they do not smell bad) as a novel biocontrol agent as well, when they are degraded in the gut. It is also reported that the addition of SCFAs in brine shrimp larvae in an environment with pathogenic *Vibrio campbellii*, significantly decrease the number of death larvae, indicating the possible utilization of SCFAs also in aquaculture (Defoirdt et al. 2009). Laranja et al. (2017) demonstrated the protective effect of PHB accumulating bacteria on Penaeus monodon larvae on exposure to pathogenic *Vibrio campbelli*. It is also reported in Wang et al. (2019) the use of PHB as feed additive for large yellow croaker fish. The study demonstrated that the fish can grow faster and gain more weight if PHB is added in the concentrations of 1% and 2%. It is also reported that polyhydroxybutyrate (PHB) can be used as a feed additive in

the animal feed, showing nutritional value and prebiotic effects in chicks, sheep, pigs, fish and prawns (Boon et al., 2013; De Schryver et al., 2010; Forni et al., 1999a,b; Najdegerami et al., 2012; Nhan et al., 2010). Boon et al. (2010) have patented the use of PHB as animal feed additive; they found that compounds of PHB as well as strains able to produce PHB have a good modulation effect on the gut flora of animals by releasing SCFA, specifically butyric acid; furthermore, they found antibacterial capacity in the gastro intestinal tract against *Vibrio*, *E. coli* and *Salmonella*. Furthermore, Suguna et al. (2014) designed a study to assess the immunostimulatory effect of poly-hydroxybutyrate-hydroxyvalerate (PHB–HV) extracted from *Bacillus thuringiensis* B.t.A102 on the immune system of fishes like *Oreochromis mossambicus*.

3.2 Focus of this work

The EU Green Deal is a complex plan wanted by the EU Commission in order to fight the climate change. More in detail, the EU Commission aims to reach carbon neutrality by 2050. In this context, the heart of the EU Green Deal is the Farm to Fork strategy which aims to reach a fair, healthy and environmentally friendly food system. This chapter has the target to try to start this path, with new researches and applications of biomasses.

Consequently, this research has the aim to study and optimize a PHA production process using a pure strain selected for its ability to store PHA, and waste stream in order to reduce the overall cost derived from the pure feeding substrate utilization.

Furthermore, preliminary attention was also given in the future possible application of the biomass thus recovered. As described above, the PHA industrial applications ranging in different fields; the focus of this research is related to the application in the feed/food sector. Indeed, this goal is also described and detailed in the last chapter (Chapter 4).

3.3 Materials and methods

3.3.1 Strain isolation

The PHA-producing bacterium used in this study was named as *Thauera* sp. Sel9. The strain was isolated from a MMC selected for PHA production at pilot scale. Five sludge samples (10_2018a, 10_2018b, 11_2018, 04_2019, 06_2019) from the

pilot plant located in Carbonera (Treviso, north of Italy) and described in Conca et al. (2020), were taken, processed and analysed for determine the microbial composition. The total bacterial DNA was extracted from the biomass and the 16S rRNA was sequenced (analysis performed by Eurofins Genomics). The analysis of microbial population was performed using the R studio software.

From the MMC, different bacterial strains were isolated and tested with the PHA staining test (as described below). The strains which showed a positive result were, thus, processed and identified through sequencing analysis. One of these strains showed a 99% of similarity to *Thauera butanivorans* NBRC 103042T. This strain, hereinafter *Thauera* sp. Sel9, was thus used for the following test.

3.3.2 Synthetic media

Several batch tests were performed using flasks under continuous agitation (150 rpm). The flasks were inoculated with the strain, previously isolated. The test was carried out with synthetic medium in order to determine the optimal concentration of VFA as chemical oxygen demand (COD). Three VFA concentrations were tested: 0.5, 1 and 2 g COD-VFA/L. Synthetic media with a ratio of acetic acid/propionic acid of 70:30 were used. The synthetic media were prepared as described in the Table 3.1 Synthetic media composition.**Errore. L'origine riferimento non è stata trovata.**. All the salts were obtained from Sigma-Aldrich. All the media tested were sterilized by autoclaving for 20 min at 121 °C (Raypa, steam sterilizer, AES series). A filtration method with a membrane at 0.22 µm of mesh size was also tested. All the tests were conducted under agitation and at the temperature of 30°C. The pH was always adjusted at around 8.

Table 3.1 Synthetic media composition.

Compound	Unit	0.5 g COD-VFA/L	1 g COD-VFA/L	2 g COD-VFA/L
CH_3COONa	g/L	0.74	1.49	2.99
CH_3CH_2COONa	g/L	0.13	0.26	0.51
$NH_4(HCO_3)$	g/L	0.28	0.54	1.00
K_2HPO_4	g/L	0.05	0.05	0.05
$MgSO_4 \cdot 7H_2O$	g/L	0.20	0.20	0.20
$CaCl_2 \cdot 2H_2O$	g/L	0.66	0.66	0.66

3.3.3 Bio-based VFA from candy wastewater fermentation

In order to test the growth performance of the strain on bio-based VFAs, a fermentation liquor derived from candy wastewater was used. The liquor derived from a lab-scale fermentation reactor with a volume of 3 L. After fermentation the liquor was centrifuged (using a centrifuge from Eppendorf model 5810 R) and the resulting supernatant was used as a feedstock for the following tests.

The liquor was then diluted in order to obtain the final concentration of 1, 2.5 and 5 g COD-VFA/L. Since it was an industrial medium, it did not maintain the same properties along the time. Before use, the diluted liquor was sterilize following the same procedure described for synthetic medium in the section 3.3.2. Ammonium chloride (NH_4Cl) and phosphoric acid (H_3PO_4) were added when it was necessary in order to provide the correct nutritional balance.

At the beginning of each test, *Thauera* sp. Sel9 was grown in an adaptation medium made with the fermented liquor diluted to 1 g COD-VFA/L and with the addition of 2.5 g/L of yeast extract and 0.5 g/L of peptone (both of them were provided by Sigma Aldrich).

3.3.4 Continuous stirred-tank reactor (CSTR)

After the batch tests performed in synthetic media, continuous tests were made in a continuous stirred-tank reactor (CSTR). The CSTR used for the experiments is shown in the Figure 3.1**Errore. L'origine riferimento non è stata trovata.**. A CSTR is a perfectly mixed vessel that works in a steady state condition to carry out different reaction. In a CSTR there are no differences in temperature, concentration, or reaction rate, so the output of the reactor has the same composition of the biomass inside the reactor.

Since there is an input and an output in continuous processes, the operating volume is always constant. The main advantages of continuous operation are reduction in the capital cost (operation with higher productivity), reduction in operating cost (labour and energy) and improved control on the process. In this context, a CSTR was chosen for its standardized characteristics that were ideals for have a good control on a pure culture process. Indeed, a CSTR can guarantee growth of microorganisms under defined conditions, that will lead to high control of the process and, in the same time, high productivity and, above all, a constant product

quality (Koller and Braunegg, 2015). Since the reactor is operated at steady state conditions (accumulation=0), the following equation show the biomass balance in a CSTR:

$$Q * X - Q * X_0 = V * r_x \qquad Eq.3.1$$

Where Q is the flow rate (L/h), X is the biomass concentration in the output (g/L), X_0 is the biomass concentration in the influent (g/L), V is the reactor volume (L) and r_x is the biomass production rate (g/Lh).

Actually, no biomass is present in the influent of the reactor, so X_0=0; the reaction will be like the Eq. 3.2:

$$Q * X = V * r_x \qquad Eq.3.2$$

Since r_x is calculated as shown in the following equation (Eq. 3.3), the overall balance will be like the Eq. 3.4.

$$r_x = \frac{dX}{dt} = \mu * X \qquad Eq.3.3$$

$$Q * X = V * \mu * X \qquad Eq.3.4$$

Where μ represents the specific growth rate (h^{-1}). In a CSTR the μ is equal to the dilution rate (D, which is equal to 1/HRT, hydraulic retention time), so the previous equation can be expressed as the following:

$$\mu = \frac{Q}{V} \qquad Eq.3.5$$

Since the Monod model is expressed with the following equation (Eq. 3.6), final equation will be as (Eq. 3.7):

$$\mu = \frac{\mu_{max} * S}{K_M + S} \qquad Eq.3.6$$

$$HRT = \frac{1}{\mu_{max}} + \frac{K_M}{\mu_{max}} * \frac{1}{S} \qquad Eq.3.7$$

Where S is the substrate concentration (g/L), μ_{max} is the maximum specific growth rate (1/h) and K_M is the Michaelis constant (L/g).

Figure 3.1 On the left continuous stirred tank reactor (CSTR). On the right CSTR operating with aeration and stirring at 30°C.

In a chemostat or a CSTR, the biomass productivity (P) is optimal when (Eq. 3.8):

$$D_{opt} = \mu_m(1 - \sqrt{\frac{K_s}{K_s+S_0}}) \qquad Eq.\ 3.8$$

Where D_{opt} is the maximum cellular productivity (h^{-1}) and S_0 is the initial substrate concentration (g/L).

3.3.5 Test in continuous with bio-based VFAs

The CSTR used in this experiment had a working volume of 1 L and was operated at 30 °C under pressure. The system was equipped with a peristaltic pump for the substrate feeding in sterile conditions (as shown in the Figure 3.1). The effluent was collected in a becher through a tap.

At the beginning of each test, the reactor was fed with the adaptation medium (described in 3.3.3) and then *Thauera* sp. was inoculated. The growth stage in the adaptation medium was settled in 48-72 hours at 30°C with continuous stirring. After adaptation, every subsequent day the following tests were carried out on the reactor effluent: optical density (OD), pH, mixed liquor suspended solids (MLSS), mixed liquor volatile suspended solids (MLVSS), cell dry mass (CDM), VFA, COD and soluble COD (sCOD) and ammonia.

The following Table 3.2 shows the experimental periods analysed in this chapter.

Table 3.2 Experimental period with CSTR and bio-based VFA.

Parameter	Unit	Period I	Period II	Period III	Period IV	Period V	Period VI
HRT	d	4	2	1	0.5	1	1
VFAs	g COD-VFA/L	1	1	1	1	5	2
OLR	g sCOD/Ld	0.9	2.1	4.9	10.1	28.9	14.3
COD/N	-	19	26	27	28	12	15
sCOD	g COD/L	3.5	4.2	4.9	5.1	28.9	14.3
NH_4-N	g/L	0.18	0.16	0.18	0.18	2.44	0.97
PO_4-P	g/L	-	-	-	-	0.45	0.04
Volume	L	1	1	1	1	1	1
pH	-	7.5	7.8	7.8	8.0	7.5	7.7
Temperature	°C	30	30	30	30	30	30

3.3.6 Analytical methods

The VFA analysis were performed with ion-chromatography analysis by using the system Thermo Fisher Dionex ICS-1100. The other analyses were performed following the standard method for water analysis (Van Loosdrecht et al., 2016; APHA, 1998).

The Total Kjeldahl Nitrogen (TKN) was also monitored during the best operating conditions following the standard method for water analysis (Van Loosdrecht et al., 2016; APHA, 1998). Then, the obtained value was multiplied by the factor 6.25 in order to indirectly calculate the content of proteins (Jones et al., 1942).

The PHAs extraction and quantification were performed following the procedure reported in Braunegg et al. (1978). For PHA staining test, Nile Blue A dying (provided by Sigma Aldrich) was used according to the procedure reported in Ostle and Holt, 1982.

The microbial growth was monitored by measuring the optical density (OD) at 600 nm using a spectrophotometer; furthermore, the colony forming units (CFU) analysis was also performed in order to monitor the growth. The OD and the CFU

were determined following the procedures described in Van Loosdrecht et al. (2016).

3.3.7 Calculations

Contents of PHA were calculated as percentage of TS on a mass basis (%PHA = g PHA/g TS∗100). Active biomass (X) was calculated as g X = g MLVSS–g PHA. The active biomass is also expressed as COD_X, multiplying the active biomass by the factor 1.42 g COD/g X.

The yields of PHA (Y_{PHA}) and the yield of active biomass (Y_X) were calculated by dividing the amount of PHA produced or biomass produced by the total amount of COD-VFA removed or sCOD consumed, respectively.

In this work the VFA concentration is always referred to COD-VFA and it is expressed as mg COD-VFA/L. The fermented wastewater was mainly composed by acetic acid (HAc), propionic acid (HPr) and butyric acid (HBt).

3.4 Results and discussion

3.4.1 Strain isolation

The microbiological characterization of a MMC deriving from a PHA-selection reactor was performed during one-year period. In detail 5 representative samples were analysed (10_2018a, 10_2018b, 11_2018, 04_2019, 06_2019) in terms of genera and families composition. The microbial community structure is an important factor in the yield of PHA and, furthermore, in the type of PHA produced. Several researches have investigated the microbial composition of biomass selected for PHA production using different molecular techniques (Sruamsiri et al., 2020; Woraittinum et al., 2017; Huang et al., 2018; Dionisi et al., 2005; Ciesielski et al., 2014). In this work the 16S rRNA sequencing was performed on all samples.

As it is possible to see from the Figure 3.2, the three main genera selected in the samples 11_2018 and 4_2019 were *Thauera*, *Paracoccus* and *Pseudoxanthomonas*. All the three genera are Gram-negative bacteria and belonging to the phylum Proteobacteria. *Thauera* and *Paracoccus* have frequently been detected in MMC selected for PHA production (Albuquerque et al., 2012; Carvalho et al., 2014; Huang et al., 2018; Coats et al., 2016). *Pseudoxanthomonas* is less reported in the MMC for PHA production, however it was observed the presence of the PHA

synthase subunit gene in the complete genome of *Pseudoxanthomonas suwonensis* which suggesting that might have PHA production capability (Woraittinun et al., 2017).

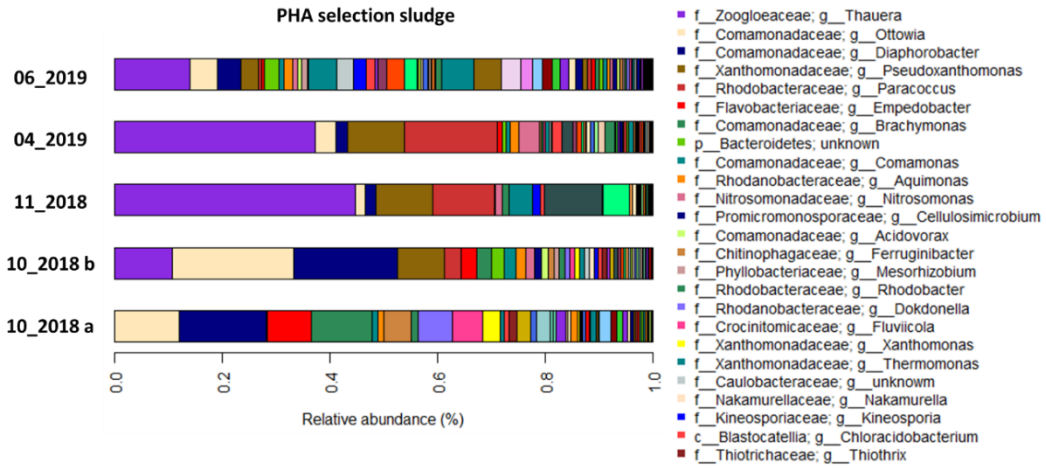

Figure 3.2 Bar plot of the microbial composition of the MMC samples. The graph shows the relative abundance of the microbial genera. Abundances were normalized to the total number of sequences. The 25 most abundant families and genera are displayed in the legend.

From this biomass several strains were isolated in order to be tested as single strain in PHA production processes. The staining test with Nile Blue A was used for screening; the bacteria resulted positive after the screening were analysed by 16S

RNA sequencing and compared with literature data. The Table 3.3 shows the results obtained after the sequencing.

Table 3.3 Bacterial strains sequenced derived from the MMC biomass for PHA recovery.

Closest bacterial strain	Accession number	Identity (%)	Class
***Sphingobacterium* sp. D1**	KU668559	99	Sphingobacteriia
***Flavobacterium mizutaii* DSM 11724T**	AJ438175	99	Flavobacteriia
***Shinella granuli* Ch06T**	AY995149	97	Alphaproteobacteria
***Flavobacterium macrobrachii* an-8T**	FJ593904	96	Flavobacteriia
***Thauera butanivorans* NBRC 103042T**	BCUG01000113	99	Betaproteobacteria
***Diaphorobacter oryzae* RF3T**	EU342381	98	Betaproteobacteria
***Brevundimonas diminuta* ATCC 11568T**	GL883089	99	Alphaproteobacteria
***Corynebacterium xerosis* ATCC 373T**	LAYS01000008	100	Actinobacteria
***Chryseobacterium haifense* H38T**	EF204450	97	Flavobacteriia

After several literature studies, *Thauera* sp. was selected as a model organism in the pure culture test described below.

Several papers reported a high abundance of this strain in biomass enriched in PHA. Some examples are: Sruamsiri et al. (2020) where *Thauera* sp. reached around 50% of relative abundance and, this 50%, constituted 80% of the total PHA accumulating cells; in Colpa et al. (2020), it is reported an increasing of *Thauera aminoaromatica* MZ1T from 24 to 40% after two months of enrichment process of the MMC. In Lemos et al. (2008) RT-PCR approach was used for biomass characterization revealing the identification of mainly 4 genera of bacterium that were the most abundant, among which *Thauera* sp. Furthermore, in Jiang et al. (2011) it is reported that the predominant genera in MMC for PHA production are *Plasticicumulans acidivorans* and *Thauera selenatis.*

The strain that showed a 99% similarity with *Thauera butanivorans* NBRC 103042T (from here referred to as "*Thauera* sp. Sel9") was thus grown in a specific medium and then stored in a cryogenic tube for further analysis and tests.

3.4.2 Batch-test on synthetic medium rich in VFAs

In order to test the growth trend of *Thauera* sp. Sel9 in the presence of VFAs, several batch tests were performed using synthetic VFA, as acetic acid (HAc) and propionic acid (HPr), with HAc:HPr ratio of 70:30. Three concentrations of COD-

VFA were tested: 0.5, 1 and 2 g COD-VFA/L. Each test was carried out for 168 h. In order to monitor the growth and to determine the best conditions for *Thauera* sp. Sel9's growth, OD, CFU and CDM were analysed during the time. Furthermore, VFA consumption as well as ammonia were analysed. Finally, PHA concentration was analysed in order to estimate the yield and to evaluate the active biomass growth (X). The OD parameter was not taken into account because it was not representative due to the formation of floccules in the growth media. The floc formation is also reported in batch culture of *Thauera aminoaromatica* described in Colpa et al. (2020).

The CFU analysis was thus used for monitoring the growth with the 3 different COD concentrations (Figure 3.3).

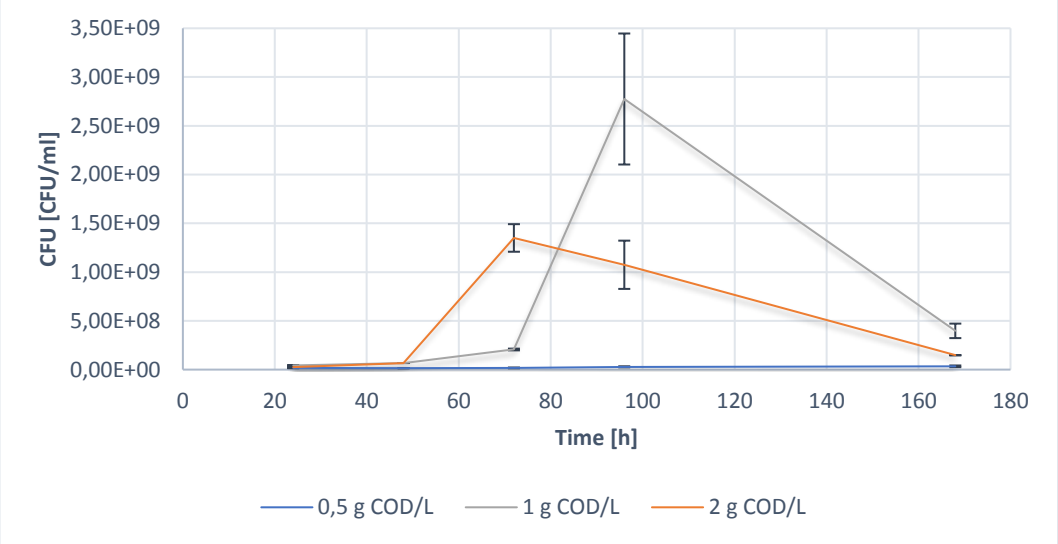

Figure 3.3 CFU trend in the synthetic test using Thauera sp. Sel9.

The Figure 3.4 shows the ammonia consumption and the CDM production over the time for all the COD concentrations tested. The ammonia removal rate was 70.9%, 69.8% and 53.2% for 0.5, 1 and 2 g COD-VFA/L respectively. While the VFAs utilization was 100% for all the test, with the only difference that for 0.5 g COD-VFA/L this removal rate was occurred after 24 h, for 1 g COD-VFA/L after 48 h and for 2 g COD-VFA/L after 96 h.

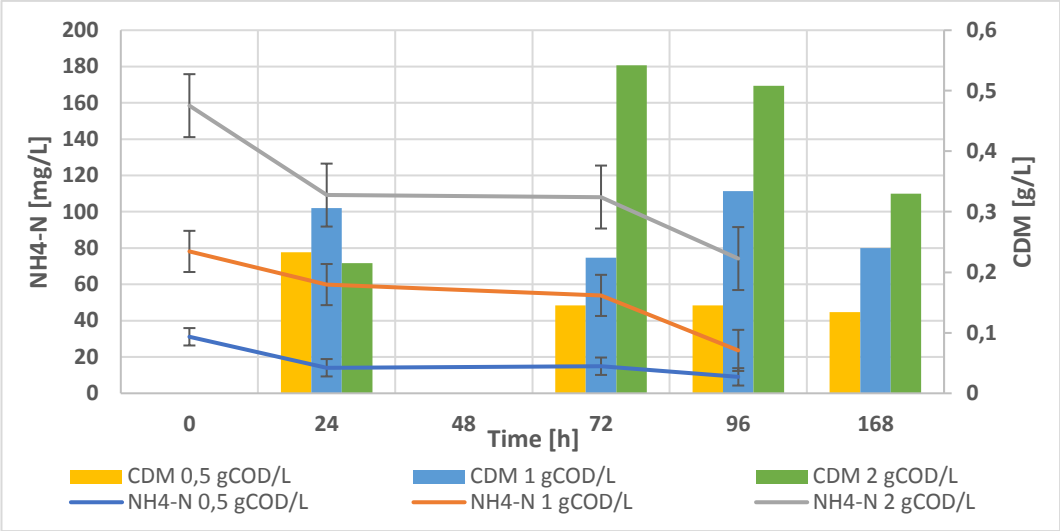

Figure 3.4 Ammonia consumption and CDM production in each test over the time.

The PHA extraction and quantification were also performed over the time of the growth phase in order to determine the strain's ability to produce PHA in the settled conditions and in order to calculate the active biomass (X). Furthermore, the growth yield (Y_X) and the PHA production yield (Y_{PHA}) was thus calculated. The Table 3.4 shows the results obtained. The PHA content was detected during the growth phase; indeed, the accumulation test was not performed with synthetic media. Considering the PHA content for the calculation of the active biomass (X) produced and considering the VFA consumed, the biomass growth yield (Y_X) was calculated. After 24 h a value of 0.42 g X/g VFA consumed was obtained for 0.5 g COD-VFA/L; in the same test, a value of 0.29 g X/g VFA consumed was obtained after 96 h. In the test with 1 g COD-VFA/L after 24 h and after 96 h the yields of 0.19 and 0.28 g X/g VFA consumed were obtained, respectively. A lower value (0.19 g X/g VFA consumed) was obtained for the test with 2 g COD-VFA/L after 96 h. As the main objective of this study is to estimate the growth performance of a pure culture on VFA, the yields for PHA production were not take in consideration. In literature it is reported a value of 0.34 g X/g COD consumed during the enrichment stage of PHA producing bacteria in case of MMC (Fernandez-Dacosta et al., 2015). It is also reported a yield of 0.36 g X/g VFA in Basset et al. (2016). Therefore, the yields here obtained are still low if compared with other studies with MMC, and further optimizations are warranted.

Table 3.4 Maximum biomass and PHA yield with different COD-VFA concentrations.

g COD-VFA/L	Y_X	Y_{PHA}
	g X/g COD-VFA	g PHA/g COD-VFA
0.5	0.42	0.04
1	0.28	0.03
2	0.19	0.07

3.4.3 Test in continuous with bio-based VFAs in real fermented substrate

The subsequent tests were performed in continuous using the CSTR system described in the Section 3.3.4 and inoculated with *Thauera* sp. Sel9; real fermented wastewater from candy industry was used as feeding. The substrate characterization is described in the Section 3.3.3. The substrate was, then, opportunely diluted and added to the reactor in order to obtain the desired conditions. The effect of different growth rates was evaluated at the steady-state conditions applying four different hydraulic retention time (HRT, 4, 2, 1 and 0.5 days) within the CSTR system as described in the Section 3.3.5 during six different periods. The Figure 3.5 shows the trend of sCOD removal efficiency during the different periods. The following picture (Figure 3.6) shows the same trend in relation to the organic loading rate (OLR) applied.

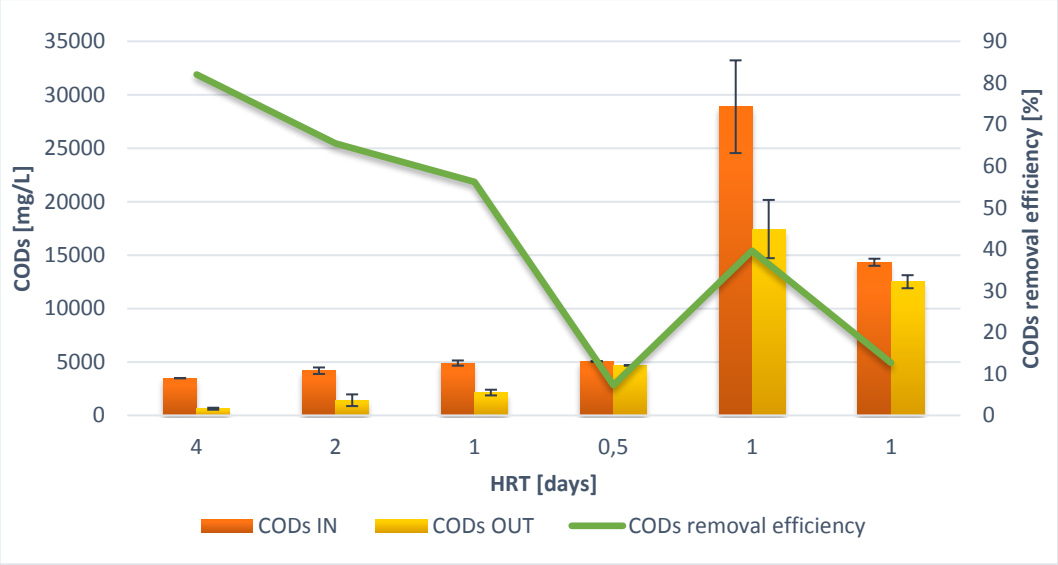

Figure 3.5 CODs removal efficiency trend in relation to the different HRT applied in the CSTR. The bars indicate the CODs in the influent and in the effluent.

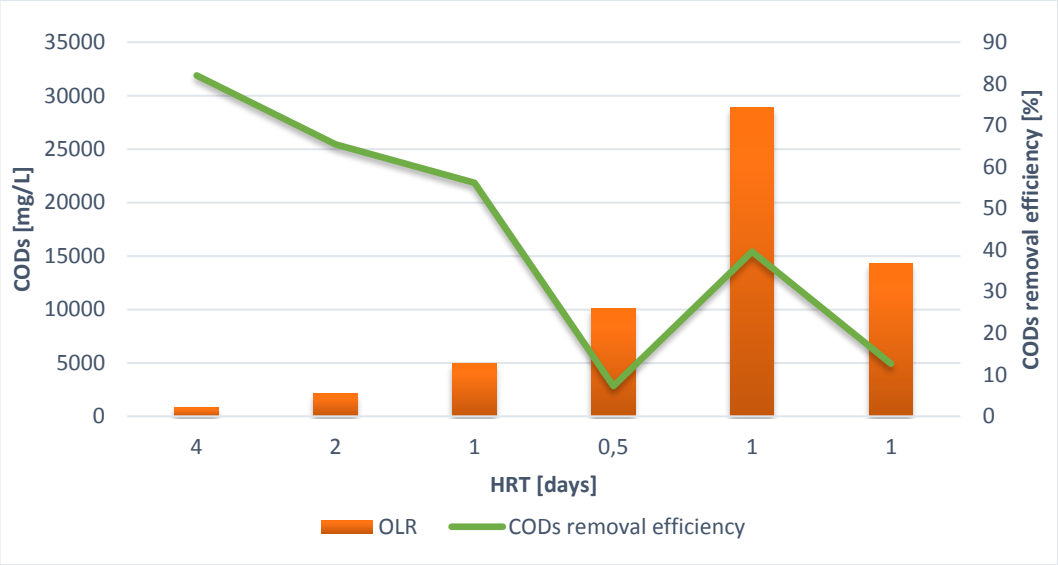

Figure 3.6 CODs removal efficiency trend in relation to the different HRT and OLR applied in the CSTR.

All the parameters analysed during the six experimental periods are summarised in the following table (Table 3.5).

Table 3.5 Summary of the influent and effluent characterization during the different experimental periods. The removal efficiencies are also summarized.

Period	I	II	III	IV	V	VI
HRT [d]	**4**	**2**	**1**	**0.5**	**1**	**1**
			Influent			
sCOD [g/d]	0.87±0.0	2.10±0.2	4.90±0.2	5.0±0.0	28.9±4.3	14.3±0.3
COD-VFA [g/d]	0.20±0.0	0.51±0.1	0.75±0.2	1.1±0.0	3.5±0.3	0.8±0.3
N-NH_4 [mg/d]	46±0.0	81±0.5	181±27	180±0.0	2439±81	969±63
			Effluent			
sCOD [g/d]	0.16±0.02	0.71±0.3	2.14±0.3	4.7±0.0	17.4±2.7	12.5±0.6
COD-VFA [g/d]	<0.01	<0.01	0.19±0.02	0.9±0.0	3.1±0.6	0.6±0.1
N-NH_4 [mg/d]	17±6	53±13	76±13	180±0.0	2098±477	733±161
MLSS [g/d]	0.107±0.02	0.460±0.14	0.690±0.13	Wash-out	0.3±0.03	0.3±0.18
MLVSS [g/d]	0.106±0.02	0.45±0.14	0.67±0.13	Wash-out	0.14±0.01	0.25±0.14
			Removal efficiency			
sCOD [%]	82%	66%	56%	7%	40%	13%
COD-VFA [%]	>99%	99%	74%	18%	11%	25%
N-NH_4 [%]	63%	34%	58%	0%	14%	25%

As it is possible to see from the Table 3.5, the sCOD removal efficiency is higher for high HRT (4 days, 82% removal), while is less than 10% for HRT of 0.5 days, where a wash-out of biomass occurred. The last two periods, with HRT of 1 day

and sCOD of 29 and 14 g/d, respectively, gave a sCOD removal efficiency lower than the previous tests, 40 and 13% respectively. The VFA were almost completely removed during period I and period II (99%), while the removal was lower for low HRT or high OLR.

During the growth phase, PHA accumulation was also determined in relation to each HRT tested. The PHA yield was calculated as well as the biomass yield. The Figure 3.7 shows the PHA and biomass production in terms of g/L during each HRT tested. The Figure 3.8 shows the PHA composition which is mainly composed by polyhydroxybutyrate (PHB), with a low percentage of polyhydroxyvalerate (PHV) during the period I.

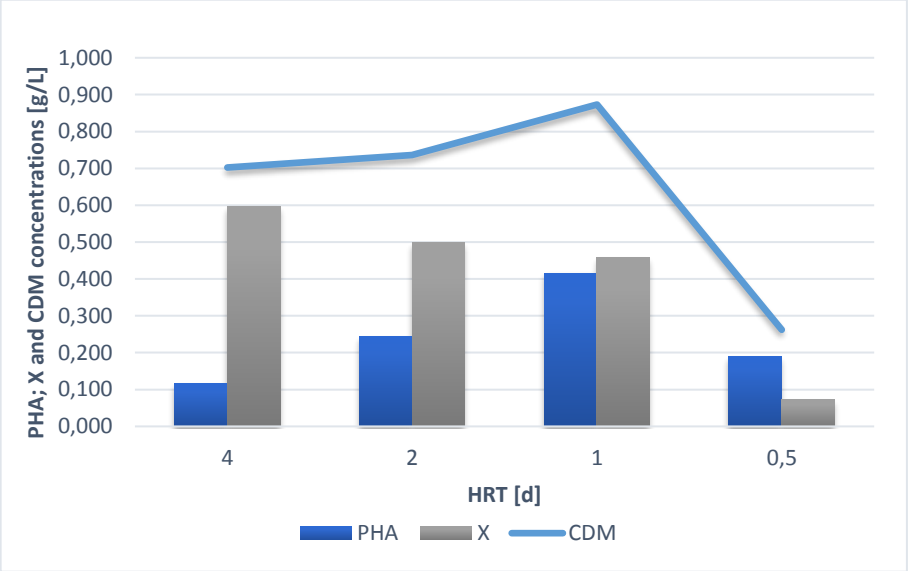

Figure 3.7 PHA and biomass production in relation to the different HRT tested.

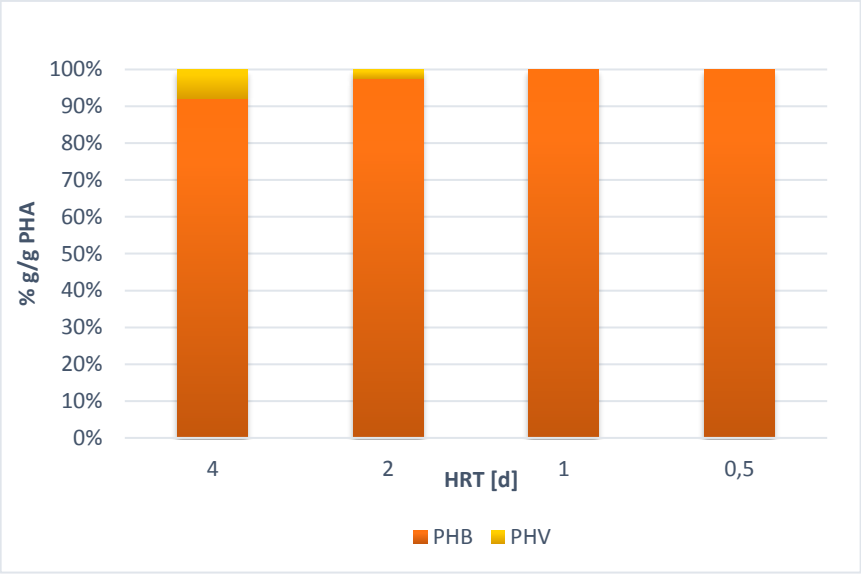

Figure 3.8 Composition of PHA accumulated in the biomass during the different tests.

Table 3.6 PHA and biomass yields during the period I-IV.

Period	HRT (d)	Y_{PHA} (g PHA/g ΔCODs)	Y_X (g X/g ΔCODs)	PHA (% as g PHA/g MLVSS)
I	4	0.044	0.275	29
II	2	0.079	0.174	26
III	1	0.147	0.196	59
IV	0.5	0.105	0.203	39

Looking at the period I, the PHA concentration in the biomass was lower (29% on MLVSS) if compared with the other periods, probably due to the longer HRT applied, which can allow more time for PHA degradation. Furthermore, the PHA yield was lower (0.044 g PHA/g ΔCODs) if compared with other studies in literature (Valentino et al., 2017). During the period II the PHA yield was still low (0.079 g PHA/g ΔCODs), while in the period III with an HRT of 1 day the PHA concentration reached a value of 59% with a PHA yield of 0.147 g PHA/g ΔCODs, which is 1.8 times more than the period II. Considering only the VFA fraction available during the period III (around 15-20%) and the VFA removal efficiency of 74% (Table 3.5), the resulting yield is 0.39 g PHA/g COD-VFA consumed.

Diniz et al. (2004) found a PHA production yield ranging from 0.15 and 0.19 g PHA/g carbohydrate consumed by a pure culture of Pseudomonas putida fed with glucose and fructose as carbon source, under limitation of nitrogen and phosphorus. However, in this work, the carbon source used was bio-based VFAs, which are considered the main chemical precursors for the production of PHAs.

From the data obtained during the test, it was possible to calculate the productivity (P) in terms of biomass (MLVSS) and PHA. The Table 3.7 summarizes the productivities calculated for each dilution tested.

Table 3.7 Productivities calculated for each dilutions tested.

D (d^{-1})	P (g MLVSS/L d)	P (g PHA/L d)
0.25	0.11	0.03
0.50	0.45	0.12
1	0.69	0.42
2	0.36	0.16

Then, it was possible to calculate the maximum productivity (P). In the following graph (Figure 3.9) it is shown the productivity trend in relation to the different dilution tested (1/day). Furthermore, the MLVSS, the sCOD and the PHA curve is reported in the graph. The same parameters, estimated experimentally, were also calculated numerically following a mathematical model described in the section 3.3.7.

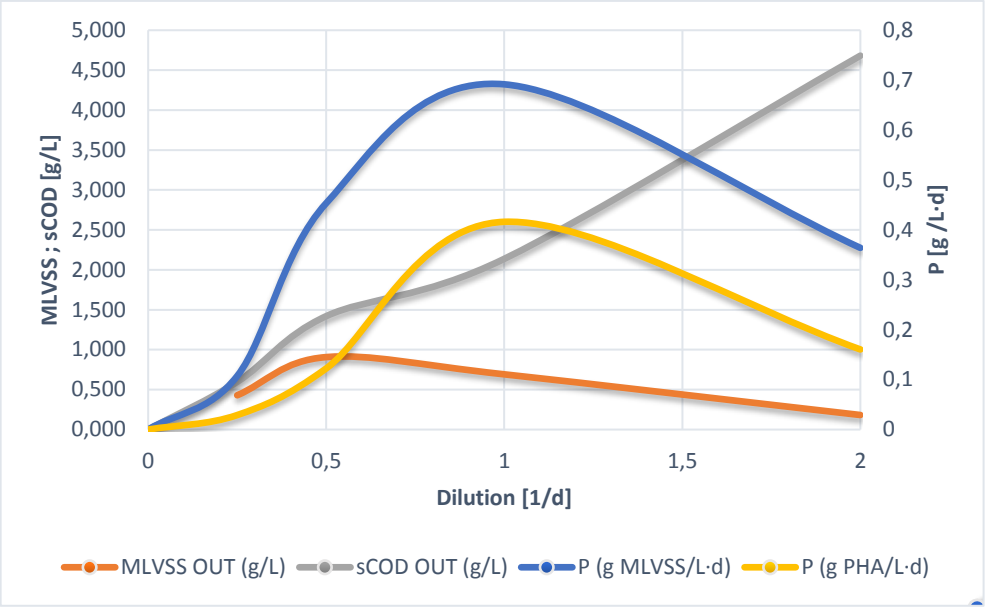

Figure 3.9 Plot correlation among dilution (1/d), productivity (P, g/L d) and biomass.

From the MLVSS curve it is possible to define the conditions in which the reactor could have the maximum productivity and, from that point, the conditions for biomass wash-out. The following graph (Figure 3.10) shows the linear trend plotting the HRT and the 1/S. From the equation obtained from the line in the graph, it was possible to estimate K_M and μ_{max}. From the equation of the graph, it was obtained a value of 60 g/L for K_M and a value of 1.20 h^{-1} for μ_{max}. The K_M value obtained in this experimentation was higher if compared with others found in literature, and this is due to the results obtained and the curve slope (Bengtsson et al., 2008).

The optimal dilution was thus calculated following the equation shown in the paragraph 3.3.4; the obtained value was 0.87 d^{-1}, corresponding to a HRT of 1.14 d; working with HRT lower than this value the process could lead to biomass wash-out.

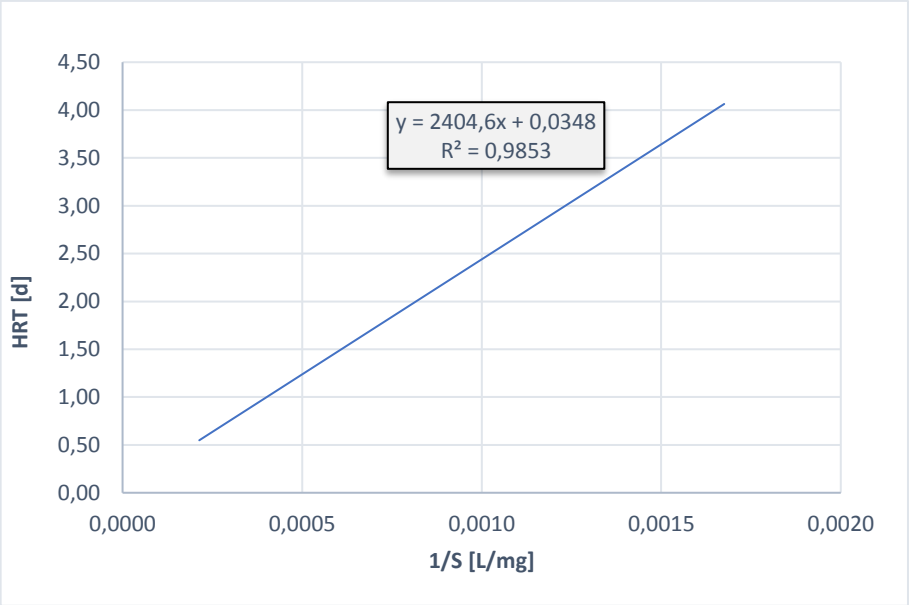

Figure 3.10 Plot of 1/S vs HRT derived from the experimental data.

3.4.4 Preliminary evaluation of nutritional value of the biomass

Basing on the biomass characterization, the nitrogen content resulted in 6.5%, which correspond to around 41% of microbial protein on MLSS. This value is in line with the protein contained in the soybean and fungi (Ghasemi et al., 2011). However, this value is a bit lower than the range of values reported by Matassa et al. (2016) as the typical concentration of crude protein in a bacterial cell, which is 50–83% based on dry matter. On the other side, the biomass here described is also enriched in PHAs (with a relatively high percentage) which can have determined the lower protein content. Furthermore, as described in the introduction, several studies demonstrated the positive effect of PHAs on animals, which can make this biomass interesting as feed additive. Following this concept, the pattern of the amino acids in the *Thauera* sp. Sel9 biomass was determined as shown in the Figure 3.11 and compared with the amino acids composition of commercial fishmeal, soybean and actual demand for trouts Figure 3.12.

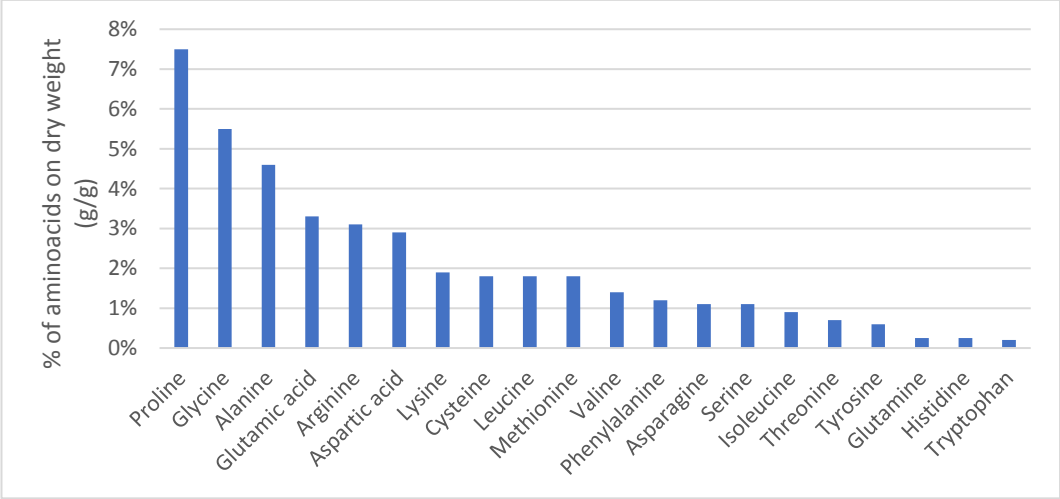

Figure 3.11 The amino acids profile of the PHA enriched biomass of Thauera sp. Sel9.

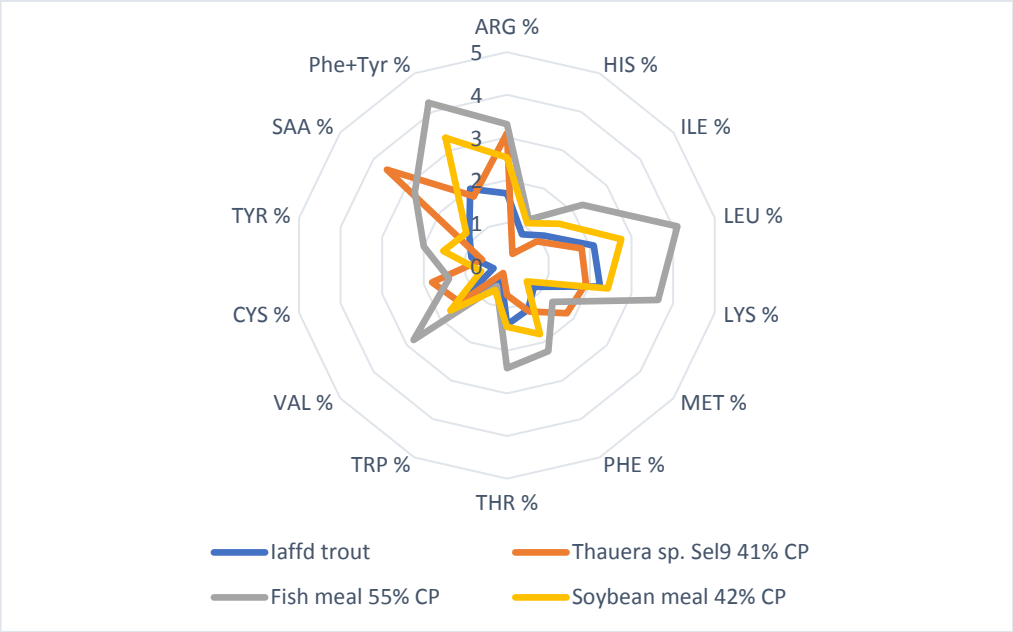

Figure 3.12 Comparison of the amino acids composition of the PHA enriched biomass compared with the commercial protein source such as soybean and fish meal. The protein content is in relation to the actual demand of amino acids of the trouts. ARG: Arginine; HIS: Histidine; ILE: Isoleucine; LEU: Leucine; LYS: Lysine; MET: Methionine; PHE: Phenylalanine; THR: Threonine; TRP: Tryptophan; VAL: Valine; CYS: Cystine; TYR: Tyrosine; SAA (Met + Cys): sulfured amino acid; Phe+Tyr: Phenylalanine + Tyrosine.

As it is possible to see from the results, the biomass showed a lack of histidine (HIS) and threonine (THR) compared with the soybeans and fishmeal, but for the remaining compositions, the % are in the right abundance for the demand required by trouts (Figure 3.12). Zhang et al. (2018) reported that *Thauera* sp., as well as other bacterial strains like *Paracoccus* sp., may increase the content of tryptophan and protein-like substance when the C/N ratio is decreasing. So, further investigation should be carried out in order to link the operating growth condition with the nutritional value of the biomass for different feed applications. On the other hand, the presence of PHAs in the biomass may give prebiotic properties, thus a higher market price compared with the current source of animal protein, like fishmeal. Ongoing research is evaluating PHAs as potential antibiotics as thus a potential feed supplement of interest for aquaculture (Defoirdt et al., 2009; De Schryver et al., 2010).

Reference

Albuquerque, P. B., & Malafaia, C. B. (2018). Perspectives on the production, structural characteristics and potential applications of bioplastics derived from polyhydroxyalkanoates. *International journal of biological macromolecules*, *107*, 615-625.

Alsafadi, D., & Al-Mashaqbeh, O. (2017). A one-stage cultivation process for the production of poly-3-(hydroxybutyrate-co-hydroxyvalerate) from olive mill wastewater by Haloferax mediterranei. *New biotechnology*, *34*, 47-53.

Basset, N., Katsou, E., Frison, N., Malamis, S., Dosta, J., & Fatone, F. (2016). Integrating the selection of PHA storing biomass and nitrogen removal via nitrite in the main wastewater treatment line. *Bioresource technology*, 200, 820-829.

Bengtsson, S., Hallquist, J., Werker, A., & Welander, T. (2008). Acidogenic fermentation of industrial wastewaters: effects of chemostat retention time and pH on volatile fatty acids production. *Biochemical Engineering Journal*, *40*(3), 492-499.

Bergeim, O. (1940). Toxicity of intestinal volatile fatty acids for yeast and *Esch. coli. The Journal of Infectious Diseases*, 222-234.

Boon, N., Defoirdt, T., De Windt, W., Van De Wiele, T., & Verstraete, W. (2013). *U.S. Patent No. 8,603,518*. Washington, DC: U.S. Patent and Trademark Office.

Chen, G. Q. (2010). Plastics completely synthesized by bacteria: polyhydroxyalkanoates. In *Plastics from bacteria* (pp. 17-37). Springer, Berlin, Heidelberg.

Ciesielski, S., & Przybylek, G. (2014). Volatile fatty acids influence on the structure of microbial communities producing PHAs. *Brazilian Journal of Microbiology*, *45*(2), 395-402.

Crutchik, D., Franchi, O., Caminos, L., Jeison, D., Belmonte, M., Pedrouso, A., ... & Campos, J. L. (2020). Polyhydroxyalkanoates (PHAs) Production: A Feasible Economic Option for the Treatment of Sewage Sludge in Municipal Wastewater Treatment Plants?. *Water*, *12*(4), 1118.

Defoirdt, T., Halet, D., Sorgeloos, P., Bossier, P., & Verstraete, W. (2006). Short-chain fatty acids protect gnotobiotic Artemia franciscana from pathogenic Vibrio campbellii. *Aquaculture*, 261(2), 804-808.

Defoirdt, T., Boon, N., Sorgeloos, P., Verstraete, W., & Bossier, P. (2009). Short-chain fatty acids and poly-β-hydroxyalkanoates:(New) Biocontrol agents for a sustainable animal production. *Biotechnology Advances*, *27*(6), 680-685.

De Schryver, P., Sinha, A. K., Kunwar, P. S., Baruah, K., Verstraete, W., Boon, N., ... & Bossier, P. (2010). Poly-β-hydroxybutyrate (PHB) increases growth performance and intestinal bacterial range-weighted richness in juvenile European sea bass, Dicentrarchus labrax. *Applied microbiology and biotechnology*, *86*(5), 1535-1541.

Diniz, S. C., Taciro, M. K., Gomez, J. G. C., & da Cruz Pradella, J. G. (2004). High-cell-density cultivation of Pseudomonas putida IPT 046 and medium-chain-length polyhydroxyalkanoate production from sugarcane carbohydrates. *Applied biochemistry and biotechnology*, *119*(1), 51-69.

Dionisi, D., Majone, M., Vallini, G., Di Gregorio, S., & Beccari, M. (2006). Effect of the applied organic load rate on biodegradable polymer production by mixed microbial cultures in a sequencing batch reactor. *Biotechnology and bioengineering*, 93(1), 76-88.

Fernández-Dacosta, C., Posada, J. A., Kleerebezem, R., Cuellar, M. C., & Ramirez, A. (2015). Microbial community-based polyhydroxyalkanoates (PHAs) production from wastewater: techno-economic analysis and ex-ante environmental assessment. *Bioresource technology*, 185, 368-377.

Forni, D., Bee, G., Kreuzer, M., & Wenk, C. (1999a). Novel biodegradable plastics in sheep nutrition, 1: Effects of untreated plastics on digestibility and metabolic energy and nitrogen utilization. *Journal of Animal Physiology and Animal Nutrition (Germany)*.

Forni, D., Wenk, C., & Bee, G. (1999b). Digestive utilization of novel biodegradable plastic in growing pigs.

Ghasemi, Y., Rasoul-Amini, S., & Morowvat, M. H. (2011). Algae for the production of SCP. *Bioprocess Sciences and Technology: Nova Science Publishers, Inc,* 163-84.

Huang, L., Chen, Z., Wen, Q., Zhao, L., Lee, D. J., Yang, L., & Wang, Y. (2018). Insights into Feast-Famine polyhydroxyalkanoate (PHA)-producer selection: Microbial community succession, relationships with system function and underlying driving forces. *Water research*, *131*, 167-176.

Jones, D. B., Munsey, V. E., & Walker, L. E. (1942). Report of committee on protein factor. *Journal of Association of Official Agricultural Chemists*, *25*(1), 118-120.

Kalia, V. C. (Ed.). (2019). *Biotechnological applications of polyhydroxyalkanoates*. Berlin: Springer.

Koller, M., & Braunegg, G. (2015). Potential and prospects of continuous polyhydroxyalkanoate (PHA) production. *Bioengineering*, 2(2), 94-121.

Kourmentza, C., Plácido, J., Venetsaneas, N., Burniol-Figols, A., Varrone, C., Gavala, H. N., & Reis, M. A. (2017). Recent advances and challenges towards sustainable polyhydroxyalkanoate (PHA) production. *Bioengineering*, *4*(2), 55.

Kucera, D., Pernicová, I., Kovalcik, A., Koller, M., Mullerova, L., Sedlacek, P., ... & Krzyzanek, V. (2018). Characterization of the promising poly (3-hydroxybutyrate) producing halophilic bacterium Halomonas halophila. *Bioresource technology*, *256*, 552-556.

Laranja, J. L. Q., Amar, E. C., Ludevese-Pascual, G. L., Niu, Y., Geaga, M. J., De Schryver, P., & Bossier, P. (2017). A probiotic Bacillus strain containing amorphous poly-beta-hydroxybutyrate (PHB) stimulates the innate immune response of Penaeus monodon postlarvae. *Fish & Shellfish Immunology*, *68*, 202-210.

Matassa, S., Boon, N., Pikaar, I., & Verstraete, W. (2016). Microbial protein: future sustainable food supply route with low environmental footprint. *Microbial biotechnology*, *9*(5), 568-575.

Mohan, S. V., Dahiya, S., Amulya, K., Katakojwala, R., & Vanitha, T. K. (2019). Can circular bioeconomy be fueled by waste biorefineries—A closer look. *Bioresource Technology Reports*, 7, 100277.

Morgan-Sagastume, F. (2016). Characterisation of open, mixed microbial cultures for polyhydroxyalkanoate (PHA) production. *Reviews in Environmental Science and Bio/Technology*, *15*(4), 593-625.

Najdegerami, E. H., Tran, T. N., Defoirdt, T., Marzorati, M., Sorgeloos, P., Boon, N., & Bossier, P. (2012). Effects of poly-β-hydroxybutyrate (PHB) on Siberian sturgeon (A cipenser baerii) fingerlings performance and its gastrointestinal tract microbial community. *FEMS Microbiology Ecology*, *79*(1), 25-33.

Nhan, D. T., Wille, M., De Schryver, P., Defoirdt, T., Bossier, P., & Sorgeloos, P. (2010). The effect of poly β-hydroxybutyrate on larviculture of the giant freshwater prawn Macrobrachium rosenbergii. *Aquaculture*, *302*(1-2), 76-81.

Ostle, A. G., & Holt, J. G. (1982). Nile blue A as a fluorescent stain for poly-beta-hydroxybutyrate. *Applied and environmental microbiology*, *44*(1), 238-241.

Poltronieri, P., & Kumar, P. (2017). Polyhydroxyalkanoates (PHAs) in industrial applications. *Handbook of Ecomaterials. Cham: Springer International Publishing*, 1-30.

Sruamsiri, D., Thayanukul, P., & Suwannasilp, B. B. (2020). In situ identification of polyhydroxyalkanoate (PHA)-accumulating microorganisms in mixed microbial cultures under feast/famine conditions. *Scientific Reports*, *10*(1), 1-10.

Suguna, P., Binuramesh, C., Abirami, P., Saranya, V., Poornima, K., Rajeswari, V., & Shenbagarathai, R. (2014). Immunostimulation by poly-β hydroxybutyrate–hydroxyvalerate (PHB–HV) from Bacillus thuringiensis in Oreochromis mossambicus. *Fish & shellfish immunology*, *36*(1), 90-97.

Tamis, J., Lužkov, K., Jiang, Y., van Loosdrecht, M. C., & Kleerebezem, R. (2014). Enrichment of Plasticicumulans acidivorans at pilot-scale for PHA production on industrial wastewater. *Journal of Biotechnology*, *192*, 161-169.

Valentino, F., Brusca, A. A., Beccari, M., Nuzzo, A., Zanaroli, G., & Majone, M. (2013). Start up of biological sequencing batch reactor (SBR) and short-term biomass acclimation for polyhydroxyalkanoates production. *Journal of Chemical Technology & Biotechnology*, *88*(2), 261-270.

Valentino, F., Morgan-Sagastume, F., Campanari, S., Villano, M., Werker, A., & Majone, M. (2017). Carbon recovery from wastewater through bioconversion into biodegradable polymers. *New biotechnology*, *37*, 9-23.

Van Immerseel, F., De Buck, J., Pasmans, F., Velge, P., Bottreau, E., Fievez, V., ... & Ducatelle, R. (2003). Invasion of Salmonella enteritidis in avian intestinal epithelial cells in vitro is influenced by short-chain fatty acids. *International journal of food microbiology*, 85(3), 237-248.

Van-Thuoc, D., Quillaguaman, J., Mamo, G., & Mattiasson, B. (2008). Utilization of agricultural residues for poly (3-hydroxybutyrate) production by Halomonas boliviensis LC1. *Journal of applied microbiology*, *104*(2), 420-428.

Wang, Y., & Chen, G. Q. (2017). Polyhydroxyalkanoates: sustainability, production, and industrialization. *Sustainable polymers from biomass. Wiley-VCH Verlag, Amsterdam, The Netherlands https://doi. org/10.1002/9783527340200. ch2*.

Wang, X., Jiang, X. R., Wu, F., Ma, Y., Che, X., Chen, X., ... & Chen, G. Q. (2019). Microbial Poly-3-Hydroxybutyrate (PHB) as a Feed Additive for Fishes and Piglets. *Biotechnology Journal*, *14*(12), 1900132.

Woraittinun, N., & Suwannasilp, B. B. (2017). polyhydroxyalkanoate production from different carbon substrates using sludge from a wastewater treatment plant: Microbial communities, polymer compositions, and thermal characteristics. *Environmental Progress & Sustainable Energy*, *36*(6), 1754-1764.

Zhang, Z., Yu, Z., Dong, J., Wang, Z., Ma, K., Xu, X., ... & Zhu, L. (2018). Stability of aerobic granular sludge under condition of low influent C/N ratio: Correlation of sludge property and functional microorganism. *Bioresource technology*, *270*, 391-399.

4 Two-steps process for the upgrading of energy-rich gases and the recovery of high-added value biomass

This chapter describes the activities carried out during an internship lasted 6 months in a Belgian company, Avecom NV, under the supervision of the Professor Willy Verstraete. The company was chosen for its experience about the optimization of microbial processes.

List of abbreviations

HOB	Hydrogen Oxidizing Bacteria
MPB	Methane-Producing Bacteria
SCP	Single Cell Protein
SOB	Sulfur Oxidizing Bacteria
SP	Sulphated Polysaccharides
SRB	Sulfate-Reducing Bacteria
TBR	Trickle-Bed Reactor

4.1 Introduction

In the previous chapter it was described a process at lab scale for the production of biomass that should be used in the feed sector. Indeed, the biomass showed characteristics compatible with the commercial feed for aquaculture sector. In the following chapter it will analysed and described a different microbial process with the same purpose: to find a potential market for recovered resources derived from the wastewater sector.

4.1.1 Sulfur cycle

Sulfur (S) is one of the most abundant elements in nature and it is present in all living organisms as a constituent of some proteins, vitamins and hormones. The S cycle contains both atmospheric and terrestrial processes. The whole cycle is shown in the Figure 4.1. Mainly, deposits of S are present as gypsum ($CaSO_4$), as metal sulfide (FeS_2), as elemental sulfur (S^0) in the earth's crust and as sulfate (SO_4^{2-}) in seawater (Lin et al., 2018).

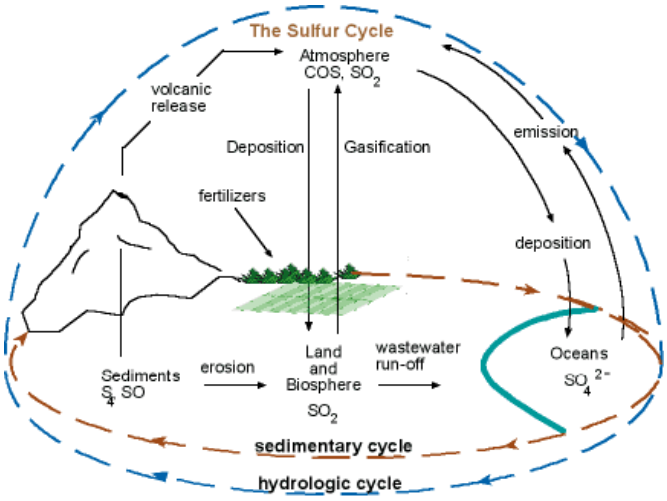

Figure 4.1 The schematization of the sulfur cycle.

The S cycle is more complex than either nitrogen or the carbon cycle. This is due to the fact that the S can occur in different redox states, such as: sulfide (S^{2-}), elemental sulfur (S^0), thiosulfate ($S_2O_3^{2-}$), sulfate (SO_4^{2-}), sulfite (SO_3^{2-}) and hydrogen sulfide (H_2S). The S cycle can be driven both chemically and biologically (Steudel, 2003). The sulfur containing proteins can be degraded by a variety of microorganism; then, the sulfur in the amino acids is converted, by another kind of microorganisms, into H_2S. H_2S exits dissolved in water as an ion (S^{2-}) under basic

conditions or in the form of gas (H_2S) under acidic conditions. H_2S is a colourless, flammable and extremely hazardous gas. It is both irritant and a chemical asphyxiant with effects on both oxygen utilization and the central nervous system. It is also very harmful for facilities and, in general, very corrosive. It can be accumulated in areas of poorly ventilated spaces and can corroding metals and concrete, representing a serious problem. Furthermore, increasing industrial activities have created significant imbalance of the sulfur cycle, leading to several environmental problems related to sulfur; some examples are odour nuisance, corrosion, sulfide toxicity, acid rain (Pikaar et al., 2014).

4.1.2 Sulfate-rich wastewater

Several industries generate wastewater with high content of sulfate, if compare with the normal concentration in the domestic wastewater (Lens et al., 1998; Muyzer and Stams, 2008). Some of these industries include sea-food processing (Omil et al., 1995), pharmaceutical plants (Li et al., 2015), pulp and paper manufacturing (Wani et al., 1999; Janssen et al., 2009), mining (Vera et al., 2013), as well as tanneries (Galiana-Aleixandre et al., 2011), natural gas processing (Tang et al., 2009) and livestock farming (Chung et al., 2001).

Typically, in untreated domestic wastewater the concentration of sulfate ranges from 20 to 60 mg/L (Moussa et al., 2006). Values between 40 to 70 mg/L are also reported in anaerobic sewage treatment, which took place in the Netherlands and in the South America (Haandel et al., 2007). It is reported also a concentration between 100 to 150 mg/L (in India) or 400 to 600 mg/L (in Arab peninsula, Haandel et al., 2007). In Xue et al. (2019) it is reported a study with a concentration of sulfate in the sewage of Hong Kong in the range of 50-500 mg/L. In Sarti and Zaiat (2011), it is reported a study using wastewater from chemical industry in which the sulfonation of vegetable oils is applied; this wastewater had an average content in sulfate of 201 g/L. It is also reported in Mendez et al. (1995), a concentration of sulfate in the water from sea food processing ranges from 600 to 2700 mg S/L (or 1800 to 8100 mg SO_4^{2-}/L).

The presence of high sulfate concentrations in wastewater restricts the application of anaerobic treatment technology, because can cause the formation of H_2S, which

is toxic and corrosive (Sarti and Zaiat, 2011). For this reason, several studies point to the beneficial application of sulfate-reducing bacteria (SRB) in wastewater treatment plants (WWTPs, Lens et al., 1998; Muyzer and Stams, 2008).

4.1.3 "Power to gas"

In this chapter we explore a novel concept based on the use of gases such as hydrogen gas (H_2), oxygen (O_2), carbon dioxide (CO_2) or methane (CH_4) as an energy source for microorganisms.

In the recent years, the reduction of fiscal incentives in the biogas production and the emergence of new challenges in the field of waste and plastic, have shifted the attention on the use of CH_4 as well as CO_2 and others as building blocks for the chemical industry (Pérez et al., 2020).

Furthermore, interest is also increasing in the investigation of protein production, such as single cell protein (SCP) using hydrogen-oxidizing bacteria (HOB). H_2 is indeed recognized as the lightest gas and a clean energy in the world (Zhang et al., 2020). HOB represent an interesting class of bacteria, whose main representatives are *Alcaligenes* and *Pseudomonas* (Matassa et al., 2016b).

4.1.4 Sulfate-reducing bacteria (SRB) and sulfur-oxidizing bacteria (SOB)

The sulfur cycle is dominated by two classes of bacteria: sulfate-reducing bacteria (SRB) and sulfur-oxidizing bacteria (SOB).

The SRB are a class of anaerobic bacteria which can respire using sulfate as an electron acceptor and to metabolise molecular hydrogen (H_2) as a primary energy source (Figure 4.2). SRB have indeed an extremely high hydrogenase activity (Martins at al., 2013), but they are also able to utilize different organic compounds. SRB can use several compounds other than H_2, such as formate, acetate, methanol, pyruvate, propionate, butyrate, higher and branched fatty acids, lactate, ethanol, higher alcohols, fumarate, succinate, malate, and aromatic compounds (Bock et al., 1994; Colleran et al., 1995).

These bacteria are ubiquitous in the environment. They have been detected in shallow marine and freshwater sediments and in deep subsurface environments. They can live in environment with extreme conditions, such as high or low pH, high

or low temperature and high or low salt concentrations. They can also occur in living organisms such as ruminants and in the human intestinal tract. Deltaproteobacteria is the class which contains most of the known sulfate reducing bacteria (Bahr et al., 2005).

Usually, SRB exist in competition with methane-producing bacteria (MPB). Factors as concentration of sulphide, organic compounds and COD/SO_4^{2-} ratio affect the relative prevalence of SRB. In case of H_2 utilizing bacteria, there is no carbon involved in the reaction, only acetate or CO_2. The carbon is thus used by the bacteria for biomass production.

Biotic sulfur oxidation can occur in areas at the interface between oxic and anoxic habitats by SOB. The Figure 4.2 represents schematically the S microbial oxidation. Biological oxidation of H_2S to sulfate in one of the major reactions of the biological sulfur cycle. The SOB are mainly present in the environment in which oxygen (O_2) or alternatively nitrate (NO_3) is available as electron acceptors. SOB are aerobic, anaerobic or facultative, they are also obligate or facultative autotrophs. They are most abundantly represented in the family of *Thiobacilliaceae* (Starosvetsky et al., 2013). Furthermore, SOB are found in four classes of the Proteobacteria, such as Alphaproteobacteria, Betaproteobacteria, Gammaproteobacteria, and Epsilonproteobacteria (Barton et al. 2014).

Sulfide in the environment is extremely toxic and represents a huge concern for biological life. There are several ways to remove sulfide, but the biological way is considered a promising alternative. SOB are, in this sense, the main actors in the detoxification from sulfide compounds. Generally, these bacteria grow by using inorganic carbon (CO_2) as a carbon source. These bacteria are reported to be able to growth under various environmental conditions and stress.

It is reported that H_2S as well as methanethiol (CH_3SH) are produced in large quantity by colonic bacteria. The colonic mucosa has already naturally enzymes that are able to detoxify these compounds, but if the system is not efficient, sulfide might be injurious to colonic mucosa. It is indeed reported in Levitt et al. (1999) that excess of sulfide production could play an important role in ulcerative colitis.

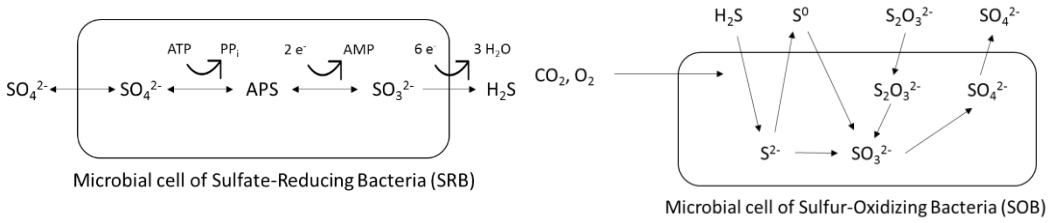

Figure 4.2 Schematization of the SRB (left) and SOB metabolism (right).

4.2 Focus of this work

The overall purpose of this work is to use and upgrade the gases that can be derived from the process of gasification (CO, CO_2, H_2, H_2S, NH_3, CH_4) of low value secondary resources in order to recovery valuable molecules that can have an increasing market demand. In order to verify this application, it was used a relatively simple reactor technology at atmospheric pressure. The H_2 gas was used to growth a biomass rich in SRB in order to generate COD in water, mainly in the form of H_2S. The solubilized COD was used to growth a microbial biomass rich in SOB with the aim to evaluate the growth yield, the H_2S utilization rate and the possible applications of the biomass.

Starting from some literature review, it was noticed high interest in sulphated polysaccharides (SPs). SPs represent an interesting class of molecules extracted mainly from seaweed, with several industrial and biological applications. The Table 4.1 shows some example of SPs extracted from seaweed with the relative industrial application. Their biological activity includes different therapeutic applications, such as anticoagulation, antithrombotic, antiviral, antioxidant, antitumor, anti-inflammatory (Raposo et al., 2013). Furthermore, SPs can be used for different industrial applications, for instance pharmaceuticals, nutraceuticals, cosmeceuticals and functional foods (Wijesinghe and Jeon, 2012). There is also some evidence that indicates that SPs can be extracted from activated sludge. Xue et al. (2019) described the recovery of this class of molecules from saline sludge. The study explores and describes a potential new source of SPs, the activated sludge, instead of marine algae, and also underlines the possibility of recovery high-value resources from sludge with an increasing market demand. In the article they reported that SPs in the sludge of a lab scale-reactor reached 342.8 ± 0.3 mg/g VSS, while the sludge from a full-scale saline wastewater treatment plant (WWTP) contained 418.1 ± 0.4

mg/g VSS of SPs. In detail they reported also the concentration of carrageenan, fucoidan and heparin (three examples of SPs) in the sludge: they obtained 159.22 ± 1.21 mg/g VSS and 184.01 ± 1.35 mg/g VSS of carrageenan in the lab-scale sludge and in the full-scale plant sludge, respectively. Furthermore, they reported a concentration of fucoidan of 23.83 ± 0.74 mg/g VSS and 40.16 ± 0.42 mg/g VSS in the lab-scale and in the full-scale, respectively. Finally, they reported the concentration of heparin: 32.49 ± 0.33 mg/g VSS in the lab-scale and 30.82 ± 0.25 in the full-scale.

Table 4.1 Some example of sulphated polysaccharides with their origins and possible applications.

Sulphated polysaccharides	Type of seaweed	Application	Reference
Carrageenan	Red seaweed (e.g. *Laurencia papillosa*)	Gelling agent in food industry	Tanna and Mishra (2019)
Fucoidan	Brown seaweed (e.g. *Splachnidium rugosum*)	Anti-inflammatory, anti-oxidative and anticoagulant	January et al. (2019)
Ulvan	Green seaweed (e.g. *Ulva*)	Antioxidant, anti-cancer in medicinal foods	Kidgell et al. (2019)
Agarans	Red seaweed (*Polysiphonia nigrescens*)	Anti-viral	Prado et al. (2008)

As an example, carrageenan is a major ingredient in the food industry and it is used for its gelling, thickening and stabilizing properties. Figure 4.3 shows the carrageenan market demand in 2018. The world carrageenan market is mainly dominated by the Asia-Pacific region. In a new report it is reported that the compound annual growth rate (CAGR) of carrageenan is going to increase up to 8.12% in the study period of 2016-2024 (https://www.mordorintelligence.com/industry-reports/global-carrageenan-market-industry). It is reported that the global production of carrageenan in 2014

was around 60 000 ton/year with a retail price of around 10 €/kg and with an approximate gross market value of around 600 million €/year (Rhein-Knudsen et al., 2015).

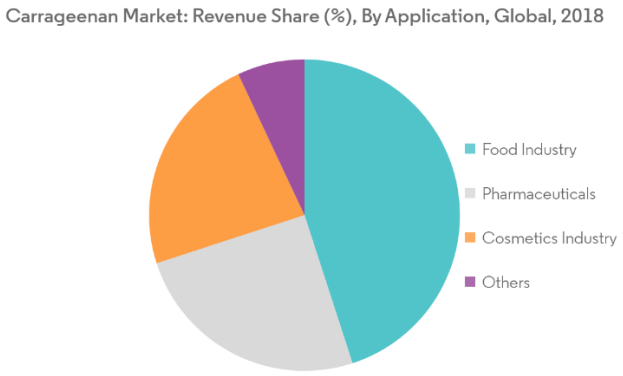

Figure 4.3 Carrageenan (an example of sulphated polysaccharides) market (source: Mordor Intelligence).

Following this possible applications and value recovery, different experimental tests were set up as described in the following paragraphs.

4.3 Materials and methods

4.3.1 Lab-scale reactors set up

The Figure 4.4 shows the experimental setup used during the experiments. The system is mainly composed of two sections: the first is dedicated to H_2S production through the upgrading of H_2 gas; the second is dedicated to the recovery of high added value molecules by using the H_2S in solution produced in the first step. The aim is to select SOB biomass.

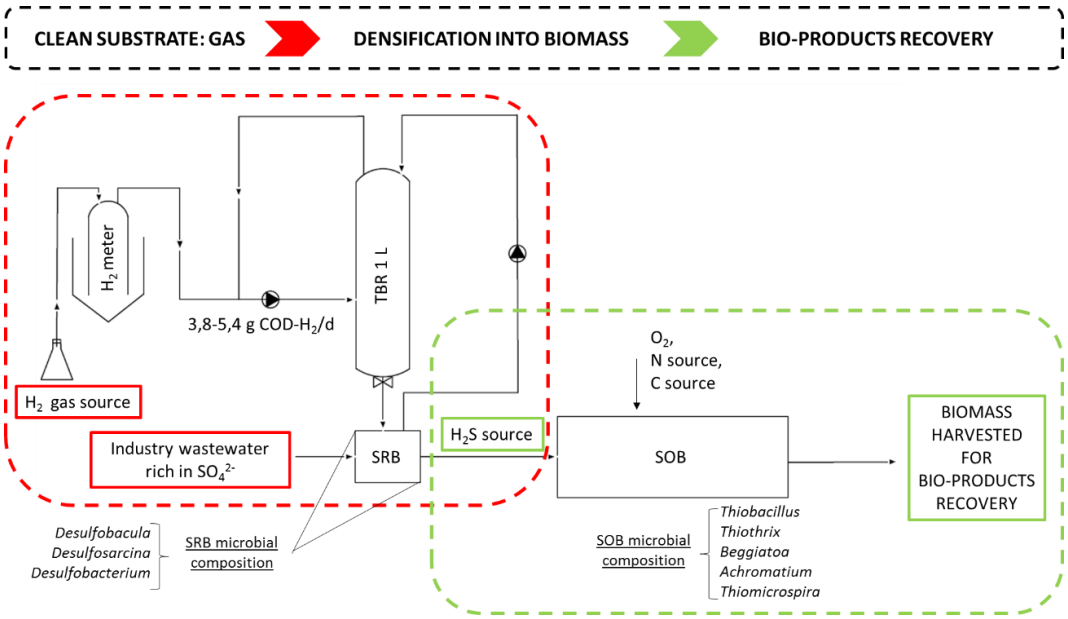

Figure 4.4 Experimental set-up at lab scale. TBR is Trickle-bed reactor.

4.3.1.1 SRB reactor

The first part is dedicated to H_2S production through the upgrading of H_2 gas (Equation 1), with a biomass that was confirmed to contain SRB (data confirmed by qPCR). The following Table 4.2 summarizes the different operational periods.

Table 4.2 Summary of the operational periods of the SRB reactor.

	Run I	Run II	Run III	Run IV
Days	1-45	61-84	85-133	134-154
V recirculation liquid [L]	10	10	6	10
HRT [d]	2.5	2.5	2.4	2.5
S-SO_4^{2-} provided [g/L TBR d]	3.7	3.8	2.7	4.1
H_2 gas consumed [g COD-H_2/L TBR d]	3.8	5.4	4.3	4.7

The H_2 gas was provided through the reaction between aluminium (Al) and sodium hydroxide (NaOH). The full reaction is described in the Equation 2. In brief: 15 g of Al foil and 32 g of sodium hydroxide are reacted in 1 L of water. So, stechiometrically, 15 g of Al (0.55 mol) produces 1.66 g of H_2 (0.83 mol), which corresponds to around 21 L of H_2 (at the experimental conditions, 33°C and 1 atm). 21 L of H_2 corresponds to 13.28 g COD-H_2. In order to optimize the SRB-H_2 contact

and to increase sulfate reduction activity, a 1 L Trickling Bed Reactor (TBR) filled with Kaldnes carriers was connected with a bin for liquid recirculation. Indeed, SRB tend to aggregate in order to have more physical protection (Jong and Parry, 2003).

$$4\,H_2 + SO_4^{2-} + H^+ \rightarrow HS^- + 4\,H_2O \qquad \textit{[Eq. 1]}$$

$$2\,\mathrm{Al} + 2\,\mathrm{NaOH} + 2\,H_2\mathrm{O} \rightarrow 2\,\mathrm{NaAl}O_2 + 3\,H_2\,(\mathrm{gas}) \qquad \textit{[Eq. 2]}$$

The SRB was fed with a synthetic wastewater (Table 4.3) containing organics, ammonia, phosphate as well as micronutrients. The wastewater was prepared with a total theoretical concentration of SO_4^{2-} of 2.8 g/L (or 29 mmol/L, or 0.9 g/L of S-SO_4^{2-}). The real value was also measured and confirmed using the Hach test kits for sulfate analysis. The pH of the medium was maintained at 6.1 ± 0.2 and the conductivity was maintained below 10 mS/cm. The reactor operated at 33°C during all the experimental activity. The hydraulic retention time (HRT) of around 2.5 days was maintained during all the runs.

Table 4.3 Composition of the synthetic wastewater used for feeding the SRB reactor.

	mmol/L	g/L
Na_2SO_4	26.4	3.75
KH_2PO_4	22.1	3
K_2HPO_4	2.9	0.5
$MgSO_4*7H_2O$	1.6	0.4
$NaHCO_3$	0.95	0.08
$CaCl_2$	0.09	0.01
$FeSO_4*7H_2O$	0.4	0.1
$(NH_4)_2SO_4$	0.75	0.1
Trace Elements [mL]	-	0.5

Once per week around 0.1-0.2 g/L of peptone was dosed to keep the SRB active and to provide to the bacteria the right amount of nitrogen as reported in Postgate, 1965. It is also reported in Dev et al. (2015) a study related to the understanding of the SRB growth performance in the presence of different nitrogen sources. In Dev et al. (2015), they analysed tryptone, corn steep liquor, yeast extract, NH_4HCO_3,

NH_4Cl and marine waste extract as different nitrogen sources. Generally, the media used for SRB contain, among others, peptone (Das et al., 2013). In the present work, it was chosen to use peptone in order to provide to the SRB not only nitrogen as in the inorganic compounds, but also amino nitrogen that can be used by SRB resulting in high growth (Wheeler and Kirchman, 1986).

4.3.1.2 SOB reactor

The second part is dedicated to the recovery of high added value biomass by using the H_2S in solution produced in the first step. The aim is to select SOB biomass and to verify the growth efficiency on H_2S gas. The Table 4.4 shows the experimental runs during the SOB activity.

Table 4.4 Summary of the operational periods of the SOB reactor.

	Run I	**Run II**	**Run III**	**Run IV**
Days	1-45	61-84	85-117	118-168
O_2 supply	Yes	Yes	Yes	No (only stirring and closed system)
C source	Sugar	Sugar	Sugar/CO_2	$NaHCO_3$
N source	$(NH_4)_2SO_4$	$(NH_4)_2SO_4$	$(NH_4)_2SO_4$	$(NH_4)_2SO_4$
H_2S [mg COD-H_2S/L reactor d]	137±21	148±28	80±19	114±49
Tot COD IN [mg/L reactor d]	486±32	497±39	150±13	186±59
V reactor [L]	20	20	10-5	5
pH	8.1-8.3	7.7-7.8	7.8-8.2	7.8-8.6
SRT [d]	4±0.5 (same as HRT, no recirculation)	17±9 (recirculation)	10±4 (recirculation)	4±0 (same as HRT, no recirculation)

The reactor was provided with oxygen through continuous aeration, during the runs I-III. In the run IV the reactor was gently shaken and also open to the air, but the

contact with the air was restricted with a cotton stopper. The Equation 3 shows the oxidation of S^{2-} to SO_4^{2-}; it could also be that the reaction only proceeds until S^0.

$$H_2S + 1.65\ O_2 + 0.35\ CO_2 + 0.35\ H_2O \rightarrow SO_4^{2-} + 0.35\ CH_2O + 2\ H^+ \quad [Eq.3]$$

The SOB reactor was fed mixotrophically during the first three runs, with the addition of 6 g of sugar per day. At the end of the run III, no more sugar was added. In the run IV $NaHCO_3$ was added as C source. The SOB was fed with the effluent derived from the SRB reactor in order to provide H_2S as energy source, during all the runs; furthermore, it was fed with a solution containing 0.1 g/L of $Fe_2(SO_4)_3$ in runs I-III. The reactor operated at 33°C during all the experimental activity.

4.3.2 Analytical procedures

The chemical oxygen demand (COD) analysis, the ammonia content and the sulfate content were determined by using Hach test kits and following the procedure described in the provided manuals. The total Kjeldahl nitrogen (TKN) analysis, the total suspended solids (TSS) and the volatile suspended solids (VSS) were determined following the standard method for water analysis (Van Loosdrecht et al., 2016). The protein content was determined by the conversion of TKN to protein by using the factor 6.25. The sulfide content was determined by using a titrimetric method (Kolthoff et al., 1969). The sugar content dissolved in the water, was determine following the colorimetric method described in Dubois et al. (1956).

4.3.3 Solid retention time (SRT)

The solid retention time (SRT) was calculated in accordance with the following equation (Equation 4).

$$SRT = \frac{(V) * (MLSS)}{(Q_W * X_r) + (Q_e * X_e)} \quad [Eq.4]$$

Where, V is the volume of the reactor; MLSS is the mixed liquor suspended solids in the reactor; Q_w is the flow rate wasted from the reactor; X_r is the concentration of the biomass wasted from the reactor; Q_e is the flow rate of supernatant after settling phase; X_e is the concentration of solids in the supernatant.

4.3.4 Chemical oxygen demand (COD) calculations

In the present text, mainly two forms of chemical oxygen demand (COD) were considered: the COD-H_2 and the COD-H_2S. If it is not specified, the COD value is referred to the total COD analysed in the biomass following the procedure described in the Analytical Procedures.

The COD-H_2 was calculated following the Equation 5. Basing on this equation, for the oxidation of 2 moles of H_2, it needs 1 mol of O_2. So, the COD conversion factor is 8 g COD/g H_2.

$$2\,H_2 + O_2 \rightarrow 2\,H_2O \qquad [Eq.5]$$

The same evaluation was done for the COD-H_2S. The Equation 6 shows the oxidation of H_2S to H_2SO_4. From this equation it is possible to estimate the COD conversion factor for H_2S that is 1.8 g COD/g H_2S.

$$H_2S + 2O_2 \rightarrow H_2SO_4 \qquad [Eq.6]$$

4.3.5 Microbiological analysis

Two samples from the SOB and the SRB reactor during the optimal conditions were recovered and the DNA was extracted using the DNeasy PowerSoil Kit by Quiagen, following the instruction manual provided. Then, the extracted DNA was stored at 20°C and the qPCR was performed by an external laboratory analysis.

4.4 Results and discussion

4.4.1 SRB reactor performance

The SRB reactor was monitored for more than 180 days. The experimental activity was divided into 4 runs, as shown in the Table 4.2. The reactor was shut down from the day 46 to the day 60 (*due to the lockdown for the Coronavirus*).

The Figure 4.5 and the Figure 4.6 show the performance of the SRB reactor during the experimental time in terms of COD, S-SO_4^{2-} reduction and S^{2-} production. The black bars indicate the different runs. During each run, a stability period was reached, and all the average data are referred to the stability periods. The Table 4.5 and the Table 4.6 show the mass balance and the % of conversion from S-SO_4^{2-} and from COD-H_2 to H_2S.

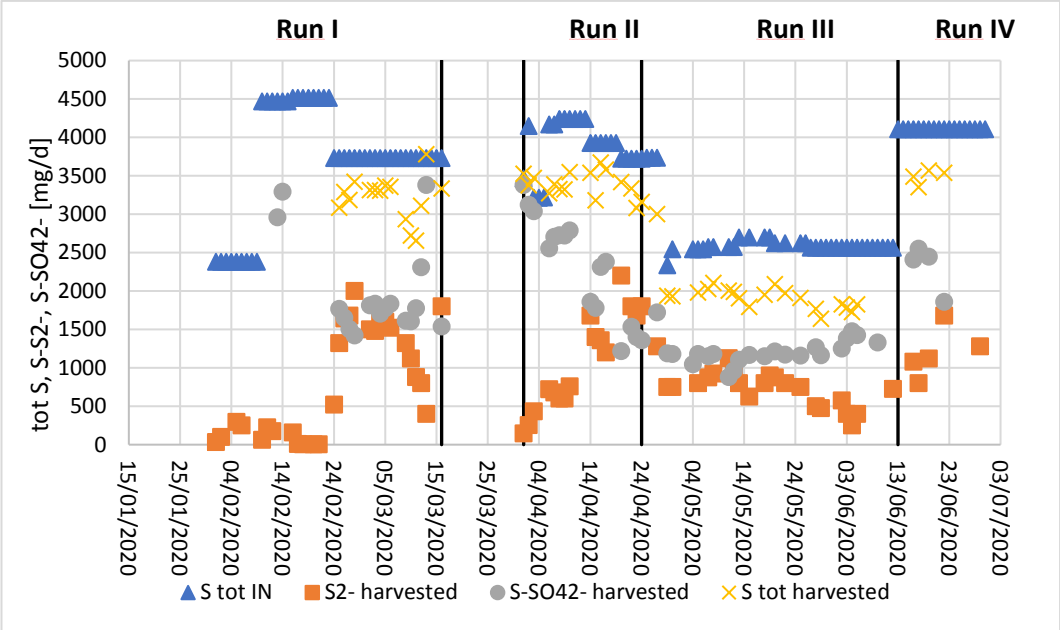

Figure 4.5 Time courses of S-SO_4^{2-}, S-S^{2-} and tot S in the SBR reactor during the experimental activity. The four black bars represent the different runs in which the experimental activity is divided.

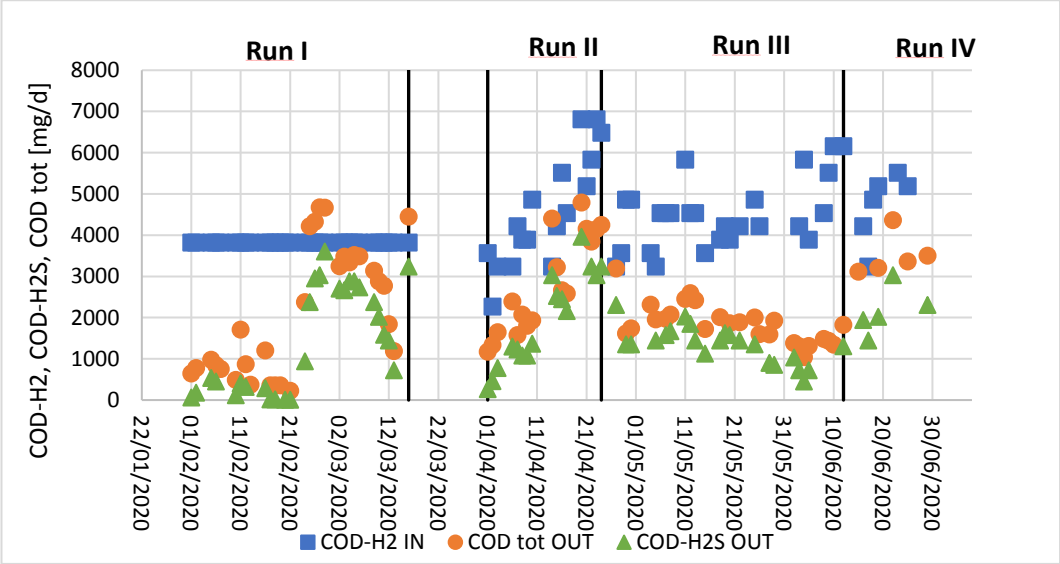

Figure 4.6 COD trend in the SRB reactor. The COD-H_2 IN is the amount of COD-H_2 that is used from the system every day; the COD tot OUT is the COD measured in the effluent from the SRB reactor; the COD-H_2S OUT is the COD estimated from the S-S^{2-} measurement multiply by the conversion factor 1.8 g COD/g H_2S. The four black bars represent the different runs in which the experimental activity is divided.

Table 4.5 S mass balance in the SRB reactor during the 4 runs.

	Run I	Run II	Run III	Run IV
Days	1-45	61-84	85-133	134-154
Recirculation liquid [L]	10	10	6	10
S-SO_4^{2-} IN [g/d]	3.7	3.8	2.6	3.7
S-S^{2-} IN [g/d]	0	0	0	0
S-SO_4^{2-} OUT [g/d]	1.7	1.7	1.1	2.3
S-S^{2-} OUT [g/d]	1.5	1.6	0.9	1.4
H_2S [mg/L]	381	410	349	350
Tot S OUT [g/d]	3.2	3.3	2.0	3.5
S-SO_4^{2-}-S-S^{2-} conversion [%]	41%	43%	34%	38%

Table 4.6 COD mass balance in the SRB reactor during all the 4 runs. The COD-H_2 IN was measured manually for the run II-IV; only for the run I, it was assumed. The COD-H_2S was calculated basing on the S-S^{2-} measured multiply by the conversion factor 1.8 g COD/g H_2S.

	Run I	Run II	Run III	Run IV
Days	1-45	61-84	85-133	134-154
Recirculation liquid [L]	10	10	6	10
COD-H_2 consumed [g/d]	3.8±0	5.4±1.2	4.3±0.7	4.7±0.8
COD-H_2 theoretical consumed [g/d]	4.1	4.2	6.8	6.3
Tot COD OUT [g/d]	3.7±0.6	3.8±0.8	2.2±0.3	3.5±0.5
COD-H_2S OUT [g/d]	2.7±0.4	2.9±0.6	1.6±0.3	2.1±0.5
COD-H_2S/tot COD [%]	74%	78%	72%	61%
% conversion COD-H_2 to tot COD [%]	97%	70%	51%	75%
% conversion COD-H_2 to COD-H_2S [%]	72%	55%	37%	46%

During the first run (days 1-45), the level of sulfate concentration in the effluent of the reactor had substantially decreased during the experimental time, resulting in a concomitant gradually increasing of sulfide concentration (Figure 4.5). During the stability period, the SRB reached an average S-S^{2-} production of 1.5 g/d (for 1 L of TBR). Due to the surplus of sulfate in the feed (around 3 g/L of SO_4^{2-} or 32 mmol/L or 1 g/L of S-SO_4^{2-}, values measured with the kit), the conversion from sulfate to sulfide was 41% in the first stability period. The surplus was chosen to make sure that the rate-limiting factor was the availability of electron donor, i.e. the transfer of hydrogen gas to the liquid. The Table 4.5 shows the total S mass balance for the run I. As it is possible to see, the efficiency in COD conversion (COD-H_2 to COD-H_2S) was around 70%.

During the second run (days 61-84, *after the lockdown due to the Coronavirus*), the sulfate in the feed was maintained at the same concentration used during the first

phase (Figure 4.5). During the stability period of the run II, the SRB reached an average of S-S^{2-} production of 1.6 g/d (for 1 L TBR). The conversion of sulfate to S-S^{2-} was, as for the first run, higher than 40%. As it possible to see from the Figure 4.5, the concentration of S-S^{2-} harvested is still increasing with time, as well as the concentration of S-SO_4^{2-} is still decreasing. The Table 4.5 shows the total S mass balance for the run II. During the second run, the COD conversion to COD-H_2S was higher than 50%.

In the run III (days 85-133) the volume of the reactor was reduced from 10 L to 6 L, in order to evaluate the effect of the low volume on the S conversion yield. In this run the % of S-S^{2-} conversion reached a lower value, around 30%. The S-S^{2-} production was around 0.9 g/d (for 1 L of TBR). The Table 4.5 shows the total S mass balance for the run III. The conversion in COD-H_2S was lower than the period before; it was indeed around 40%.

Then, during the run IV (days 134-154), due to the reduction of the S conversion reached in the previous run, the volume of the reactor was changed to 10 L again. Here, the % of S-S^{2-} conversion reached around 40% with a S-S^{2-} production of 1.4 g/d (for 1 L of TBR); furthermore, an increment in COD conversion was observed in the last run (up to more than 50%).

Following the Equation 2, stoichiometrically with 15 g of Al (0.55 mol) it is possible to produce 0.83 mol of H_2 (gas) which corresponds (at 33°C and 1 atm) to 21 L. During the first run, in the system every day was measured a maximum of 15-16 L of gas produced. As every g of H_2 correspond to 8 g COD, and the system used every day around 6 L of gas, it is possible to determine that every day 3.82 g COD-H_2 was consumed by the system. As it is possible to see in the Figure 4.6, in the first period the value of COD-H_2 was considered constant (around 4 g COD-H_2/d). During the run II, III, IV and V, the H_2 level was measured differently, and the values considered were closer to the real COD-H_2 produced and consumed. From the Equation 1 it is possible to determine the amount of total COD-H_2 that is needed for the reduction of SO_4^{2-}. For every g of SO_4^{2-}, it needs 0.67 g COD-H_2. So, as it is shown in the Table 4.6, it is possible to estimate the theoretical COD-H_2 that should be consumed for the reduction of SO_4^{2-}. The real values and the

theoretical values are different from each other, but it may be due to the limitations in the H_2 level measurement.

The pH trend is shown in the Figure 4.7; as it is possible to see from the graph, the pH starts at around 6-7 and increases during the fed batch reaction to 8-9. At this pH value, almost 100% of H_2S produced is in the form of HS^- (Figure 4.7).

During the optimal and stable conditions, one sample from the SRB reactor was taken in order to proceed with the genomic extraction procedure and, then, with the qPCR analysis. The detection was made searching the APS-reductase gene, which occurs in anaerobic reducing sulfates to sulfides bacteria. The results showed the presence of bacteria correlated mainly to the Desulfobacteraceae family, which comprise bacteria involved in the reduction of sulfate.

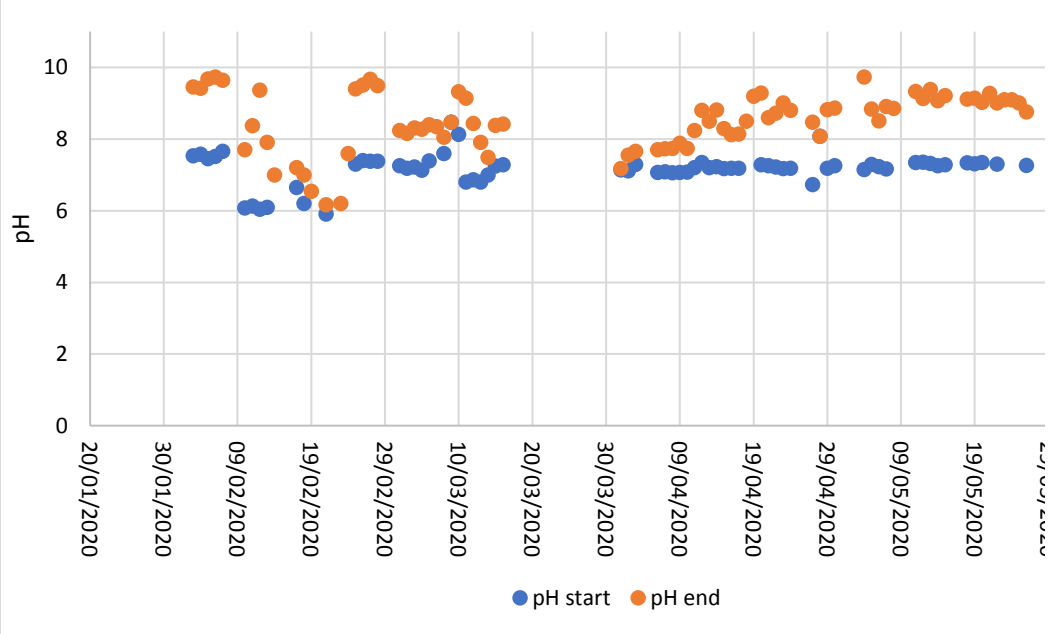

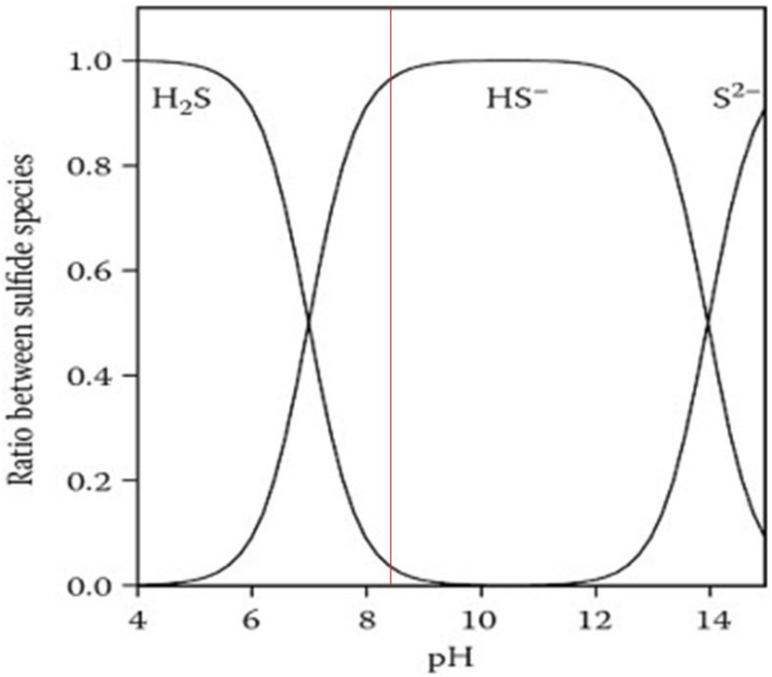

Figure 4.7 The upper picture shows the pH trend in the SRB reactor. The lower graph shows the relation between sulfide species and pH (source: Park et al., 2014). The red line represents the value of pH (8.5) at which sulfide is present mainly in solution in the form of HS^-.

The SRB reactor during all the experimental runs was fed with only H_2 gas. The volume of the TBR was maintained constant during all the experimental period, i.e. 1 L; two volumes of liquid reservoir were tested during the activity: 10 L and 6 L, for gaining information about the effect of the H_2S dilution.

The simple approach of a TBR allows to achieve a good rate of COD-H_2 conversion to total COD; as shown in the Table 4.6, except for the run III, it was obtained a conversion of the COD-H_2 in the range of 70-97%. Furthermore, it is possible to notice that in all the runs, around 70% of the total COD in the effluent is COD-H_2S.

From the data show in the Table 4.5, it is evident that in all the runs the concentration of H_2S was always maintained below 500 mg/L; it is indeed reported in Reis et al. (1992) that a concentration higher than 547 mg/L have a toxic effect on the bacteria.

The SO_4^{2-} concentration in the influent to the SRB reactor was maintained during all the runs around 1100-1300 mg/L. In literature (Dev et al., 2016) it is reported a study to verify the performance of SRB in a packed bed reactor. In that article, the concentration of sulfate ranging from 600 to 2000 mg/L, with an increment of 200 mg/L. Furthermore, in the same work they observed a gradual increase in specific

growth rate when sulfate concentration in the system varied from 600 to 1000 mg/L. However, in the present study, the main objective was to analyse and optimize the solubilization of a gas (in this case H_2) to a biomass. The experiments were set up mainly to optimize the COD-H_2 conversion to the COD-biomass and to optimize the H_2S production, instead of optimize biomass growth. For this reason, the SO_4^{2-} concentration in the influent was always maintained in excess in order to avoid limitation in the reaction. And, thus, the COD/SO_4^{2-} ratio was for all the runs below the minimum COD/SO_4^{2-} ratio of 0.67 which is required for sulfate removal (Choi and Rim, 1991; Lens et al., 1998). It is also reported that with ratio of 1.7 to 2.7, there is a competition between sulfate reducers and methane formers (Brahmacharimayum et al., 2019), which, in this process, was to be avoided, in order to optimize H_2S production in solution.

For full scale application, the process has to be optimized. One possible application can be related to the use of sulfate-rich wastewater as sulfate source, mainly generated by several industrial processes, such as fermentation or see food processing industry, pharmaceutical plants, pulp and paper industry, mining industry, as well as electroplating, tannery and metal processing tannery industries (Lens et al., 2002; Lens et al., 1998). The gas source, as previously reported, can be derived from the use of syngas or biogas, as low-cost energy vectors.

4.4.2 SOB reactor performance

In order to investigate the effect of the S^{2-} as energy source on the biomass selected, the SOB reactor was operated differently in four runs, as shown in the Table 4.4.

SOB biomass is often used in the biological removal of H_2S from biogas (Pokorna and Zabranska, 2015). Several technologies have been developed and practiced in the last years in order to treat gaseous sulfide stream or large volumes of polluted aqueous stream with high sulfide concentrations (Lin et al., 2018). Additionally, these bacteria offer several opportunities for resources recovery such as metals (Rawlings, 2005), elemental sulfur to be applied as fertilizer (Valdés et al., 2016) and polyhydroxyalkanoates (PHAs, Lin et al., 2018).

Basing on the desired product, the amount of oxygen supplied in the reactor has to be controlled. As an example, in case elemental sulfur is the main product, the

reaction has to proceed under oxygen-limiting conditions (Janssen et al., 1995), because sulfide can be oxidize to sulfate in the presence of excess oxygen. Furthermore, SOB bacteria can growth in autotrophic conditions, fixing CO_2 as well as in heterotrophic conditions using organic C-sources. Here, both conditions were studied.

In this work, SOB were tested to verify if, in some conditions, they are able to produce externally SPs. Indeed, it is reported that some bacteria, that usually live in marine environments, are able to produce exopolysaccharides with a sulfated group (Vliet et al., 2019) which have a protection function against degradation. In Xue et al., 2019 it is reported the recovery of sulphated polysaccharides from wastewater rich in sulfur.

In this work the idea is to couple the advantages of this technology for the sulfide removal, with the recovery of high added value molecules.

As for the SRB reactor, the SOB reactor was shut down from the day 46 to the day 60 (*due to the lockdown for the Coronavirus*).

It is possible to divide the four runs in two periods:

1) without pH control from run I to run III;
2) with pH set point at start only during the last run (run IV).

4.4.2.1 SOB reactor without pH control (run I-III)

The Figure 4.8 shows the TSS and VSS trend during the experimental time (run I-III) in the reactor. The black bars indicate the periods of each run. During the first two runs the content of ashes was very high and it is a problem for possible future applications of the biomass. In order to calculate the yield, the amount of salts derived from the SRB effluent was considered in order to not overestimate the yields. In the last run (run III) the reactor was fed without the supply of sugar, differently from the others runs. This was done in order to evaluate the effect of the only $S\text{-}S^{2-}$ as energy source on the biomass growth and in order to select autotrophic bacteria.

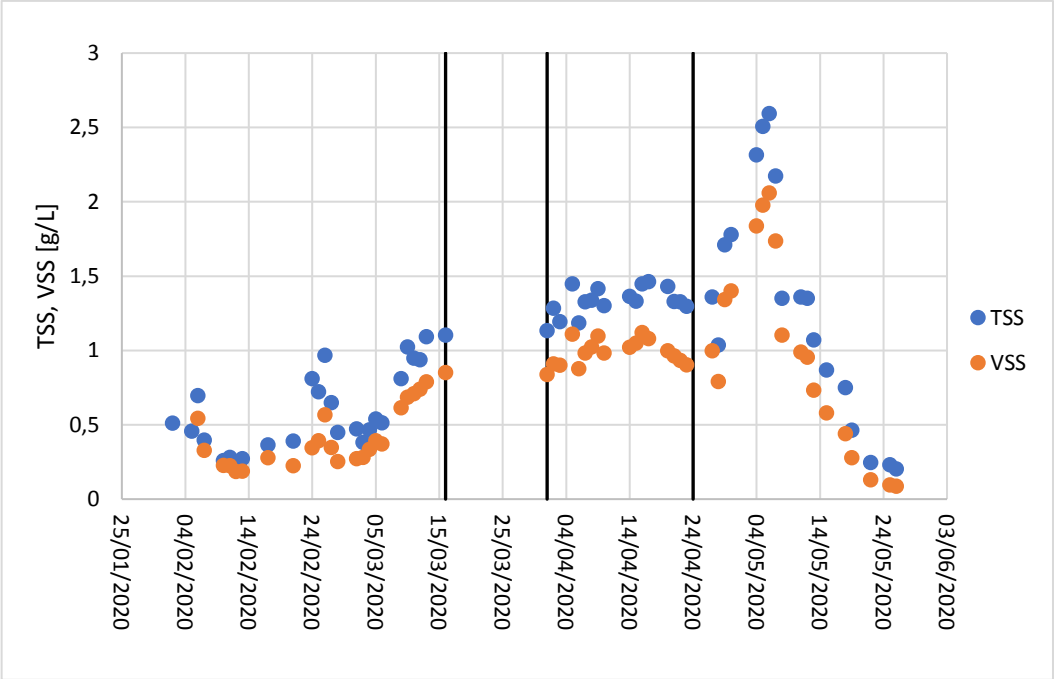

Figure 4.8 TSS and VSS trend in the SOB rector during the first period (3 runs). The black bars indicate the 3 runs. In the first period (run I and II) the VSS/TSS was around 0.6; in the second period (run III) this ratio was consistently lower, 0.16.

The Figure 4.9 shows the trend of S in the system during the runs I-III. The Figure 4.10 shows the pH trend in the same runs.

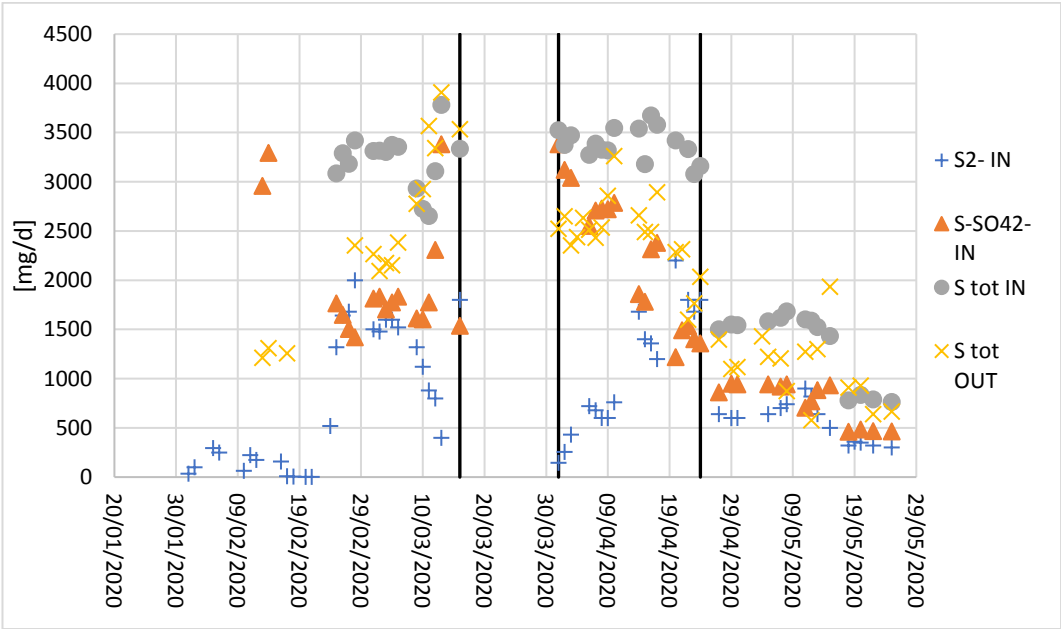

Figure 4.9 Overall trend of S compounds in the SOB reactor during the experimental activity (run I-III). The bac bars indicate the different runs.

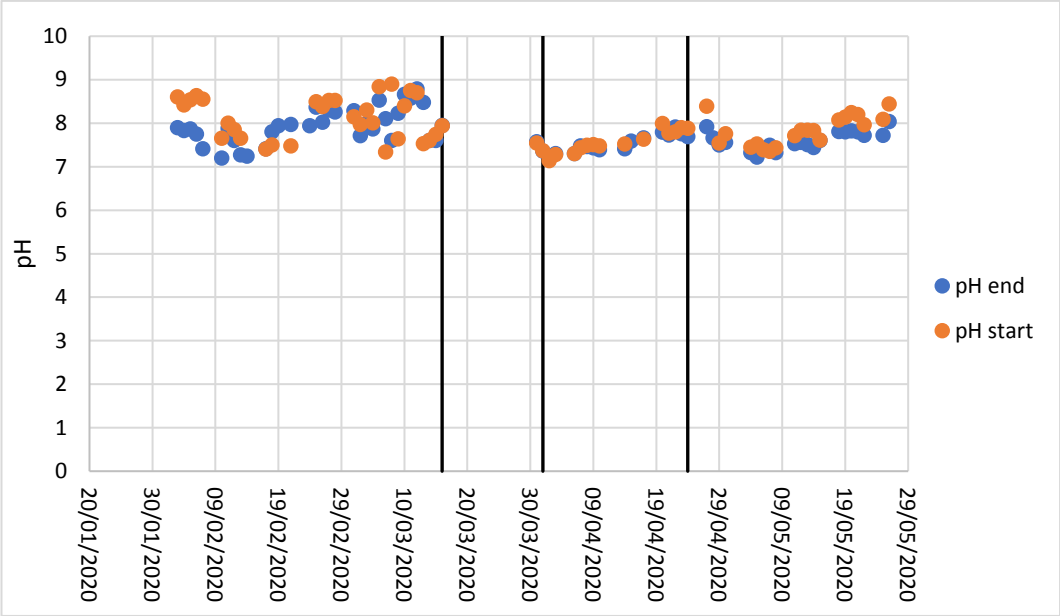

Figure 4.10 pH trend in the SOB reactor during the runs I-III. As it is possible to see, the pH at the end of the reaction was around 7.7 during all the 3 runs, while it was around 7.9 at the beginning of the reaction.

As it is possible to see in the Figure 4.8, the run III was substantially a "transition run" from the mixotrophic period (run I and run II) to the autotrophic one (run IV, in the next paragraph). In the very first part of the run III, the reactor was still fed with sugar, then both volume and feeding procedure were changed causing the "wash-out" of the biomass. Indeed, no-external C source were applied when the sugar was stopped (only CO_2 from the air).

In run I (1-45), every day the SOB reactor, with a working volume of 20 L, was fed with 4 L derived from the SRB reactor and with 1 L of a solution containing 0.1 g/L of $Fe_2(SO_4)_3$ and 6 g of sugar. 5 L of the SOB reactor was harvested every day from the reactor. In this way, the HRT and the SRT were maintained around 4 days. The pH in the reactor was maintained around 8-8.2. The Table 4.7, Table 4.8, Table 4.9 and Table 4.10 show the COD in the influent and in the effluent of the system and the S-mass balance.

Table 4.7 COD characterization in the SOB influent. COD-Sugar is the amount of external sugar added during the mixotrophic runs (I and II). COD-SRB is the COD measured using the COD kit in the SRB effluent. COD-H_2S is calculated converting the H_2S produced by the SRB to COD-H_2S, multiplying by the factor 1.8 g COD/g H_2S. COD total is the total amount of COD feeding in the SOB system.

		INFLUENT			
Runs	**Days**	**COD-Sugar mg/d**	**COD-SRB mg/d**	**COD-H_2S mg/d**	**COD TOT mg/d**
I	1-45	6000	3725±631	2746±412	9725±631
II	61-84	6000	3782±782	2952±568	9782±782
III	85-117	0	749±66	581±37	749±66

Table 4.8 COD total, TSS and VSS in the effluent of the SOB.

		EFFLUENT			
Runs	**Days**	**COD TOT mg/d**	**TSS g/d**	**VSS g/d**	**VSS/TSS**
I	1-45	2644±379	2.54±0.9	1.64±0.6	0.64
II	61-84	2364±1507	2.83±1.8	1.75±1.2	0.62
III	85-117	77±16	0.19±0.06	0.03±0.02	0.17

Table 4.9 S-compounds in the influent to the SOB.

		INFLUENT		
Runs	**Days**	**S-SO_4^{2-} mg/d**	**S-S^{2-} mg/d**	**Tot S mg/d**
I	1-45	1683±138	1525±229	3209±214
II	61-84	1731±436	1640±316	3371±218
III	85-117	469±11	323±21	792±31

Table 4.10 S-compounds in the effluent from the SOB.

		EFFLUENT			
Runs	**Days**	**S-SO_4^{2-} mg/d**	**S-S^{2-} mg/d**	**Tot S mg/d**	**ΔS mg/d**
I	1-45	2391±304	0	2391±304	818
II	61-84	2278±447	0	2278±447	1093
III	85-117	786±155	0	786±155	0

During the stability period, the totality of S^{2-} was converted to SO_4^{2-}. However, the amount of total S in the output did not correspond to the amount in the influent. Indeed, 3.2 g/d of total S was fed in the reactor, while only 2.4 g/d of total S were found in the output. So, around 0.8 g/d of total S could probably be present in a form different from sulfate or sulfide (e.g. thiosulfate), or can be lost (or stripped)

as a result of high volatile nature of sulfide, or can be attached to the EPS around the cells as sulfated groups.

In order to have a confirmation of this last point, and to motivate the S-mass balance, the biomass was analysed for verify the presence of sulphated polysaccharides (SPs). In detail the % of sulfur in the biomass was analysed, and only 0.6% of sulfur was found in the biomass.

So, the theory of stripping was evaluated. The reason why the S-mass balance was not closed, could be due to the pH value used during the runs. Indeed, as it is reported in the Figure 4.10, with pH lower than 8 or around 8, almost 50% of the S is in the form of H_2S gas. So, it was assumed that around 50% of the COD-H_2S was lost for stripping. In this way, the yields shown in the Table 4.11 were calculated. Assuming a yield of 0.35 g TSS/g COD for heterotrophic bacteria growing on sugar (Shuler and Kargi, 2002; Simonic et al., 2017), it was estimated an amount of TSS harvested of 2.1 g TSS/d. In the first run, it was harvested 2.54 g TSS/d, so 0.44 g TSS/d (and 0.28 g VSS/d) could derive from the part of COD not related to sugar. Calculating the specific yield for autotrophic growth (on COD-H_2S), it is possible to obtain a yield of 0.16 g TSS/g COD-H_2S consumed. However, considering only 50% of COD-H_2S used (due to the stripping), the resulting yield is 0.32 g TSS/g COD-H_2S consumed or 0.21 g VSS/g COD-H_2S consumed.

Table 4.11 Yields calculated for each run. All the COD are referred to the COD consumed. The COD-H_2 consumed is referred to the amount (in L) of SRB effluent gave to the SOB reactor.

		YIELD		
Runs	**Days**	**g VSS/g ΔCOD-H2 (+sugar)**	**g TSS/g ΔCOD-H2S**	**g VSS/g ΔCOD-H2S**
I	1-45	0.0003*	0.32**	0.21**
II	61-84	0.0003*	0.49**	0.31**
III	85-117	0.02	0.33	0.06

**These two yields are referred to a mixotrophic period. So, the VSS harvested derived not only from COD-H_2S (which derive, in turns, from the COD-H_2 consumed) but also from COD-sugar. For this reason, the yield is calculated considering the COD-H_2 and the COD-sugar consumed. It was used a value of 0.35 g TSS/g COD removed (Shuler and Kargi, 2002).*

***These yields are calculated following these 2 points:*

a) *Taking into account the amount of TSS and VSS derived from only COD-H_2S (and not sugar).*

b) Taking into account a loss of COD-H_2S (due to pH) of around 50%, for the first two runs.

During the second run (61-84), the SOB reactor had a working volume of 20 L, as in the previous period; every day the SOB reactor was fed with 4 L derived from the SRB reactor, 1 L of a solution containing 0.1 g/L of $Fe_2(SO_4)_3$, 6 g/d of sugar and 0.2 g/d of $(NH_4)_2SO_4$. The Table 4.7 and the Table 4.8 show the COD-mass balance, the Table 4.9 and the Table 4.10 show the S-mass balance; as it possible to see, also in the second run around 1 g/d of tot S is lost and it is not found in the tot S out. The second run had, basically, the same characteristics of the first run; indeed, for calculating the biomass growth yield factor was followed the same approach. Considering 6 g COD-sugar/d, it should be obtained 2.1 g TSS/d; during the second run it was obtained 2.83 g TSS/d, so 0.73 g TSS/d could derive from autotrophic growth. Considering only the amount of COD-H_2S consumed (always 50% due to the stripping), the yield should have a value of 0.49 g TSS/g COD-H_2S consumed or 0.31 g VSS/g COD-H_2S (Table 4.11).

Then, in the run III (85-117), the reactor working volume was changed from 20 to 10 L and then to 5 L. The influent and effluent flow rate were changed in order to maintain the same HRT. The feeding procedure was maintained the same as for the previous runs. The Table 4.7, the Table 4.8, the Table 4.9 and the Table 4.10 show the S and COD mass balance. The biomass growth yield factor during the run III was calculated. No sugar was added during this run, so the biomass selected was mainly autotrophic. This run was an intermediate run between mixotrophic and full autotrophic period.

During the first two runs the nutrient composition used was suitable for mixotrophic rather than heterotrophic or autotrophic growth; the reactor was feed with sugar and with H_2S as energy sources.

In Kuenen and Beudeker (1982) it is reported a study about the evaluation of the microbiology of *Thiobacillus* and other SOB in different conditions, such as autotrophic, mixotrophic and heterotrophic. They discovered that *Thiobacillus* display remarkable flexibility with respect to the substrates; it can indeed utilize both inorganic and organic substrates. Same aspects were also reported in

Kantachote et al. (2008) where they performed a selection study of SOB to enhance biogas production. Here, they reported a better growth in a mixotrophic conditions than in heterotrophic.

4.4.2.2 SOB with pH set point at start (run IV)

After the analysis of the results obtained in the first three runs shown above, it is observed that the differences in the S mass balance may be due to the loss of S^{2-}. Indeed, looking at the pH values shown in the Figure 4.7 (in which is shown the relation between sulfide species and pH), and looking at the Figure 4.10, which shown the pH trend in the SOB reactor in the first 3 runs, around the 50% of the S compounds should be in the form of H_2S gas.

Due to this evaluation, the SOB reactor was set up in order to maintain the pH higher than 8.5 (Figure 4.13). The reactor had a working volume of 5 L and it was under continuous stirring in a closed system, at the temperature of 33 °C. The reactor was fed daily with SRB effluent. In the first 9 days the reactor was fed with 1 L of SRB effluent per day, and 0.25 L/d of biomass was recirculated to the reactor. After 10 days, the reactor was fed with 1.2 L of SRB effluent per day, 1.5 g/d of $NaHCO_3$ as carbon source and no-recirculation was applied to the system. The HRT was, thus, maintained at around 4 days. Then, due to the low amount of nitrogen in the reactor, 1 g/d of $(NH_4)_2SO_4$ was added.

The reactor was monitored for around 50 days, after the pH control was started. During this time COD, S compounds, TSS and VSS were monitored. The Figure 4.11 shows the TSS and VSS trend in the reactor. The Figure 4.12 shows the S trend in the reactor during the overall period. As it is possible to see, differently from the SOB reactor before the pH control, the S mass balance fits better than in the previous period, no loss of S is shown (Table 4.12 and Table 4.13). The Table 4.14 and the Table 4.15 show the COD-mass balance.

Table 4.12 S-compounds in the influent to the SOB.

		INFLUENT		
Runs	**Days**	**S-SO_4^{2-} mg/d**	**S-S^{2-} mg/d**	**Tot S mg/d**
IV	118-168	660±75	265±105	925±108

Table 4.13 S-compounds in the effluent from the SOB.

		EFFLUENT			
Runs	**Days**	**S-SO_4^{2-} mg/d**	**S-S^{2-} mg/d**	**Tot S mg/d**	**ΔS mg/d**
IV	118-168	974±115	0	974±115	0

Table 4.14 COD characterization in the SOB influent. COD-Sugar is the amount of external sugar added during the mixotrophic runs (I and II). COD-SRB is the COD measured using the COD kit in the SRB effluent. COD-H_2S is calculated converting the H_2S produced by the SRB to COD-H_2S, multiplying by the factor 1.8 g COD/g H_2S. COD total is the total amount of COD feeding in the SOB system.

		INFLUENT			
Runs	**Days**	**COD-Sugar mg/d**	**COD-SRB mg/d**	**COD-H_2S mg/d**	**COD TOT mg/d**
IV	118-168	0	932±295	568±247	911±303

Table 4.15 COD total, TSS and VSS in the effluent of the SOB.

		EFFLUENT			
Runs	**Days**	**COD TOT mg/d**	**TSS g/d**	**VSS g/d**	**VSS/TSS**
IV	118-168	169±42	0.22	0.11	0.48

Then, the yields of the process were estimated as shown in the Table 4.16.

Table 4.16 Yields calculated for last run. All the COD are referred to the COD consumed. The COD-H_2 consumed is referred to the amount (in L) of SRB effluent gave to the SOB reactor.

		YIELD		
Runs	**Days**	**g VSS/g ΔCOD-H2**	**g TSS/g ΔCOD-H2S**	**g VSS/g ΔCOD-H2S**
IV	118-168	0.07	0.39	0.19

Considering the overall process, from H_2S production starting from H_2, to SOB biomass selection, the yield is in the order of 0.07 g COD-biomass/g COD-H2 consumed by the SRB system (g COD_B/g COD-H_2, or g VSS/ g COD-H_2). This yield is comparable with other yields reported in literature related to hydrogen-oxidizing bacteria (HOB) selection processes. In Ehsani et al., (2019), it is reported an increasing in the yield of HOB bacteria, from 0.02 to 0.07 g COD_B/g COD-H_2. Furthermore, in Matassa et al. (2016b) it is reported a biomass yield for HOB in the range of 0.07-0.28 g CDW/g COD-H_2. However, due to this low yield, the overall process is not yet economically affordable and further improvements are necessary.

In terms of H_2S used, in this work it is observed a biomass yield of 0.39 g TSS/g COD-H_2S consumed. However, due to the high amount of ashes in the biomass, VSS are more representative and a yield of 0.19 g VSS/g COD-H_2S consumed was estimated, as shown in the Table 4.16. These values demonstrate well the assumptions did in the first two mixotrophic runs. Indeed, as shown in the Table 4.11, in the run I a yield of 0.32 g TSS/g COD-H_2S consumed was estimated basing on the assumption described above (or 0.21 g VSS/ g COD-H_2S consumed).

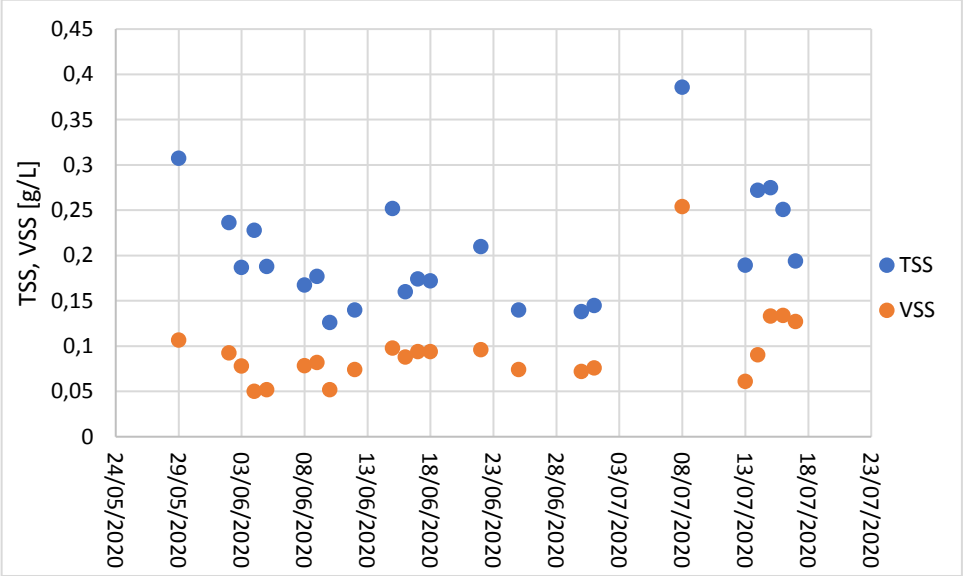

Figure 4.11 TSS and VSS trend in the SOB reactor during the run IV. The VSS/TSS is around 0.5.

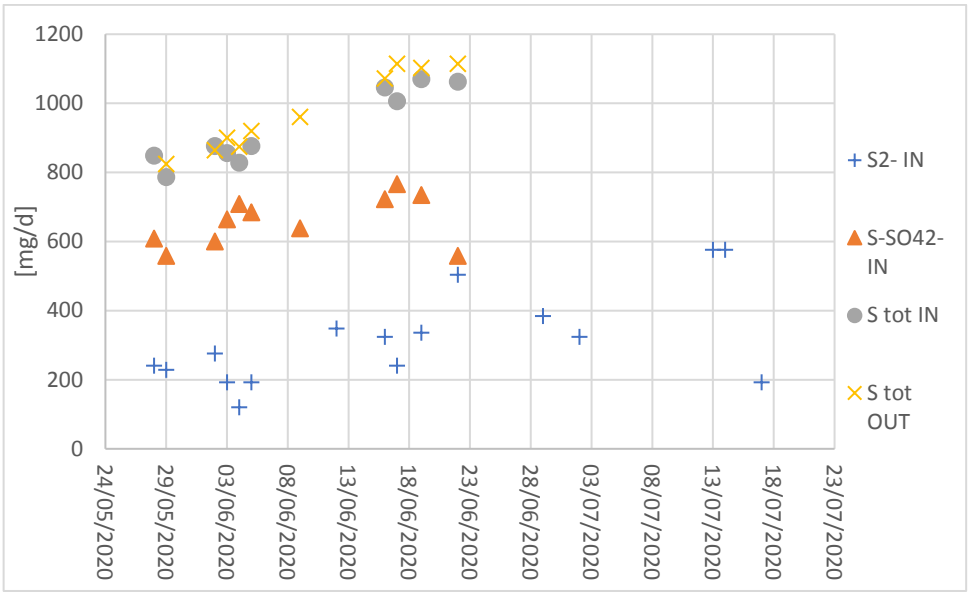

Figure 4.12

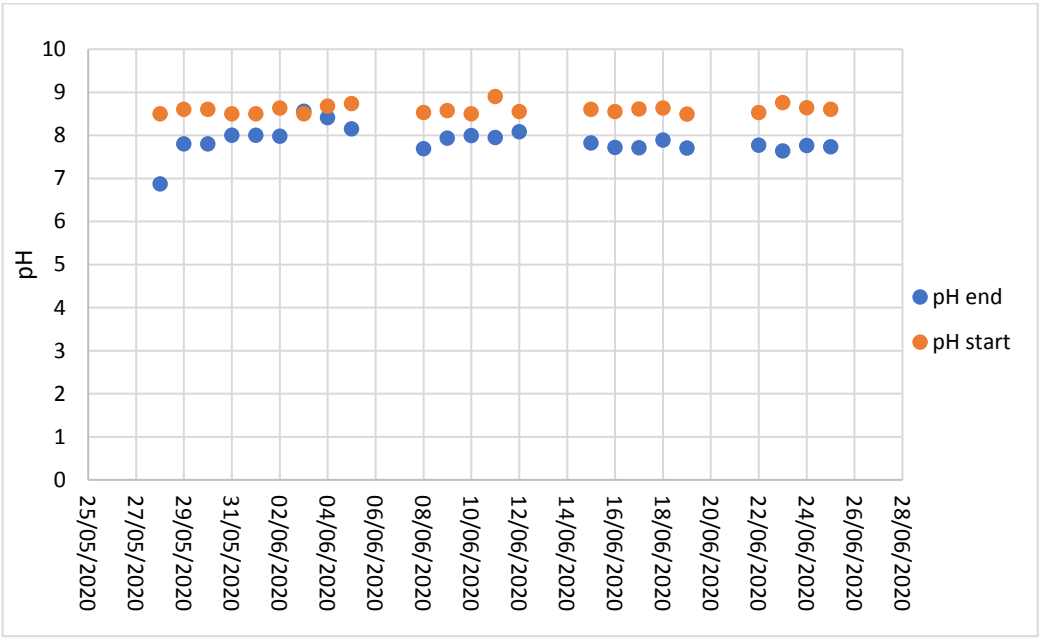

Figure 4.13 pH trend during the last run in the SOB reactor.

4.4.3 SOB harvested biomass

The biomass harvested every day from the SOB reactor, was also characterized in terms of TKN, organic N, proteins, carbohydrates, COD, TSS and VSS content. The Table 4.17 shows the main results obtained from a preliminary analysis of the biomass during run I, run II and run IV.

Table 4.17 Main characterization of the SOB biomass during different runs.

Run	Run I	Run II	Run IV
Days	1-45	61-84	117-151
mg protein/g VSS*100 [%]	74	71	52
mg sugar/g VSS*100 [%]	4	10	-

Sublette and Sylvester (1987) were the first to study in detail the dynamic of growth of *Thiobacillus* on H_2S as the sole energy source. In the study, it is reported the use of *Thiobacillus denitrificans* for desulfurization of natural gas. Some controversies are reported in that paper about the real capacity of *Thiobacillus* to growth on sulfide as the sole energy source. Obviously, soluble sulfide is toxic to several microorganisms, as well as to *Thiobacillus*, if it is provided at high concentrations (they reported 5-8 mM which correspond to 160-256 mg/L of sulfide). In subsequent studies, higher concentrations of sulfide were tested with *Thiobacillus denitrificans* (up to 15 mM which correspond to 500 mg/L, Wang et al., 2005).

In the Sublette and Sylvester (1987) they demonstrate that *Thiobacillus* can growth on sulfide as energy source (in the study they employed up to 2.2 mM of sulfide which correspond to 70 mg/L). Furthermore, in these conditions, it is reported a % of protein of 60±3% by weight. In the present work, the amount of protein as mg protein/g VSS*100 (%) was in the range of 52-74% (as shown in the Table 4.17). The results here obtained are in line with what is reported in literature for *Thiobacillus* grown on H_2S. However, the process can be further improved.

The biomass was also characterized in terms of microbiological composition through quantitative polymerase chain reaction (qPCR). The biomass was analysed for the presence of *Thiobacillus, Thiothrix, Beggiatoa, Achromatium* and *Thiomicrospira*, as well as for the total Eubacteria. The results obtained showed that around 16% of the total community is related to the genera listed above. The most representative genus was *Thiobacillus.*

In Maestre et al., (2010) it is described the bacterial community composition of a gas-phase bio-trickling filter for biogas desulfurization. Indeed, they reported that after 105 days of activity, more than 45% of the inoculum was composed of bacteria

related to the sulfur cycle. However, the setup used in the present work in the run V, has been running for around only 30 days. In Kiragosyan et al. (2020) it is reported a value around 40%.

Reference

Bahr, M., Crump, B. C., Klepac-Ceraj, V., Teske, A., Sogin, M. L., & Hobbie, J. E. (2005). Molecular characterization of sulfate-reducing bacteria in a New England salt marsh. *Environmental Microbiology*, *7*(8), 1175-1185.

Barton, L. L., Fardeau, M. L., & Fauque, G. D. (2014). Hydrogen sulfide: a toxic gas produced by dissimilatory sulfate and sulfur reduction and consumed by microbial oxidation. In *The Metal-Driven Biogeochemistry of Gaseous Compounds in the Environment* (pp. 237-277). Springer, Dordrecht.

Bock, A. K., Prieger-Kraft, A., & Schönheit, P. (1994). Pyruvate—a novel substrate for growth and methane formation in Methanosarcina barkeri. *Archives of microbiology*, *161*(1), 33-46.

Brahmacharimayum, B., Mohanty, M. P., & Ghosh, P. K. (2019). Theoretical and practical aspects of biological sulfate reduction: a review. *Global NEST Journal*, *21*(2), 222-244.

Choi, E., & Rim, J. M. (1991). Competition and inhibition of sulfate reducers and methane producers in anaerobic treatment. *Water science and technology*, *23*(7-9), 1259-1264.

Chung, Y. C., Huang, C., & Tseng, C. P. (2001). Biological elimination of H2S and NH3 from wastegases by biofilter packed with immobilized heterotrophic bacteria. *Chemosphere*, *43*(8), 1043-1050.

Colleran, E., Finnegan, S., & Lens, P. (1995). Anaerobic treatment of sulphate-containing waste streams. *Antonie van Leeuwenhoek*, *67*(1), 29-46.

Das, B. K., Gauri, S. S., & Bhattacharya, J. (2013). Sweetmeat waste fractions as suitable organic carbon source for biological sulfate reduction. *International Biodeterioration & Biodegradation*, *82*, 215-223.

Dev, S., Patra, A. K., Mukherjee, A., & Bhattacharya, J. (2015). Suitability of different growth substrates as source of nitrogen for sulfate reducing bacteria. *Biodegradation*, *26*(6), 415-430.

Dev, S., Roy, S., & Bhattacharya, J. (2016). Understanding the performance of sulfate reducing bacteria based packed bed reactor by growth kinetics study and microbial profiling. *Journal of environmental management*, *177*, 101-110.

Dubois, M., Gilles, K. A., Hamilton, J. K., Rebers, P. T., & Smith, F. (1956). Colorimetric method for determination of sugars and related substances. *Analytical chemistry*, *28*(3), 350-356.

Ehsani, E., Dumolin, C., Arends, J. B., Kerckhof, F. M., Hu, X., Vandamme, P., & Boon, N. (2019). Enriched hydrogen-oxidizing microbiomes show a high diversity of co-existing hydrogen-oxidizing bacteria. *Applied microbiology and biotechnology*, *103*(19), 8241-8253.

Galiana-Aleixandre, M. V., Mendoza-Roca, J. A., & Bes-Piá, A. (2011). Reducing sulfates concentration in the tannery effluent by applying pollution prevention techniques and nanofiltration. *Journal of Cleaner Production*, *19*(1), 91-98.

Haandel, A., & Lubbe, J. (2007). Handbook of biological wastewater treatment. *Design and optimization of activated sludge systems. Leidschendam, The Netherlands: Quist Publishing*.

Janssen, A. J. H., Sleyster, R., Van der Kaa, C., Jochemsen, A., Bontsema, J., & Lettinga, G. (1995). Biological sulphide oxidation in a fed-batch reactor. *Biotechnology and bioengineering*, *47*(3), 327-333.

Janssen, A. J., Lens, P. N., Stams, A. J., Plugge, C. M., Sorokin, D. Y., Muyzer, G., ... & Buisman, C. J. (2009). Application of bacteria involved in the biological sulfur cycle for paper mill effluent purification. *Science of the total environment*, *407*(4), 1333-1343.

January, G. G., Naidoo, R. K., Kirby-McCullough, B., & Bauer, R. (2019). Assessing methodologies for fucoidan extraction from South African brown algae. *Algal Research*, *40*, 101517.

Jong, T., & Parry, D. L. (2003). Removal of sulfate and heavy metals by sulfate reducing bacteria in short-term bench scale upflow anaerobic packed bed reactor runs. *Water research*, *37*(14), 3379-3389.

Kantachote, D., Charernjiratrakul, W., Noparatnaraporn, N., & Oda, K. (2008). Selection of sulfur oxidizing bacterium for sulfide removal in sulfate rich wastewater to enhance biogas production. *Electronic Journal of Biotechnology*, *11*(2), 107-118.

Kidgell, J. T., Magnusson, M., de Nys, R., & Glasson, C. R. (2019). Ulvan: A systematic review of extraction, composition and function. *Algal research*, *39*, 101422.

Kiragosyan, K., Picard, M., Sorokin, D. Y., Dijkstra, J., Klok, J. B., Roman, P., & Janssen, A. J. (2020). Effect of dimethyl disulfide on the sulfur formation and microbial community composition during the biological H2S removal from sour gas streams. *Journal of hazardous materials*, *386*, 121916.

Kolthoff, I. M., Sandell, E. B., Meehan, E. J., and Bruckenstein, S., 1969, *Quantitative Chemical Analysis* (4th ed.): New York, Macmillan, p. 857.

Kuenen, J. G., & Beudeker, R. F. (1982). Microbiology of thiobacilli and other sulphur-oxidizing autotrophs, mixotrophs and heterotrophs. *Philosophical Transactions of the Royal Society of London. B, Biological Sciences*, *298*(1093), 473-497.

Lens, P., Vallerol, M., Esposito, G., & Zandvoort, M. (2002). Perspectives of sulfate reducing bioreactors in environmental biotechnology. *Reviews in Environmental Science and Biotechnology*, *1*(4), 311-325.

Lens, P. N. L., Visser, A., Janssen, A. J. H., Pol, L. H., & Lettinga, G. (1998). Biotechnological treatment of sulfate-rich wastewaters. *Critical reviews in environmental science and technology*, *28*(1), 41-88.

Levitt, M. D., Furne, J., Springfield, J., Suarez, F., & DeMaster, E. (1999). Detoxification of hydrogen sulfide and methanethiol in the cecal mucosa. *The Journal of clinical investigation*, *104*(8), 1107-1114.

Lin, S., Mackey, H. R., Hao, T., Guo, G., van Loosdrecht, M. C., & Chen, G. (2018). Biological sulfur oxidation in wastewater treatment: A review of emerging opportunities. *Water research*, *143*, 399-415.

Li, W., Niu, Q., Zhang, H., Tian, Z., Zhang, Y., Gao, Y., ... & Yang, M. (2015). UASB treatment of chemical synthesis-based pharmaceutical wastewater containing rich organic sulfur compounds and sulfate and associated microbial characteristics. *Chemical Engineering Journal*, *260*, 55-63.

Maestre, J. P., Rovira, R., Álvarez-Hornos, F. J., Fortuny, M., Lafuente, J., Gamisans, X., & Gabriel, D. (2010). Bacterial community analysis of a gas-phase biotrickling filter for biogas mimics desulfurization through the rRNA approach. *Chemosphere*, *80*(8), 872-880.

Martins, M., & Pereira, I. A. (2013). Sulfate-reducing bacteria as new microorganisms for biological hydrogen production. *International journal of hydrogen energy*, *38*(28), 12294-12301.

Matassa, S., Verstraete, W., Pikaar, I., & Boon, N. (2016b). Autotrophic nitrogen assimilation and carbon capture for microbial protein production by a novel enrichment of hydrogen-oxidizing bacteria. *Water research*, *101*, 137-146.

Mendez, R., Lema, J. M., & Soto, M. (1995). Treatment of seafood-processing wastewaters in mesophilic and thermophilic anaerobic filters. *Water Environment Research*, *67*(1), 33-45.

Moussa, M. S., Fuentes, O. G., Lubberding, H. J., Hooijmans, C. M., Van Loosdrecht, M. C. M., & Gijzen, H. J. (2006). Nitrification activities in full-scale treatment plants with varying salt loads. *Environmental technology*, *27*(6), 635-643.

Muyzer, G., & Stams, A. J. (2008). The ecology and biotechnology of sulphate-reducing bacteria. *Nature reviews microbiology*, *6*(6), 441-454.

Omil, F., Méndez, R., & Lema, J. M. (1995). Anaerobic treatment of saline wastewaters under high sulphide and ammonia content. *Bioresource technology*, *54*(3), 269-278.

Park, K., Lee, H., Phelan, S., Liyanaarachchi, S., Marleni, N., Navaratna, D., ... & Shu, L. (2014). Mitigation strategies of hydrogen sulphide emission in sewer networks–a review. *International Biodeterioration & Biodegradation*, *95*, 251-261.

Pérez, V., Mota, C. R., Muñoz, R., & Lebrero, R. (2020). Polyhydroxyalkanoates (PHA) production from biogas in waste treatment facilities: Assessing the potential impacts on economy, environment and society. *Chemosphere*, 126929.

Pikaar, I., Sharma, K. R., Hu, S., Gernjak, W., Keller, J., & Yuan, Z. (2014). Reducing sewer corrosion through integrated urban water management. *Science*, *345*(6198), 812-814.

Pokorna, D., & Zabranska, J. (2015). Sulfur-oxidizing bacteria in environmental technology. *Biotechnology Advances*, *33*(6), 1246-1259.

Prado, H. J., Ciancia, M., & Matulewicz, M. C. (2008). Agarans from the red seaweed Polysiphonia nigrescens (Rhodomelaceae, Ceramiales). *Carbohydrate research*, *343*(4), 711-718.

Raposo, M. F. D. J., De Morais, R. M. S. C., de Morais, B., & Miranda, A. M. (2013). Bioactivity and applications of sulphated polysaccharides from marine microalgae. *Marine drugs*, *11*(1), 233-252.

Rawlings, D. E. (2005). Characteristics and adaptability of iron-and sulfur-oxidizing microorganisms used for the recovery of metals from minerals and their concentrates. *Microbial cell factories*, *4*(1), 13.

Reis, M. A. M., Almeida, J. S., Lemos, P. C., & Carrondo, M. J. T. (1992). Effect of hydrogen sulfide on growth of sulfate reducing bacteria. *Biotechnology and bioengineering*, *40*(5), 593-600.

Rhein-Knudsen, N., Ale, M. T., & Meyer, A. S. (2015). Seaweed hydrocolloid production: an update on enzyme assisted extraction and modification technologies. *Marine drugs*, *13*(6), 3340-3359.

Sarti, A., & Zaiat, M. (2011). Anaerobic treatment of sulfate-rich wastewater in an anaerobic sequential batch reactor (AnSBR) using butanol as the carbon source. *Journal of Environmental Management*, *92*(6), 1537-1541.

Shuler, M. L., & Kargi, F. (2002). Bioprocess considerations in using plant cell cultures. *Bioprocess engineering (Basic concepts), 2nd edn. Prentice-Hall Inc., USA*, 405-419.

Simonič, M., Goršek, A., & Petrovič, A. (2017). Nitrate Removal from Groundwater with Membrane Bioreactor. *Nitrification and Denitrification*, 93.

Steudel, R. (2003). Aqueous sulfur sols. In *Elemental sulfur and sulfur-rich compounds I* (pp. 153-166). Springer, Berlin, Heidelberg.

Sublette, K. L., & Sylvester, N. D. (1987). Oxidation of hydrogen sulfide by Thiobacillus denitrificans: desulfurization of natural gas. *Biotechnology and bioengineering*, *29*(2), 249-257.

Tanna, B., & Mishra, A. (2019). Nutraceutical potential of seaweed polysaccharides: Structure, bioactivity, safety, and toxicity. *Comprehensive reviews in food science and food safety*, *18*(3), 817-831.

Tang, K., Baskaran, V., & Nemati, M. (2009). Bacteria of the sulphur cycle: an overview of microbiology, biokinetics and their role in petroleum and mining industries. *Biochemical Engineering Journal*, *44*(1), 73-94.

Valdes, F., Camiloti, P. R., Rodriguez, R. P., Delforno, T. P., Carrillo-Reyes, J., Zaiat, M., & Jeison, D. (2016). Sulfide-oxidizing bacteria establishment in an innovative microaerobic reactor with an internal silicone membrane for sulfur recovery from wastewater. *Biodegradation*, *27*(2), 119-130.

Van Loosdrecht, M. C., Nielsen, P. H., Lopez-Vazquez, C. M., & Brdjanovic, D. (Eds.). (2016). *Experimental methods in wastewater treatment*. IWA publishing.

Van Vliet, D. M., Palakawong Na Ayudthaya, S., Diop, S., Villanueva, L., Stams, A. J., & Sánchez-Andrea, I. (2019). Anaerobic degradation of sulfated polysaccharides by two novel Kiritimatiellales strains isolated from Black Sea sediment. *Frontiers in microbiology*, *10*, 253.

Vera, M., Schippers, A., & Sand, W. (2013). Progress in bioleaching: fundamentals and mechanisms of bacterial metal sulfide oxidation—part A. *Applied microbiology and biotechnology*, *97*(17), 7529-7541.

Wang, A. J., Du, D. Z., Ren, N. Q., & Van Groenestijn, J. W. (2005). An innovative process of simultaneous desulfurization and denitrification by Thiobacillus denitrificans. *Journal of Environmental Science and Health*, *40*(10), 1939-1949.

Wani, A. H., Lau, A. K., & Branion, R. M. (1999). Biofiltration control of pulping odors–hydrogen sulfide: performance, macrokinetics and coexistence effects of organo-sulfur species. *Journal of Chemical Technology & Biotechnology: International Research in Process, Environmental & Clean Technology*, *74*(1), 9-16.

Wheeler, P. A., & Kirchman, D. L. (1986). Utilization of inorganic and organic nitrogen by bacteria in marine systems 1. *Limnology and Oceanography*, *31*(5), 998-1009.

Wijesinghe, W. A. J. P., & Jeon, Y. J. (2012). Biological activities and potential industrial applications of fucose rich sulfated polysaccharides and fucoidans isolated from brown seaweeds: A review. *Carbohydrate Polymers*, *88*(1), 13-20.

Xue, W., Zeng, Q., Lin, S., Zan, F., Hao, T., Lin, Y., ... & Chen, G. (2019). Recovery of high-value and scarce resources from biological wastewater treatment: Sulfated polysaccharides. *Water research*, *163*, 114889.

Zhang, W., Niu, Y., Li, Y. X., Zhang, F., & Zeng, R. J. (2020). Enrichment of hydrogen-oxidizing bacteria with nitrate recovery as biofertilizers in the mixed culture. *Bioresource Technology*, 123645.

5 General conclusion

This chapter provides the main conclusions of the PhD work.